University of South-Eastern Norway
Faculty of Technology, Natural Sciences and Maritime Studies

Doctoral dissertation no. 11
2018

Michal Sposob

Biological hydrogen sulfide removal with nitrate

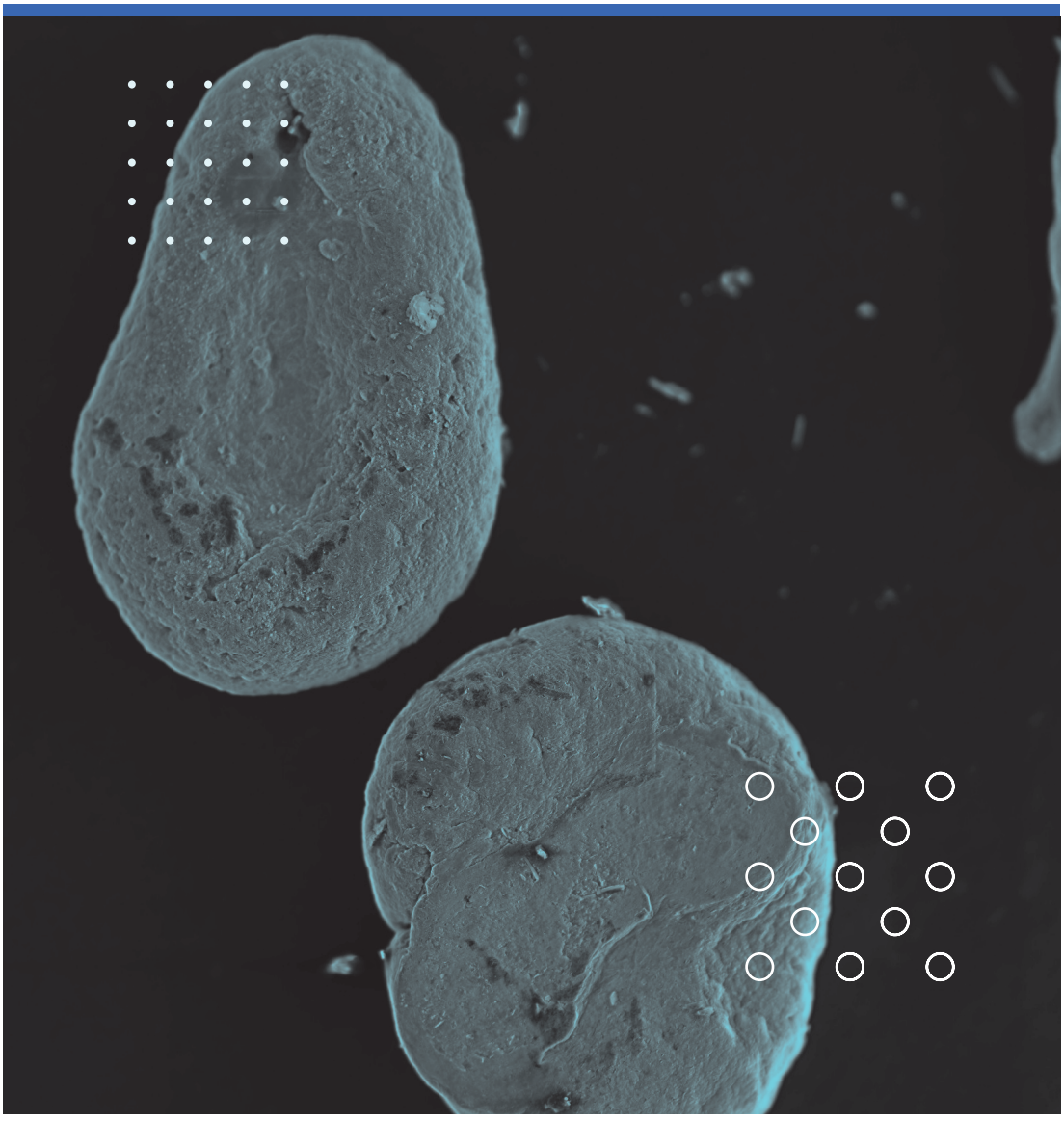

Michal Sposob

Biological hydrogen sulfide removal with nitrate

A PhD dissertation in
Process, Energy and Automation Engineering

Faculty of Technology, Natural Sciences and Maritime Studies
University of South-Eastern Norway
Porsgrunn, 2018

Doctoral dissertations at the University of South-Eastern Norway no. 11

ISSN: 2535-5244 (print)
ISSN: 2535-5252 (online)

ISBN: 978-82-7206-485-2 (print)
ISBN: 978-82-7206-486-9 (online)

Print: University of South-Eastern Norway

Acknowledgments

First and foremost, I wish to express my deep gratitude to my advisors: Associate Professor Carlos Dinamarca and Professor Rune Bakke, thank you for the opportunity to pursue my Ph.D. at the University of South-Eastern Norway (USN). Thank you for your guidance and support.

I would like to express my gratefulness to Associate Professor Agnieszka Cydzik-Kwiatkowska (University of Warmia and Mazury, Poland) and Assistant Professor Slawomir Gulkowski (Lublin University of Technology, Poland) for their research cooperation during this period. I am grateful to Associate Professor Jacek Czerwinski (Lublin University of Technology, Poland) that inspired me to scientific work and thanks to him I had a chance to come to University of South-Eastern Norway (former Telemark University College). I would like to thank Hildegunn Hegna Haugen and Nora Cecilie Furuvik for help with laboratory issues. Thanks to Espen Johansen and Jon Hovland (Tel-Tek/Sintef) for their cooperation. Frank Aarvak and 'Team Skruf,' thank you for the weekly quizzes. Special thanks to all my friends that distracted/helped me during my Ph.D. studies. Among of them are Joanna Kazmierczak, Jan Kudlicka, Gamunu Samarakoon, Veralia Gabriela Sanchez, Christoffer J.V. Wille, my master's students Jens Podevyn and Valerii Vyshniakov, research group mates, and fellow Ph.D. students.

Finally, I am grateful to my parents Grazyna and Piotr Sposob and my brother Dominik for their love, help, and support. This would not be possible without them.

Abstract

Aim

Hydrogen sulfide is a major occupational hazard in agriculture, industry, and sewage processing; its presence leads to corrosion. Thus, hydrogen sulfide removal is obligatory. These investigations aim to evaluate the temperature (25-10 ^{o}C) and N/S ratio influence on simultaneous NO_3^- and H_2S removal and products distribution. The dynamics of microbial communities under temperature stress was examined and a method for indirect H_2S measurements was developed.

Materials and methods

The experimental work was performed in an expanded granular sludge bed (EGSB) reactor in two trials. Before the start of each trial, an acclimatization period of around 1 month has been assured to obtain stable conditions when the test started. The reactor was continuously fed with laboratory prepared synthetic wastewater that consisted of nitric acid (HNO_3) as the electron acceptor and sodium sulfide nonahydrate ($Na_2S{\cdot}9H_2O$) as the electron donor. The electron acceptor and donor solutions were prepared and supplied in separate tanks. A pH buffer was supplied together with the electron donor while macro-, microelements, and vitamins were supplied dissolved together with the electron acceptor. The first short-term trial was focused on the evaluation whether the process can run at frequent temperature changes (25-10 ^{o}C) and elemental sulfur (S^0) can be accumulated in the granular sludge (details are given in Article I). The main trial was performed over 150 days (excluding the acclimatization period). During this trial, the temperature impact (25-10 ^{o}C) in a longer time span and different N/S ratios (0.35-1.30) were studied (details are given in Articles II-IV). The obtained results were analyzed considering Gibbs free energy and electron balance. The microbial communities in biomass samples were also examined to better understand the observed temperature adaptation.

Results and discussion

Performed experimental studies on temperature and feed composition impact show that the granular sludge bed autotrophic denitrification process can operate in the 25-10 °C temperature range with high HS^- removal rate and extent from 98 % (at 25 °C) to 89.2 % (at 10 °C) with a complete NO_3^- removal. Feed N/S ratio can be tuned to enhance the sludge associated S^0 accumulation, so that S^0 enriched sludge can be harvested.

The temperature influence was not only limited to changes in HS^- removal. Changes in temperature also influenced the product characteristics under invariable feeding conditions. Increased SO_4^{2-} production and decreased of S^0 was observed with decreasing temperature. The average S^0 yield ranged from 83.7 % at 25 °C to 67 % at 10 °C, while the SO_4^{2-} presence increased from 14.4 % (25 °C) to 22.1 % (10 °C).

The Gibbs free energy analysis revealed that the changes in HS^- removal and products distribution between S^0 and SO_4^{2-} allowed the microbial community to maintain similar reaction energy (for catabolism) at each temperature. This metabolic shift allowed biomass to obtain more energy per HS^- consumed. It is hypothesized to be a microbial response to compensate for the temperature changes.

The observed metabolic shift could be due to changes in metabolism within the microorganisms or changes in the microbial community. A significant population shift was confirmed by the microbial community analysis at 25 and 10 °C which showed that under mesophilic conditions (25 °C) *Thauera* sp. and *Alicycliphilus* sp. (both *β*-Proteobacteria) prevailed and comprised over 57 % of all identified sequences, while *ε*-Proteobacteria (mostly *Sulfurimonas* sp., 31.3 %) predominated under psychrophilic conditions (10 °C). Changes in relative abundance of these Proteobacteria classes are similar to the relative changes in product composition, particularly in case of S^0_{acc}. Its production decreased 2.5 times from 25 to 10 °C, while the presence of *β*-Proteobacteria (*Thauera* sp. and *Alicycliphilus* sp.) decreased by 2.3 times. Thus, it can be suggested that their presence is connected with the HS^- oxidation to S^0 and its accumulation.

Effects of different N/S ratios (0.35, 0.40, 0.60, and 1.30) were studied under psychrophilic conditions (10 °C). The HS^- removal was the highest at the lowest and highest studied N/S ratios, 89.2 % and 89.6 %, respectively. Lower HS^- removal was obtained at N/S=0.40 and 0.60 with the lowest 76.9 % at N/S=0.60. Product formation deviated from the theoretical predictions, suggesting that the reactions in continuous flow bioreactors are more complex than assumed in the standard stoichiometric models. Increasing N/S feed ratio increased the SO_4^{2-} production and decreased of S^0. The S^0 accumulated at low N/S feed ratio was utilized at higher N/S leading to higher SO_4^{2-} production. This phenomenon can explain the lower removal of HS^- at mid-N/S ratios and the higher total effluent sulfur concentration than fed at N/S=1.30.

Keywords: autotrophic denitrification; elemental sulfur recovery; N/S ratio impact; sulfide removal; temperature impact

Popular scientific summary

The controlled stabilization of organic matter is one of the solutions for carbon footprint reduction. One of the methods for organic matter stabilization is the biogas production by anaerobic digestion. Biogas is mainly a mixture of methane and carbon dioxide, but it also contains small amounts of other gases like hydrogen sulfide. Hydrogen sulfide causes corrosion and is a major occupational hazard in agriculture, aquaculture, biogas processing, industry, and sewage processing. Thus, its removal is necessary.

We have investigated a biological method for hydrogen sulfide removal using nitrate as an electron acceptor in a granular sludge bed. The method is an autotrophic denitrification process producing a low amount of sludge. Proposed concept overcomes the complexity of physicochemical methods, enabling the granular sludge to accumulate elemental sulfur that can be harvested for recovery.

The experiments were performed in a high rate reactor, demonstrating the efficiency of the approach. Experimental work was focused on the temperature impact on the process, important for cold-climate countries like Norway. Effects of the ratio between feed nitrate and hydrogen sulfide on sulfur accumulation were also investigated.

The process is much more sensitive to nitrate and hydrogen sulfide ratio changes than temperature. The feed ratio between nitrate and hydrogen sulfide that enhance the elemental sulfur accumulation was experimentally determined. Higher feed ratios caused the oxidation of earlier accumulated elemental sulfur as sulfate.

Hydrogen sulfide removal decreased with temperature but was still efficient at the lowest investigated level (10 °C). It implies that the autotrophic sulfide removal can be a feasible option in cold climates. Elemental sulfur accumulation decreased with temperature more than sulfide removal, which can be explained by a temperature induced changes in microbial communities. There was less microbial diversity at lower temperature implying that fewer psychrophilic than mesophilic organisms are involved in the autotrophic sulfide oxidation. Mesophilic dominating (25 °C) microorganisms *β*-Proteobacteria (*Thauera* sp. and *Alicycliphilus* sp.) were replaced by *ε*-Proteobacteria (*Sulfurimonas* sp.) at 10 °C.

Populærvitenskapelig sammendrag

En kontrollert stabilisering av organisk materiale er en av løsningene for å redusere karbonutslipp. En av metodene for stabilisering av organisk materiale er biogassproduksjon gjennom anaerob utråtning. Biogass er hovedsakelig en blanding av metan og karbondioksid, men inneholder også andre gasser i små mengder, som hydrogensulfid. Hydrogensulfid fører til korrosjon og er en stor yrkesfare i landbruk, fiskeoppdrett, biogassanlegg, prosessanlegg og ved rensing av kloakk. Derfor er det nødvendig å fjerne hydrogensulfid i mange ulike sammenhenger.

Vi studerte en biologisk metode for fjerning av hydrogensulfid ved å bruke nitrat som en elektronakseptor i en kultur som vokser i granuler. Metoden er en autotrof denitrifikasjons-prosess som produserer lite slam. Det foreslåtte konseptet unngår kompleksiteten av fysisk-kjemiske metoder. Det granulære slammet kan akkumulere elementær svovel som kan hentes ut for gjenvinning. Eksperimentene ble utført i en høyhastighetsreaktor, som demonstrerer effektiviteten av metoden.

Eksperimentelt arbeid var fokusert på temperaturenes påvirkning av prosessen, viktig for land med kaldt klima som i Norge. Effekten på svovelakkumuleringen som følge av forholdet mellom matet nitrat og hydrogensulfid ble også undersøkt.

Prosessen er mye mer sensitiv til endringer i forholdet mellom nitrat og hydrogensulfid enn temperaturendringer. Mateforholdet mellom nitrat og hydrogensulfid som maksimerer akkumulering av elementær svovel ble eksperimentelt bestemt. Høyere mateforhold forårsaket oksidasjon av tidligere akkumulert svovel til sulfat.

Fjerningen av hydrogensulfid ble redusert med fallende temperatur, men var fortsatt effektiv ved 10 ^{o}C, den laveste temperaturen som det ble undersøkt. Dette impliserer at autotrof fjerning av sulfid kan bli et effektivt alternativ i kaldt klima. Elementer svovelakkumulering ble redusert mer enn fjerningen av sulfid med fallende temperatur, forklart gjennom endringer i kulturen. Det var mindre mikrobielt mangfold ved lavere temperaturer, noe som antyder at færre psychofile enn mesofile organismer kan være involvert i autotrof sulfidoksidasjon. Dominerende mesofile (25 ^{o}C) mikroorganismer, *β*-Proteobacteria (*Thauera* sp. og *Alicycliphilus* sp.), ble erstattet av *ε*-Proteobacteria (*Sulfurimonas* sp.) ved 10 ^{o}C.

Preface

This dissertation is submitted to the University of South-Eastern Norway (USN) in partial fulfillment of the requirements for the degree of Philosophiae Doctor (Ph.D.). This work has been carried out under the supervision of Associate Professor Carlos Dinamarca and Professor Rune Bakke.

The dissertation contains two parts. In the first part, a literature review and overall discussion are given. The articles that the dissertation is based on are included in the second part.

A major part of the research was carried out at USN. The reactor design, construction, and operation together with the chemical analyses were performed at USN. The microscopy imaging of granular biomass by scanning electron microscopy was performed in collaboration with Assistant Professor Slawomir Gulkowski at the Lublin University of Technology (Poland), while the microbial analysis of reactor's sludge was performed at the University of Warmia and Mazury (Poland) by Associate Professor Agnieszka Cydzik-Kwiatkowska.

During the study period, I have participated in two international conferences. In addition, I was involved in other projects taking place at USN.

List of papers

Article I

Sposob, M., Dinamarca, C., & Bakke, R. (2016). Short-term temperature impact on simultaneous biological nitrogen-sulphur treatment in EGSB reactor. *Water Science and Technology*, 74(7), 1610-1618.

Article II

Sposob, M., Bakke, R., & Dinamarca, C. (2017). Metabolic divergence in simultaneous biological removal of nitrate and sulfide for elemental sulfur production under temperature stress. *Bioresource Technology*, 233, 209-215.

Article III

Sposob, M., Cydzik-Kwiatkowska, A., Bakke, R., & Dinamarca, C. (2018). Temperature-induced changes in microbial community under autotrophic denitrification with sulfide. *Process Biochemistry,* 69, 161-168.

Article IV

Sposob, M., Bakke, R., & Dinamarca, C. (2017). Effects of N/S molar ratio on products formation in psychrophilic autotrophic biological removal of sulfide. *Water*, 9(7), 476.

Article V

Sposob, M., Bakke, R., & Dinamarca, C. (2017). Modeling N/S ratio and temperature effects in simultaneous biological denitrification and sulfide oxidation. *Proceedings of the 58th Conference on Simulation and Modelling (SIMS 58)*, 138, 41-47.

Conference papers

Sposob, M., Dinamarca, C., & Bakke, R. (2016). Temperature impact on autotrophic sludge bed sulfide oxidation. *The 13th IWA Leading Edge Conference on Water and Wastewater Technologies*. Abstract.

Sposob, M., Bakke, R., & Dinamarca, C. (2017). Modeling N/S ratio and temperature effects in simultaneous biological denitrification and sulfide oxidation. *The 58th International Conference of Scandinavian Simulation Society*. Paper.

Other contributions

Østgaard, K., Kowarz, V., Shuai, W., Henry, I. A., Sposob, M., Haugen, H. H., & Bakke, R. (2017). Syringe test screening of microbial gas production activity: Cases denitrification and biogas formation. *Journal of Microbiological Methods*, 132, 119-124.

Wen, Q., Ji, Y., Hao, Y., Huang, L., Chen, Z., & Sposob, M. (2018). Effect of sodium chloride on polyhydroxyalkanoate production from food waste fermentation leachate under different organic loading rate. *Bioresource Technology*, 267, 133-140.

Abbreviations and nomenclature

–SH – Thiol group

AAGBR – Anaerobic Attached-Growth Bioreactor

ANAMMOX – Anaerobic Ammonia Oxidation

ATP – Adenosine triphosphate

BOD_7 – Biological Oxygen Demand, 7 days

$Ca(NO_3)_2$ – Calcium nitrate

$CaCO_3$ – Calcium carbonate

$CaSO_4$ – Calcium sulfate

$CH_{1.8}O_{0.5}N_{0.2}/CH_2O_{0.5}N_{0.15}$ – Biomass

Cl^- – Chloride ion

ClO_4^- – Perchlorate

CO_2 – Carbon dioxide

CO_3^{2-} – Carbonate ion

COD – Chemical Oxygen Demand

CPBD – Carrier-Packed Biological Deodorization

Cr_2O_3 – Chromium (III) oxide

CrO_4^{2-} – Chromate ion

Cu^{2+} – Cupper (II) ion

DEAMOX – Denitrifying Ammonium Oxidation

DMDS – Dimethyl disulfide

DMS – Dimethyl sulfide

DMSO – Dimethyl sulfoxide

DMTS – Dimethyl trisulfide

DO – Dissolved Oxygen

e^- – Electron

EDTA – Ethylenediaminetetraacetic acid

EGSB – Expanded Granular Sludge Bed

EPA – Environmental Protection Agency

Fe – Iron

Fe^{2+} – Iron (II) ion

$Fe(NO_3)_2$ – Iron (II) nitrate

$Fe(OH)_3$ – Iron (III) hydroxide

$FeCl_3$ – Iron (III) chloride

FeO – Iron (II) oxide

FeS – Iron (II) sulfide

FeS_2 – Iron (II) disulfide

FNA – Free Nitrous Acid

IC_{50} – Half-maximal inhibitory concentration

H^+ – Hydrogen ion

H_2 – Hydrogen gas

H_2O_2 – Hydrogen peroxide

$H_2S/HS^-/S^{2-}$ – Hydrogen sulfide and its ions

HCO_3^- – Bicarbonate ion

HNO_3 – Nitric acid

HRT – Hydraulic Retention Time

$KMnO_4$ – Potassium manganate (VII)

KOH – Potassium hydroxide

MFC – Microbial Fuel Cell

MnO_2 – Manganese (IV) oxide

MnO_4^- – Manganate (VII) ion

N/S – NO_3^- to HS^- molar ratio

N_2 – Nitrogen gas

N_2O – Nitrous oxide

NH_4^+ – Ammonium ion

NaCl – Sodium chloride

$Na_2S \cdot 9H_2O$ – Sodium sulfide nonahydrate

NiO – Nickel (II) oxide

NO_2^- – Nitrite ion

NO_3^- – Nitrate ion

O_2 – Oxygen

OH^- – Hydroxide ion

PAO – Polyphosphate Accumulating Organisms

PbO_2 – Lead (IV) oxide

pK_a – Logarithm of the acid dissociation constant

pH – Measure of hydrogen ion concentration

PO_4^{3-} – Phosphate ion

PP – Polypropylene

ppb – Parts per billion

ppm – Parts per million

ppm_v – Parts per million by Volume

RFLR – Reverse Fluidized Loop Reactor

S – Sulfur

S^0 – Elemental Sulfur

SANI – Sulfate reduction, Autotrophic denitrification, Nitrification Integrated

SAOB – Sulfide Antioxidation Buffer

SO_x – Sulfur Oxides

SO_2 – Sulfur Dioxide

SO_3^{2-} – Sulfite Ion

SO_4^{2-} – Sulfate Ion

$S_2O_3^{2-}$ – Thiosulfate Ion

SEM – Scanning Electron Microscopy

SOB – Sulfide Oxidizing Bacteria

SRB – Sulfate Reducing Bacteria

SRT – Sludge Retention Time

UASB – Up-flow Anaerobic Sludge Blanket

VFA – Volatile Fatty Acid

VSS – Volatile Suspended Solids

Zn^{2+} – Zinc (II) Ion

°C – Degree Celsius

Table of contents

Part I

1 Introduction - literature review

1.1 Hydrogen sulfide properties, sources, and role in sulfur cycle

1.1.1 Properties and presence

Hydrogen sulfide (H_2S) is a colorless, easily soluble, and heavier than air toxic gas, with a characteristic smell of 'rotten eggs.' The solubility of H_2S in water is equal to 150 mM/L at 10 °C and decreases with temperature (Carroll and Mather, 1989).

Depending on pH, H_2S dissociates forming HS^- (pK_{a1}=7.04) and S^{2-} (pK_{a2}=11.96), as presented in Figure 1.1. The aqueous, non-ionized H_2S is characterized by its instability and can be released to the gas phase. The release of H_2S is correlated with a mass transfer between gas and liquid. Since the investigations carried out in this thesis were focused on HS^- removal from the liquid phase, the experiments were conducted at pH>8.0 to minimize the H_2S-gas release.

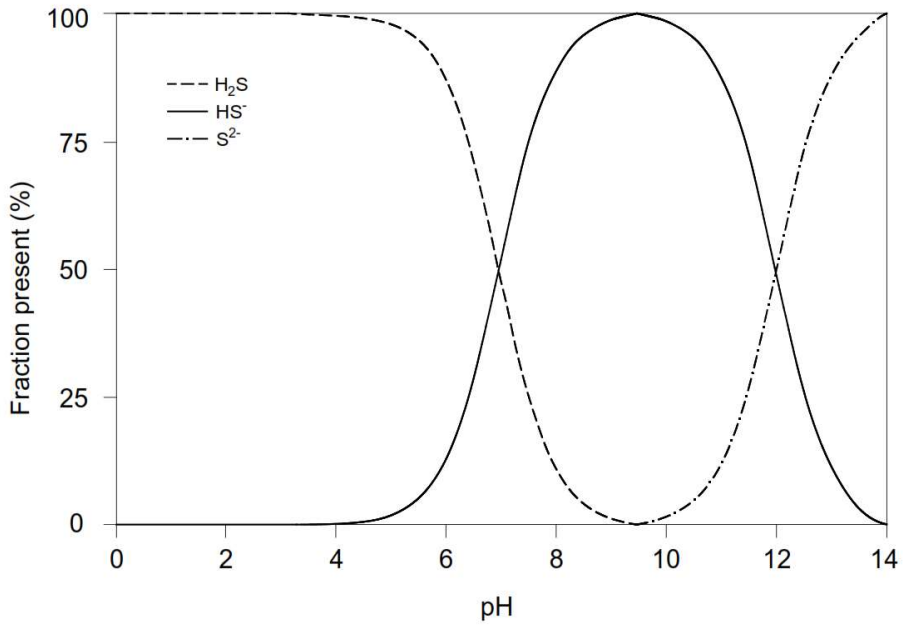

Figure 1.1: pH dependence of sulfide speciation (adapted from Chen et al., 2015).

High H_2S concentrations can be found naturally in sulfur-laden mineral springs. The presence of H_2S in most wastewater streams is moderately low. Domestic wastewater typically has a HS^- content of around 10 mg/L (Pikaar et al., 2011). Taking into account that wastewater pH is usually neutral, the fraction of non-ionized H_2S is around 50 %, which causes the unpleasant odor release.

The H_2S-containing gases and wastewaters are present in many branches of industry like fish, food, mining, oil, paper, and tannery (Cai et al., 2008). Their presence is also typical for biogas plants, landfills, and livestock manure. H_2S concentration in wastewater treatment plants has been reported to be around 1000 ppm; however, concentrations up to 10000 ppm can be reached (Rasi et al., 2011). Biogas can contain from 500 ppm_v up to 20000 ppm_v of H_2S (Pokorna and Zabranska, 2015). Their presence and abundance depend on various factors, e.g., pH, carbon source, and operational conditions.

1.1.2 Sources

H_2S in wastewaters originates from both proteins degradation and sulfate (SO_4^{2-}) reduction. Amino acids like cysteine and methionine comprise a thiol (–SH) group that is liberated under protein decomposition caused by, e.g., pH changes. During the SO_4^{2-} reduction, SO_4^{2-} serves as an electron acceptor used by sulfate reducing bacteria (SRB) under anaerobic conditions (Hao et al., 1996). This reduction often requires a source of organic carbon. The organic carbon uptake by SRB in anaerobic digestion reduces the biogas yield. The reaction below is presented according to Tchobanoglous et al. (2003):

$$\text{organic carbon} + SO_4^{2-} \rightarrow S^{2-} + H_2O + CO_2 \quad (1.1)$$

$$S^{2-} + 2H^+ \rightarrow H_2S \quad (1.2)$$

The reaction mentioned above usually occurs in wastewater treatment plants during influent pretreatment and sludge treatment (e.g., stabilization, dewatering) where O_2 is depleted (Colomer et al., 2012; Rasi et al., 2011). A typical composition of Norwegian

wastewater facilitates formation of H_2S where around 20 mg SO_4^{2-}/L and 150 mg BOD_7/L can be found (Ødegård, 1992).

SO_4^{2-} and organic matter rich wastewaters are typically present in the industry. It was shown that SO_4^{2-} is often found as a co-contaminant of NO_3^- in wastewaters from, e.g., aquaculture, mining processes, petroleum industry, and others (Chen et al., 2017; Hubert et al., 2009; Keränen et al., 2015).

1.1.3 Toxicity and corrosivity

The toxicity of H_2S is mainly related to its non-ionized form. H_2S can diffuse through a cell membrane and react with heavy metals, e.g., Fe cytochromes inhibiting the oxidative phosphorylation (Chen et al., 2010).

Given the characteristic smell (perceptible at >0.02 ppm) and lack of accumulation in the human body, the deadly toxic effect of H_2S is uncommon. However, the prolonged exposure to low H_2S concentrations can lead to eye irritation and olfactory nerve paralysis. High concentrations (>500 ppm) usually found in the industry have a more severe impact, where the loss of consciousness and subsequent death is immediate (Hendrickson et al., 2004).

H_2S is corrosive due to the biological production of SO_4^{2-} that damages, e.g., concrete walls, gas boilers, and piping (De Gusseme et al., 2009). The corrosion of concrete walls can reach up to 10 mm per year, generating high maintenance costs (Zhang et al., 2008). Worldwide maintenance costs of the degraded concrete structures amount to several billion of dollars per year (Huber et al., 2016). Gas motors fueled by H_2S-containing gases like, e.g., unupgraded biogas, emit SO_x shortening the service life of motor (Gayh et al., 2010). To avoid corrosion of heat and power generation units (commonly used for biogas combustion), the H_2S concentration in biogas should not exceed 300 ppm (Bayrakdar et al., 2016). Due to these adverse properties, the H_2S removal is deemed to be necessary.

1.1.4 Inhibition of biological processes

Apart from toxic and corrosive properties, H_2S can be inhibitory towards biological processes under certain conditions (Visser et al., 1993). The negative H_2S influence is mainly correlated with its non-ionized form. Two stages of microorganisms inhibition by H_2S were distinguished: denaturation of native proteins and interference of the sulfur assimilatory metabolism (Zehnder, 1988).

The H_2S concentrations above 200 mg/L have been reported as inhibitory (Tchobanoglous et al., 2003). However, other reports state that both ionized and non-ionized forms can decrease the efficiency of biological processes. The concentrations of 100-800 mg HS^-/L and 50-400 mg H_2S/L were found inhibitory, indicating that ionized HS^- is less severe than H_2S (Parkin et al., 1990). Interestingly, the H_2S presence can negatively influence the process responsible for its generation by reduction of SRB activity (Moosa and Harrison, 2006).

Several studies on the H_2S inhibition towards specific processes are found. The H_2S presence at 60 mg H_2S/L in anaerobic metabolism of polyphosphate-accumulating organisms (PAO) limits the acetate uptake to 50 % (Saad et al., 2017). Nitrification can also be negatively influenced by HS^-; at 100 µM of HS^-, nitrification was reduced by 100 % where the process recovery was slow (Joye and Hollibaugh, 1995). The IC_{50} of HS^--S for anaerobic ammonium oxidation (ANAMMOX) was reported to be equal to 264 mg/L at initial total nitrogen of 200 mg/L (ratio between NH_4^+:NO_2^-=1:1) (Jin et al., 2013).

The concentrations range for H_2S inhibition towards biological processes is wide and variable depending on process parameters. Thus, the establishment of a single value above which the processes are inhibited is not possible, especially taking into account that some microorganisms possess the ability to adapt to H_2S (Cohen et al., 1986).

1.1.5 Sulfur cycle

Sulfur (S) has an important role in the environment and living organisms. Historically, the properties of S gained a noticeable interest. S^0 has been known and used for several thousands of years. In *Genesis*, it was referred to as brimstone, while Homer used it for disinfection. Chinese used S^0 as a gunpowder ingredient around 2000 years ago.

S is one of the six major elements making up the composition of biomolecules. Plants, algae, and many microorganisms assimilate S from SO_4^{2-} as –SH to build proteins. The direct assimilation of S^{2-} into proteins has been reported as impossible due to its inhibitory properties (Atlas and Bartha, 1981). S is present in many substances crucial for living organisms, like glutathione, thiamine, biotin, lipoic acid, coenzyme A, *etc.* (Siegel, 1975).

Large S reservoirs are found in metal rocks (e.g., $CaSO_4$ and FeS_2), S^0 deposits, and fossil fuels, while the oceans are the most significant reservoir of SO_4^{2-}. Due to the human activity, including strip mining and fossil fuels burning, a part of these reservoirs is released, leading to pollution.

The broad presence of S is related to its wide range of oxidation states. This makes the biological sulfur cycle more complex than, e.g., the nitrogen cycle. The oxidation states of S range from –II to +VI, giving 8 electrons (e^-) difference between the most reduced to the most oxidized form (Table 1.1). SO_4^{2-} is the most oxidized S compound, while the most reduced ones are H_2S and –SH.

Table 1.1: Oxidation states of sulfur compounds.

Compound	Oxidation state
Organic S (R–SH)/H_2S	-II
S^0	0
$S_2O_3^{2-}$	-II/+VI
SO_2/SO_3^{2-}	+IV
SO_4^{2-}	+VI

Depending on the oxidation state, S compounds can serve as an electron acceptor or donor. Thus, even if the environmental S concentrations are reported as low, the sulfur fluxes are high (Shao et al., 2010). This unique property is used in the SANI (sulfate reduction, autotrophic denitrification, nitrification integrated) process, where S compounds play both role of electron acceptor (heterotrophic SO_4^{2-} reduction) and electron donor (autotrophic denitrification) (Wang et al., 2009). In terms of oxidation and reduction, the transitions in the biological sulfur cycle take place in anoxic and oxic environment (Figure 1.2).

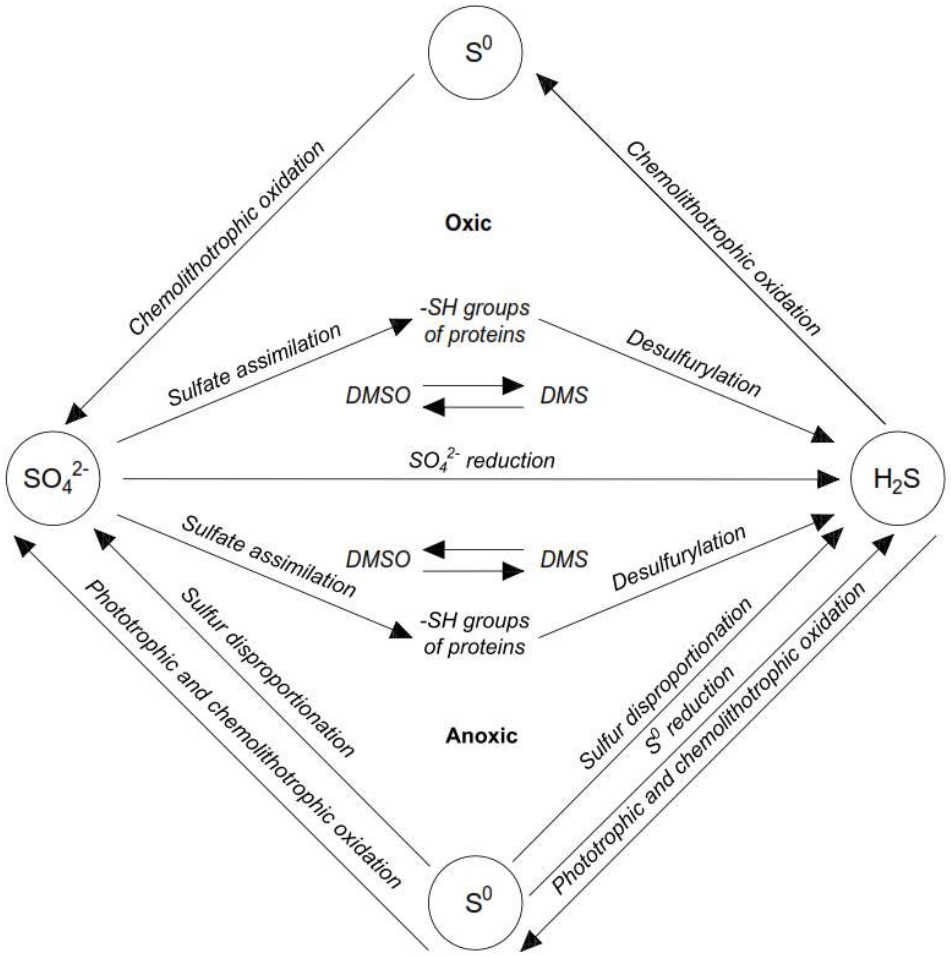

Figure 1.2: The biological sulfur cycle (adapted from Muyzer and Stams, 2008).

H_2S is used as the electron donor by chemolithotrophic sulfide oxidizing bacteria (SOB) like *Thiobacillus* under both the aerobic and anaerobic conditions yielding in S^0 and SO_4^{2-}. Similarly, S^0 can be oxidized by SOB to SO_4^{2-}. One of the consequences of the high production of SO_4^{2-} can be drastic environment acidification. Besides SOB, the oxidation of H_2S can be performed by green and purple phototrophic bacteria (Madigan et al., 1997).

SO_4^{2-}, as a product of H_2S oxidation, can be reduced anaerobically back to H_2S by sulfate reducing bacteria (SRB) that are auto- and heterotrophic, like *Desulfovibrio*, sulfate reducing archaea, *Desulfobacter*, and hyperthermophilic archaea (Schicho et al., 1993; Taylor and Parkes, 1983). Due to low organic carbon availability in the oceans, the SO_4^{2-} reduction is limited.

The organic forms of S compounds like dimethyl sulfide (DMS), dimethyl disulfide (DMDS), and dimethyl trisulfide (DMTS) are present and cycled in the environment. The most abundant one is DMS that is produced in marine environments. DMS, similarly to DMDS and DMTS can be released during zooplankton grazing on phytoplankton and decay (Dacey and Wakeham, 1986). It was estimated that 90 % of the total sulfur flux from marine comes from organosulfur compounds (e.g., DMS) yielding in H_2S (Ibañez et al., 2010).

In addition to the biologically maintained transformations in the S cycle, metals can selectively precipitate HS^-. HS^- reacts violently with many metal oxides, especially with transition metals, such as lead (IV) oxide (PbO_2), nickel (II) oxide (NiO), chromium (III) oxide (Cr_2O_3), and iron (II) oxide (FeO).

Historically, a common method for H_2S removal was to use the iron sponge impregnated on wood chips. The H_2S combines with Fe^{2+} to form iron (II) sulfide (FeS) that is insoluble in water. The iron salts, typically iron (III) chloride ($FeCl_3$) are used to precipitate dissolved HS^-. These salts are supplied in liquid form, which facilitates simple storage. In addition to Fe^{2+}, the combinations of other metal cations like Cu^{2+} or Zn^{2+} are also used (Costa et al., 2017).

According to Wei et al. (2017), the S^{2-} precipitated with Fe^{2+} can be further used for biological denitrification as a source of electron donor (Eqs. 1.3, 1.4).

$$10FeS + 18NO_3^- + 16H_2O \rightarrow 9N_2 + 10\ Fe(OH)_3 + 10SO_4^{2-} + 2H^+ \quad (1.3)$$

$$10Fe(OH)_2 + 2NO_3^- + 6H_2O \rightarrow 10Fe(OH)_3 + N_2 + 2OH^- \quad (1.4)$$

1.2 Biological removal of hydrogen sulfide

The biological treatment methods have many advantages over the physicochemical treatment. The latter is expensive, safe only under limited conditions (temperature and pressure) and generates a sludge that is difficult to handle. Sludge from chemical H_2S precipitation may consist of a high amount of heavy metals, e.g., iron (Fe) or other metal cations used for precipitation. The chemicals supplied in physicochemical treatment can lead to aggressive corrosion and often need to be replaced or dosed in high quantities. On the other hand, the physicochemical methods are characterized by high removal efficiencies and stable operational performance. Biological methods have lower operational costs as a result of the operation at ambient temperatures, atmospheric pressure, less chemicals addition, less sludge production and in terms of HS^- oxidation the resource (S^0) can be recovered (Li et al., 2016).

In biological processes, microorganisms are used to remove contaminants by performing the redox reaction through which they derive energy. Chemotrophic microorganisms obtain energy from chemicals. Depending on the carbon source, chemotrophs can be divided into chemolithotrophs (autotrophs) which use CO_2 to synthesize new organic matter and chemoorganotrophs (heterotrophs) that use organic compounds as a carbon source (Madigan et al., 1997). The microorganisms that can grow either auto- or heterotrophically are called mixotrophs. Aerobes derive energy only under O_2 presence as the source of the electron acceptor. Others, capable of obtaining energy only in the absence of O_2 are called anaerobes. Facultative aerobes can gain energy both under the aerobic and anaerobic conditions. In this thesis, inorganic carbon was supplied

for simultaneous NO_3^- and HS^- removal; thus, chemolithotrophs were cultivated during this work.

The redox reaction conducted by microorganisms leads to energy generation. An electron donor is used by microorganisms as the source of energy. Electrons are transferred from the electron donor to the electron acceptor to provide energy for maintenance and growth. That leads to the electron donor oxidation and electron acceptor reduction.

The electrons portion used to synthesize biomass from organic carbon is much higher than for inorganic carbon. This is because a considerable amount of energy has to be used by autotrophs to reduce inorganic carbon (oxidation state +IV) to approximately oxidation state 0 (pyruvate) (Rittmann and McCarty, 2001). Consequently, the biomass synthesis, measured as biomass yield from electron donor consumed, in the aerobic processes is always higher than from the anaerobic ones. Thus, depending on the microbial metabolism, the growth yield will differ (Table 1.2).

Table 1.2: Typical synthesis yield coefficients (Tchobanoglous et al., 2003).

Growth condition	Electron donor	Electron acceptor	Synthesis yield
Aerobic	Organic compound	Oxygen	0.40 g VSS/g COD
Aerobic	Ammonia	Oxygen	0.12 g VSS/g NH_4^+-N
Anoxic	Organic compound	Nitrate	0.30 g VSS/g COD
Anaerobic	Organic compound	Organic compound	0.06 g VSS/g COD
Anaerobic	Acetate	Carbon dioxide	0.05 g VSS/g COD

1.2.1 Electron acceptors

A few electron acceptors promoting the microbial activity for biological H_2S removal can be distinguished: NO_2^-, NO_3^-, and O_2. Usually, the methods related with electron acceptor supplementation require the prior retention of gaseous H_2S in the liquid. That can be achieved by, e.g., pH elevation using a gas scrubbing.

1.2.1.1 Electron acceptors comparison

So far, O_2 is the most widely used electron acceptor in the biological H_2S removal. Chen et al. (2006) suggested that HS^- oxidation in the presence of O_2 is thermodynamically more favorable than NO_3^-. However, O_2 supply into biological processes faces a few constraints like mass transfer limitations and proper dosing. Lab-scale biotricking filters used at short contact time (under 120 seconds) for H_2S removal (concentrations up to 12000 ppm_v), showed that the mass transfer was a limiting factor in H_2S removal with O_2 (Fortuny et al., 2011). Excessive supply of O_2 may lead to negative effects like pH decrease as well as the biogas quality and yield deterioration. The biogas flammability limits can be exceeded at too high O_2 presence. Thus, the O_2 supply must be carefully controlled.

Due to the high reactivity of H_2S, the O_2 presence can lead to its simultaneous biological and chemical oxidation (Díaz and Fdz-Polanco, 2012). Ramos et al. (2013) confirmed that the control between the biological and chemical removal with O_2 is challenging.

Limitations with mass transfer and possible increase in biogas flammability are absent when NO_3^- is used. On the basis of the physical properties, O_2 has a much lower solubility compared to NO_3^- (Figure 1.3). Therefore, NO_3^- can be an alternative electron acceptor to O_2 such as when high concentrations of H_2S need to be treated.

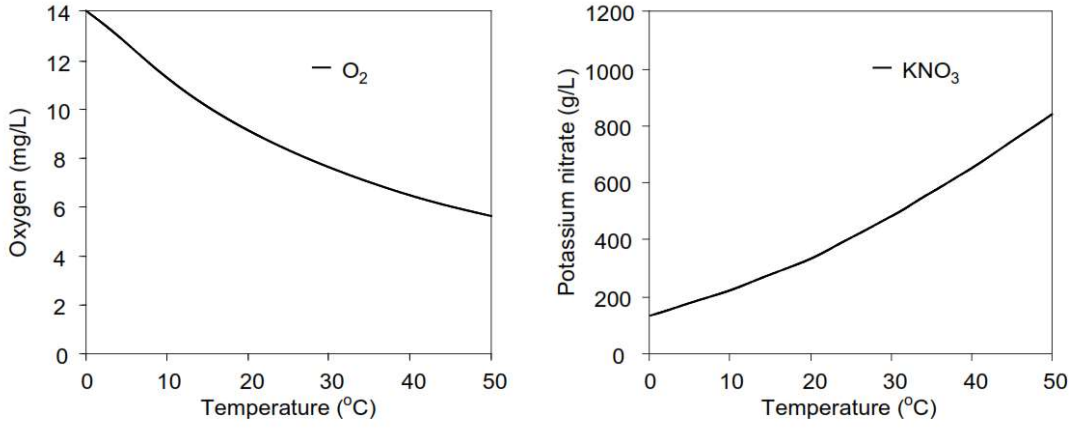

Figure 1.3: Solubility of electron acceptors in water.

O_2 inhibits NO_3^- removal (denitrification) deteriorating the activity of denitrifiers with an inhibition threshold of 0.1 mg O_2/L (Oh and Silverstein, 1999). Nevertheless, studies combining and comparing these two electron acceptors have been performed. The combination of NO_3^- and O_2 was found to enhance the S^0 production (Wang et al., 2015; Xu et al., 2017).

The combination of NO_2^- and O_2 seems to be even more promising than a combination of NO_3^- and O_2. The NO_2^- reductase appeared to be less sensitive to O_2 inhibition than NO_3^- reductase, with an inhibitory threshold of 2.5 mg O_2/L (Korner and Zumft, 1989). NO_2^- supplementation studies were performed by Doğan et al. (2012) where it is reported that at HRT between 8.4-2.0 h the HS^- removal reached over 80 % with a load of 0.47-2.16 kg S/m^3·d. Conversely, NO_2^- was found as inhibitory on denitrification at concentrations of 36-60 mg NO_2^--N/L (Fajardo et al., 2014).

1.2.1.2 Oxygen

The electron acceptor dosage plays a crucial role in biological H_2S oxidation not only due to the increased flammability of biogas (in case of O_2 supply) but also due to the level of H_2S oxidation. Under micro-aerobic (O_2 limited) conditions, the oxidation of H_2S is incomplete and leads to S^0 production as the main product, while at higher O_2 concentrations, SO_4^{2-} is produced (Eqs. 1.5-7).

$$H_2S + 0.5O_2 \rightarrow S^0 + H_2O \quad (1.5)$$

$$S^0 + H_2O + 1.5O_2 \rightarrow SO_4^{2-} + 2H^+ \quad (1.6)$$

$$H_2S + 2O_2 \rightarrow SO_4^{2-} + 2H^+ \quad (1.7)$$

The way of O_2 supply can be different; it can involve air, pure oxygen or oxygen obtained from electrolysis during the MFCs operation (Díaz et al., 2010; Lee et al., 2012; Zhang and Angelidaki, 2015).

Proper control of O_2 dosage, at a right ratio between the electron acceptor and donor is challenging due to a variable concentration of the influent H_2S. The control of O_2 dosage

can be performed by redox measurements. The optimal redox potential range for S^0 formation has been reported between -147 and -137 mV (H_2 reference electrode, 30 °C, pH 8) (Janssen et al., 1998). This control protocol was used in a reverse fluidized loop reactor (RFLR) for S^0 recovery, where the S^0 recovery reached up to 95 % at 11 kg $HS^-/m^3 \cdot d$ (Krishnakumar et al., 2005).

The studies on O_2 were performed at different configurations where O_2 supply was implemented in separate units, directly or its generation was *in situ*.

Several studies on separate units for biological desulfurization with O_2 have been carried out. In the fluidized bed reactor, the introduction of low airflow (0.7-0.9 $m^3/m^3 \cdot d$) at O_2/S molar ratio between 8-10 resulted in H_2S reduction to an undetectable level producing S^0, $S_2O_3^{2-}$, and polysulfides, implying that the reaction proceeds faster at higher O_2/S molar ratio (van der Zee et al., 2007). The external chamber for micro-aerobic desulfurization reached the removal of H_2S up to 94 % while 60 % of S was recovered as S^0 (Ramos et al., 2013). Similar studies were performed in the airlift reactor, where the S^0 recovery reached up to 95 % at DO<0.2 mg/L (Zytoon et al., 2014). The most well-known industrial application of O_2 for H_2S removal is the THIOPAQ® process, which includes H_2S scrubbing in alkaline solution and controlled O_2 supply (Cline et al., 2003).

The direct O_2 supply creating micro-aerobic conditions inside the anaerobic digesters has also been studied. It has been reported that at HRT=20 d and 0.25 NL of O_2/L of feed sludge, the removal of H_2S was higher than 98 %, resulting in S^0 production where the methane concentration in biogas was not affected (Díaz et al., 2011, 2010). Similar positive effects of micro-aeration were reported in up-flow anaerobic sludge blanket (UASB) reactor used for brewery wastewater removing 73 % of H_2S without affecting the COD removal and methanogenic activity (Krayzelova et al., 2014).

The electrochemical HS^- oxidation by O_2 produced *in situ* is frequently studied. Anodic HS^- oxidation to S^0 coupled with cathodic caustic recovery has been reported, where the high current density results in more oxidized sulfur species (Vaiopoulou et al., 2016). Pikaar et al. (2011) obtained the highest HS^- removal rate at 11.8 ± 1.7 g S/(m^2 of anode

surface·h), wherein the final oxidation products were SO_4^{2-}, $S_2O_3^{2-}$, and S^0. Another study, combining SO_4^{2-} reduction and HS^- oxidation on hexacyanoferrate cathodic electrode reported a total removal of HS^- up to 98 % and acetate up to 46 % (Rabaey et al., 2006).

Due to the fact that SOB such as *Thiobacillus denitrificans* has a very good immobilization capability, various packing materials were tested to enhance the removal of H_2S with O_2 (Ma et al., 2006). Materials such as activated carbon, porous lava, ceramics, peat, dolomite, and polymers were examined by Midha et al. (2012). Pall rings were also used as a packing material for biotrickling filtration of biogas (Montebello et al., 2013). The relationship between different carriers in carrier-packed biological deodorization (CPBD) reactor was studied concluding that cylindrical carriers with high porosity were the most efficient (Shinabe et al., 2000). Thus, high porosity (large surface) enhances the process efficiency, where higher loads can be treated.

1.2.1.3 Nitrate

The interest in NO_3^- as an alternative electron acceptor for H_2S removal was already expressed over 80 years ago. One of the first industrial applications of NO_3^- for HS^- removal in paper mills was reported by Fales (1929), while Allen (1949) described the NO_2^- usage for the same purpose. However, the aforementioned trials encountered a problem with the lack of an electron acceptor dosing control leading to overdosing.

Nowadays, the two commercially used NO_3^- salts for H_2S removal are: calcium nitrate $Ca(NO_3)_2$ and iron (II) nitrate $Fe(NO_3)_2$ known under the trade name Nutriox® and Anaerite 263®, respectively. Both these compounds are supplied with complete systems including a chemical feed pump, control unit, and storage tanks. The controlled dosage of NO_3^- salts proved to be effective in the H_2S control and increased the BOD removal (Bentzen et al., 1995). It has been reported that dosing of $Ca(NO_3)_2$ resulted in maximum H_2S removal (>94.7 %) in both gas and liquid phase (Garcia de Lomas et al., 2006).

The autotrophic biological oxidation of H_2S with NO_3^-, which constitutes the topic of this thesis, leads to simultaneous denitrification and desulfurization as a clear advantage of

this approach. In the denitrification process, the dissimilatory transformation of NO_3^- to N_2 takes place (Knowles, 1982). Usually, denitrification is performed with organic carbon as an electron donor. In autotrophic denitrification, the organic carbon is not required that leads to cost savings on organic carbon supply (e.g., methanol), lower sludge production, and process maintenance (Bayrakdar et al., 2016).

Economic reports show that the upgrading cost of 1 m^3 of biogas using $FeCl_3$ and chemical scrubbing ranges between 0.024 and 0.30 €/m^3, while the cost of anoxic biofiltration approximates 0.016 €/m^3 (Lebrero et al., 2016). The life cycle assessment indicates that in comparison with commodity chemicals, nitrate/free nitrous acid (FNA) production from urine for HS^- control would lower operational costs by approximately 2/3 and greenhouse gas emission by 1/3 in 20 years (Zheng et al., 2017). The denitrification process supplemented by reduced sulfur compounds, instead of the commonly used organic carbon source is much cheaper, whereas the prices of S^0 and methanol were reported as 0.1 and 0.7/0.91 $/kg, respectively (Park and Yoo, 2009; Yang et al., 2017). However, so far, autotrophic denitrification for H_2S removal is not a widespread technology.

Similarly as for O_2, the products formation (level of H_2S oxidation) depends on the NO_3^- availability (Eqs. 1.8, 1.9). Better solubility than O_2 makes it easily applicable for sewer systems and point-H_2S-emission sources (Auguet et al., 2016).

$$HS^- + 0.4NO_3^- + 1.4H^+ \rightarrow S^0 + 0.2N_2 + 1.2H_2O \quad (1.8)$$

$$HS^- + 1.6NO_3^- + 0.6H^+ \rightarrow SO_4^{2-} + 0.8N_2 + 0.8H_2O \quad (1.9)$$

The stable isotope fractioning of HS^- showed that its oxidation under NO_3^- presence was a biological process (De Gusseme et al., 2009). This implies that the oxidation of HS^- with NO_3^- is controlled only by microorganisms.

On the basis of catabolic reactions, at N/S=0.40, HS^- is oxidized to S^0 that is stored in the microbial inclusion bodies (Shively, 1974). HS^- can be oxidized to the highest oxidation

state (to SO_4^{2-}) at catabolic N/S=1.60. The ratios within the discussed range can lead to mixed products composition (S^0 and SO_4^{2-}) (Cai et al., 2008).

Feed ratios out of the 0.40<N/S<1.60 range lead to incomplete NO_3^- removal (too high N/S ratio) or incomplete HS^- removal (too low N/S ratio) (Dolejs et al., 2015). The excess of NO_3^- in drinking water can cause the 'blue-baby' syndrome, carcinogenic compounds formation, and eutrophication (Knobeloch et al., 2000; McIsaac et al., 2001). NO_3^- presence can inhibit volatile fatty acids (VFAs) production, methanogens, and consequently methane production (Auguet et al., 2016; Wong and Lee, 2011; Zhou et al., 2012).

In systems rich in organic matter, the depletion of NO_3^- leads to the reduction of SO_4^{2-} and S^0 to HS^- (Jiang et al., 2009). However, organic carbon supply can enhance the denitrification rate with HS^- (Cardoso et al., 2006; Wei et al., 2018).

To fully account for the process, the biomass production should be taken into account. Kleerebezem and Mendez (2002) used the 'energy dissipation' method developed by Heijnen (2002) and proposed the following stoichiometric equations (Eqs. 1.10, 1.11) for autotrophic denitrification with HS^- as electron donor.

$$3HS^- + 3.9NO_3^- + 0.2NH_4^+ + HCO_3^- + 1.7H^+ \rightarrow CH_{1.8}O_{0.5}N_{0.2} + 1.95N_2 + 3SO_4^{2-} + 2.3H_2O \quad (1.10)$$

$$14.5HS^- + 5NO_3^- + 0.2NH_4^+ + HCO_3^- + 20.3H^+ \rightarrow CH_{1.8}O_{0.5}N_{0.2} + 2.5N_2 + 14.5S^0 + 17.4H_2O \quad (1.11)$$

The extended reactions show that the N/S ratio for S^0 is equal to 0.35, while for SO_4^{2-} to 1.30. These N/S ratios derived from the combined anabolic and catabolic reactions were applied in this work.

The NO_3^- supply for HS^- removal was extensively studied at different reactor configurations, conditions, and feeding properties. Operating parameters such as dissolved oxygen, loading rate, pH, and sludge retention time (SRT) do not only influence the removal and activity but also result in long term succession of community structure and diversity (Cardoso et al., 2006; Lu et al., 2014).

Since this thesis was focused on the operational parameters like N/S ratio and temperature at specific pH range, these issues are elaborated in Chapter 1.3 (Factors influencing the simultaneous nitrate and sulfide removal).

1.2.2 Reactor design

Two main reactor configurations for a simultaneous NO_3^- and HS^- removal have been reported: packed bed and fluidized bed (Di Capua et al., 2015).

The packed bed reactors are used to enhance performance by keeping a high biomass concentration in the attached biofilm. Fernández et al. (2013) supplied NO_3^- to a biotrickling filter packed with polypropylene Pall rings to remove H_2S from biogas reaching 99 % removal efficiency at 120 g S/m^3·h. Pall rings and hollow plastic balls were also used by Deng et al. (2009) for H_2S removal from biogas originating from swine wastewater (using NO_3^- and NO_2^-) where the hollow plastic balls proved to be more efficient. In a biotrickling filter packed with open-pore polyurethane foam, the loads up to 130 g S/m^3·h could be treated with 99 % of H_2S removal (Fernández et al., 2014). Another packing material like sponge cubes was used in an anaerobic attached-growth bioreactor (AAGBR) for biogas desulfurization, completely removing H_2S at loads 0.1-1.8 g S/L·d and short HRT (2.67 h) converting 88.4 % of HS^- to S^0 (Li et al., 2009). The comparison studies on immobilization materials showed that an alginate matrix exhibits better performance than polyurethane foam or granular activated carbon (Ravichandra et al., 2009). The accumulation of S^0 in packed bed reactors causes clogging of packing material, decreasing its lifetime (Fortuny et al., 2008).

The second most commonly used configuration (fluidized bed reactor) is usually employed as up-flow anaerobic sludge blanket (UASB) reactor. The concept was developed in the 1970s and became the most popular high-rate reactor for biological wastewater treatment (Lettinga et al., 1980). The fluidized bed reactors can tolerate high loading rates up to 6.09 kg S/m^3·d and short hydraulic retention time down to 3.12 h in simultaneous NO_3^- and H_2S removal (Cai et al., 2007; Chen et al., 2008b). Regarding S^0 recovery, the fluidized bed reactors can handle the accumulation and retrieval of S^0 by

the removal of granular sludge excess. It has been reported that by shortening the height and consequently the volume of UASB reactor, the S^0 recovery rate can be improved from 7.4 to 78.8 %, while complete removal of acetate, HS^-, and NO_3^- was achieved (Huang et al., 2016).

The studies performed in fluidized bed reactors often report that the collected effluent samples are visually characterized by a yellow 'straw' color, suggesting unattached and freely dispersed elemental sulfur/polysulfides (Chen et al., 2008a; Krishnakumar et al., 2005).

1.2.3 Involved microorganisms and their properties

Chemolithotrophic SOB (also known as colorless sulfur-oxidizing bacteria) can derive energy from reduced sulfur compounds (H_2S, $S_2O_3^{2-}$, S^0). Most of these microorganisms are members of Proteobacteria phylum and were frequently demonstrated as a dominant group in laboratory-scale bioreactors performing the studied process (Chen et al., 2008a; Ontiveros-Valencia et al., 2014). The species belonging to *α*-, *β*-, *γ*-, and *ε*-Proteobacteria classes showed the ability to perform autotrophic denitrification (Shao et al., 2010).

The most studied microorganism carrying out autotrophic denitrification using reduced sulfur compounds is *Thiobacillus denitrificans* (*β*-Proteobacteria class) that is a strictly autotrophic and facultative anaerobe (Mohseni-Bandpi et al., 2013; Sublette and Sylvester, 1987). *Sulfurimonas denitrificans* (*ε*-Proteobacteria) is also often reported in autotrophic denitrification, its metabolism is versatile and it has been demonstrated as a major hydrothermal vent chemolithotroph (Shao et al., 2010). The HS^- oxidizers can oxidize it to S^0 and SO_4^{2-}.

The studies on different feeding conditions and working parameters showed that the microbial community composition usually changes within a Proteobacteria phylum. The *α*-, *β*-, and *γ*-Proteobacteria were found as most active denitrifiers in mature reactors (Tan et al., 2016; Viviantira et al., 2012). *β*-Proteobacteria and *ε*-Proteobacteria are especially abundant in S^0 regeneration (Wang et al., 2015). The denitrifying *β*-

Proteobacteria are considered the most efficient bacteria in breaking down aromatic compounds in various environments (Viviantira et al., 2012).

To enhance the S^0 regeneration Tan et al. (2016) used *Thiopseudomonas denitrificans* X2 for HS^-, NO_3^-, and acetate removal increasing S^0 recovery from 20-37 % to 45-70 %. Another method for enhancing the S^0 accumulation was reported by Borkenstein and Fischer (2006), where the mutant *Allochromatium vinosum* (*γ*-Proteobacteria) strain 21D was used. The studied strain contained an inactivated *dsrB* gene that makes the further oxidation of stored S^0 to SO_4^{2-} impossible.

Changes in salinity impact the microbial diversity. It has been reported that in simultaneous acetate, HS^- and NO_3^- removal at 0 g NaCl/L *Thauera* prevailed (21 %), while at high salinity (75 g/L) its presence diminished to 13 % and the *Halomonas* was predominant (40 %) (Liu et al., 2016). According to Zhou et al. (2017), the changes in up-flow velocity within 0.25-3.3 m/h does not impact the microbial structure, while at 7.7 m/h, the presence of *Thiothrix* (*γ*-Proteobacteria) increased to 10 %. The N/S ratio studies performed by increasing NO_3^- concentration (500 and 3500 mg/L) enriched *γ*-Proteobacteria (*Pseudomonas*) and *ε*-Proteobacteria (*Arcobacter* and *Sulfurospirillum*) while the share of SRB (*Desulfobulbus*) decreased (Chen et al., 2017). In another study focused on N/S ratio impact, *Thiobacillus denitrificans* and *Thiomicrospira denitrificans* were detected at low abundance (lower than 5 %) using fluorescent *in situ* hybridization (Dolejs et al., 2015).

Many of Proteobacteria are facultative; SOB, e.g., *Sulfurosirillum* has an ability to use NO_3^- and O_2 under microaerobic conditions (Kodama and Watanabe, 2004; Oyarzún et al., 2003). Studies using NO_3^- and O_2 for HS^- oxidation to S^0 under heterotrophic conditions showed that microbial community comprised SRB (*Desulfomicrobium* sp.), heterotrophic (*Pseudomonas aeruginosa* and *Sulfurospirillum* sp.), and autotrophic denitrifiers (*Sulfurovum* sp. and *Paracoccus denitrificans*), where at higher NO_3^- and HS^- load the SRB activity decreased (Chen et al., 2008a). The studies on the competition between organic and inorganic carbon in a culture enriched with *Thiomicrospira* sp. CVO show that under

the presence of acetic acid, the chemolithotrophic denitrification occurs and is followed by heterotrophic NO_3^- reduction after HS^- depletion (An et al., 2010).

Depending on the hydraulic properties of the reactor, stratification of Proteobacteria through the sludge bed can be obtained. In experiments conducted in the UASB reactor focused on microbial stratification in the sludge bed, *Azoarcus* (28.8 %) and *Thauera* (23.9 %) dominated in the lowest 10 cm while *Thiobacillus* was dominant both at 20 (65.4 %) and 30 cm (73.8 %). This indicates that the microbial community responded to the chemical gradient (Huang et al., 2017). Relatively fast development of *Thauera* and *Azoarcus* has been observed when non-efficient seeding sludge using quinole adapted within 6-weeks reaching 74 % abundance, while their presence in seeding sludge was minor (4 %) (Liu et al., 2006).

It has been reported that microorganisms oxidizing S^0 and other reduced sulfur compounds generating SO_4^{2-} can solubilize and convert the insoluble phosphorus compounds to a simple plant-available phosphorus compounds (Ullah et al., 2014). However, the presence of potassium phosphate made *Acidithiobacillus thiooxidans* (former *Thiobacillus thiooxidans*) cells more hydrophobic and less adhesive to S^0 (Takeuchi and Suzuki, 1997).

Besides colorless bacteria, phototrophic purple sulfur bacteria oxidize HS^- to S^0 and store it in cellular sulfur globules (Madigan et al., 1997).

1.2.4 Resource recovery

Facilitation of biological S^0 production has been suggested as the best way to break a sulfur cycle yielding an insoluble product (Kuenen and Robertson, 1992). The production of S^0 is more sustainable than the one of SO_4^{2-}, which can lead to corrosion or be reduced back to H_2S in low redox environments. This approach can be used for complete S removal (Reyes-Avila et al., 2004).

Under the already mentioned conditions, the production and storage of S^0 in bacterial inclusion bodies (internal or external) can occur (Dahl and Prange, 2006; Shively, 1974).

Winogradsky gave the first descriptions of these phenomena in 1887 where the build-up and disappearance of sulfur inclusion bodies by *Beggiatoa* was described. Microbial S^0 globules can reach up to 1 µm and are deposited as cell oxidize and grow in H_2S presence. The inclusion bodies are often surrounded by a protein envelope to be purely structural in function (Berg et al., 2014). S^0 globules can be deposited both extra- and intracellularly. *Thermothrix thioparus*, deposits sulfur globules extracellularly (Caldwell et al., 1976), while *Thermotrix azorensis* forms globules intracellularly in the presence of $S_2O_3^{2-}$ and pH>7.0 (Odintsova et al., 1996). After depletion of reduced sulfur compounds, SOB oxidize the accumulated elemental sulfur to SO_4^{2-}, deriving energy from this process (Schedel and Trüper, 1980). However, the mechanism involved in the formation and oxidation of sulfur globules remains unknown (Holkenbrink et al., 2011).

The biologically produced S^0 has to be recovered; usually, physical and physicochemical methods like sedimentation, centrifugation, membrane separation, extraction, and coagulation are used for this purpose (Cai et al., 2017). The S^0 incorporated into inclusion bodies is characterized by a lower density and different crystalline structure than the orthorhombic sulfur, increasing the buoyant density (Berg et al., 2014; Mas and van Gemerden, 1987). The main difference between chemically and biologically obtained S^0 is related to water interaction: the chemical S^0 is hydrophobic, while the biological S^0 is hydrophilic (Holkenbrink et al., 2011; Janssen et al., 2009). These characteristics facilitate the use of biological S^0 as a soil fertilizer or fungicide (Tan et al., 2016).

Kleerebezem and Mendez (2002) suggested that the capacity of partial HS^- oxidation is species specific and that the biomass capacity for S^0 retention is limited. Different S^0 recovery yields are reported in the literature. Values like 50, 71, 79, and 88 % are reported by Cardoso et al. (2008), Huang et al. (2016), Krishnakumar and Manilal (1999) and Li et al. (2009a), respectively.

The biologically produced S^0 can also be further used as an alternative electron donor for denitrification due to its hydrophilicity and high specific surface area (Di Capua et al., 2016; Wang et al., 2011). Particulate S^0 were colonized by sulfur oxidizers, reaching

maximum NO_3^- removal of 90 % at neutral pH (Moon et al., 2004). It has been reported that the oxidation rate of S^0 to SO_4^{2-} is 15 % faster than the one of HS^- to S^0 (Jiang et al., 2009).

1.2.4.1 Kinetics

The production of S^0 is not the only possibility for resource recovery from H_2S oxidation. For example, other reduced sulfur compounds, e.g., $S_2O_3^{2-}$ obtained by H_2S oxidation, can serve as a further electron donor in autotrophic or heterotrophic denitrification. Studies comparing different sulfur reduced compounds reported that the highest denitrification rate can be obtained with $S_2O_3^{2-}$ and follows the order: $S_2O_3^{2-}>S^{2-}>>S^0$ (Cardoso et al., 2006). Another, the more recent study reports the following order: $S_2O_3^{2-}$>biogenic-S^0>chemically-synthetized S^0 powder>S^0 lentils (Di Capua et al., 2016). According to Trouve et al. (1998), the denitrification rate of S^0 is lower than with FeS and FeS_2. Due to the high denitrification rate of $S_2O_3^{2-}$ it has been used in autotrophic denitrification of micro-polluted water (Zhou et al., 2016).

The electron acceptor source has also been reported as important for desulfurization rate; the utilization rate of NO_3^- was reported as 2.5 times higher than NO_2^- in $S_2O_3^{2-}$ presence (Campos et al., 2008).

The kinetic parameters of autotrophic denitrification with HS^- were studied. The maximum specific growth rate (μ_{max}) was reported in the wide range from 0.45 to 4.25 d^{-1}, depending on the experimental conditions and estimation method (An et al., 2010; Wang et al., 2010; G. Xu et al., 2016). Similarly, for a half-saturation constant of NO_3^- and HS^-, it ranged from 0.01 to 110 mg NO_3^--N/L and from 1.5 to 58 mg S^{2-}/L.

1.2.4.2 N_2O emissions

N_2O was detected during H_2S-driven autotrophic denitrification studies. The N_2O emissions can cause a greenhouse effect that is more potent than CO_2. Its presence increases when the N/S ratio increases (Yang et al., 2016). Thus, the conditions facilitating the S^0 recovery through denitrification may decrease the N_2O emissions. It has been reported that N_2O reductase enzyme can be inhibited by the S^{2-} concentration above 200

mg/L (Fajardo et al., 2014). However, in heterotrophic denitrification, the N_2O emissions are higher than in autotrophic reaching up to 14.6 % of nitrogen load (Kampschreur et al., 2009). The studies on S^0-driven mixotrophic denitrification reported that longer sludge retention time (SRT) and higher influent COD/N ratio reduces N_2O emissions (Liu et al., 2017). The N_2O emissions during heterotrophic denitrification are also dependent on the pH (Pan et al., 2013).

1.3 Factors influencing the simultaneous nitrate and sulfide removal

1.3.1 N/S molar ratio

The N/S molar ratio is a critical factor determining the products formation in HS^- oxidation. Redox equations refer to the N/S=0.40 for S^0 production and 1.60 for SO_4^{2-}, while in case of a reaction including anabolism and catabolism – 0.35 for S^0 and 1.30 for SO_4^{2-}. Several studies focused on N/S ratio impact; usually, batch experiments or separate continuous experiments were performed. It has been reported that at the N/S ratio higher than 0.80 (e.g., 1.10 and 1.70), HS^- is oxidized to SO_4^{2-}, while at lower than 0.80, HS^- was oxidized to S^0 accumulating in sludge (Dolejs et al., 2015). In the study conducted in a sequence mode, at N/S ratio 1.0 the 26.5 % influent S was converted to S^0 (250-300 mg S^{2-}/L) (Xu et al., 2018). At similar N/S ratio (1.0), An et al. (2010) reported that HS^- was completely oxidized to SO_4^{2-}, while at ratio lower than stoichiometric (0.32) only 4.4 % of HS^- was converted to SO_4^{2-}. Doğan et al. (2012) reported that at N/S above 1.48 (NO_2^- as electron acceptor), SO_4^{2-} is the main product, while below, the mixture of SO_4^{2-} and S^0 was obtained. The complete oxidation of HS^- to SO_4^{2-} was observed at ratios equal or exceeding stoichiometric requirements (Garcia de Lomas et al., 2006).

In addition to the HS^- oxidation level, the N/S ratio affects the H_2S removal efficiency. It has been reported that when the N/S ratio increased from 0.28 to 1.43 (biotrickling filter), the removal efficiency of H_2S was raised from 66 to 100 %, while the NO_3^- removal decreased from 100 to 70 % (Li et al., 2016).

In this work, the studies on different N/S ratios applied in continuous flow EGSB reactor were performed showing a possible release of the earlier accumulated S^0. The detailed description is given in Article IV.

Besides the N/S ratio, in heterotrophic denitrification the CH_3COO^-/NO_3^- ratio was reported as an important parameter for the H_2S oxidation to either S^0 or SO_4^{2-} (Cardoso et al., 2008).

The studies on S^0 recovery reported different levels of S^0 recovery at various N/S ratios. It should be mentioned that the analytical methodologies differ between studies and the balances for S^0 calculation are based on more or less detailed effluent sulfur speciation. Huang et al. (2017) reported 77.9 % of S^0 recovery when the ratio between acetate/NO_3^-/HS^- was set to 1.9/1.6/0.7 kg/m^3·d. The recovery of 68 ± 16 % was reported at N/S=0.46 by Fernández et al. (2013).

The studies coupling the denitrifying ammonium oxidation (DEAMOX) with autotrophic denitrification and ANAMMOX were performed, suggesting the S^0 accumulation at N/S=1.0 molar ratio according to the stoichiometry proposed by Liu et al. (2015):

$$S^{2-} + NO_3^- + H_2O \rightarrow S^0 + NO_2^- + 2OH^- \quad (1.12)$$

Alternatively, novel processes assuming simultaneous nitrogen and sulfur removal for S^0 recovery combining, ANAMMOX and autotrophic desulfurization-denitrification have been described by Guo et al. (2016):

$$2NH_4^+ + 2.64NO_2^- + 1.3S^{2-} + 0.132HCO_3^- + 3.38H^+ \rightarrow 2.3N_2 + 1.3S^0 + 0.132CH_2O_{0.5}N_{0.15} + 5.62H_2O \quad (1.13)$$

1.3.2 Temperature

The optimal temperature for denitrification was reported within 20-30 °C (Grady Jr et al., 2011). Biological processes are very sensitive to temperature and their transitions. In anaerobic digestion process, it is therefore recommended to limit the temperature variation to less than 1 °C (Grady Jr et al., 2011). Temperature strongly influences

the rates of conversion, activity of microbial groups, and the structure of microbial consortia (Bialek et al., 2012; Rebac et al., 1995; Sumino et al., 2012). Almost all full-scale biological treatment systems operate under mesophilic or thermophilic conditions.

The temperature requirements are variable depending on the microorganism. The optimal temperature of *Thiobacillus denitrificans* growth for denitrification was reported as 32.8 °C (Kelly and Wood, 2000). The other most commonly reported autotrophic denitrifier *Sulfurimonas denitrificans* exhibits the optimum growth at 22 °C (Takai et al., 2006). Microorganisms conducting autotrophic denitrification are mostly mesophilic and thermophilic (Syed et al., 2006).

The optimum temperature for autotrophic denitrification is 33-35 °C (Oh et al., 2000). The studies on low temperatures related to the simultaneous NO_3^- and HS^- removal are rarely performed. Temperature studies in batch cultures in the range of 15-30 °C were performed by Y. Xu et al. (2016) where complete NO_3^- removal was obtained. A few studies, dealing with other reduced sulfur compounds like $S_2O_3^{2-}$ and S^0 have been found as well. Batch experiments on denitrification under the $S_2O_3^{2-}$ presence comparing different temperatures revealed that a few *Thiobacillus denitrificans* strains are capable of denitrifying at 10 and 5 °C (Trouve et al., 1998). It has been reported that a complete $S_2O_3^{2-}$-driven denitrification in 3-20 °C temperature range can be performed. On the other hand, at low temperatures, the bed expansion, and cell detachment were observed, not affecting the denitrification performance (Di Capua et al., 2017). In S^0-driven autotrophic denitrification, the temperature lower than 10 °C led to the decrease in denitrification efficiency to 60-70 % (Sahinkaya et al., 2014). In this work, the temperature studies in EGSB reactor were performed in the range of 25-10 °C and are presented later in this thesis.

Temperature is not only related to appropriate microbial growth conditions but also to the economic feasibility. Substantial energy input is required to heat a bioreactor to the treatment temperature. It has been reported that heating of wastewater prior to treatment, can consume up to 30 % of the energy produced in the anaerobic digestion

(Scully et al., 2006). The operation at low temperatures (or temperatures equal to the influent temperature) can reduce the heating requirements.

Temperature has an impact on the physical parameters of water. As the temperature drops, the water density, and viscosity increases, limiting the substrate diffusion into the biofilm (Sumino et al., 2012) (Figure 1.4). Low temperatures affect the cellular processes like cell membrane fluidity, mass transfer, and protein folding (D'Amico et al., 2006). Thus, the proteins structure and cell membrane characteristic substantially differ at low temperatures. The membranes fluidity can be improved at low temperatures through changes in the membrane lipid composition and synthesis of 'cold-shock' proteins to sustain a regular protein synthesis (McKeown et al., 2012).

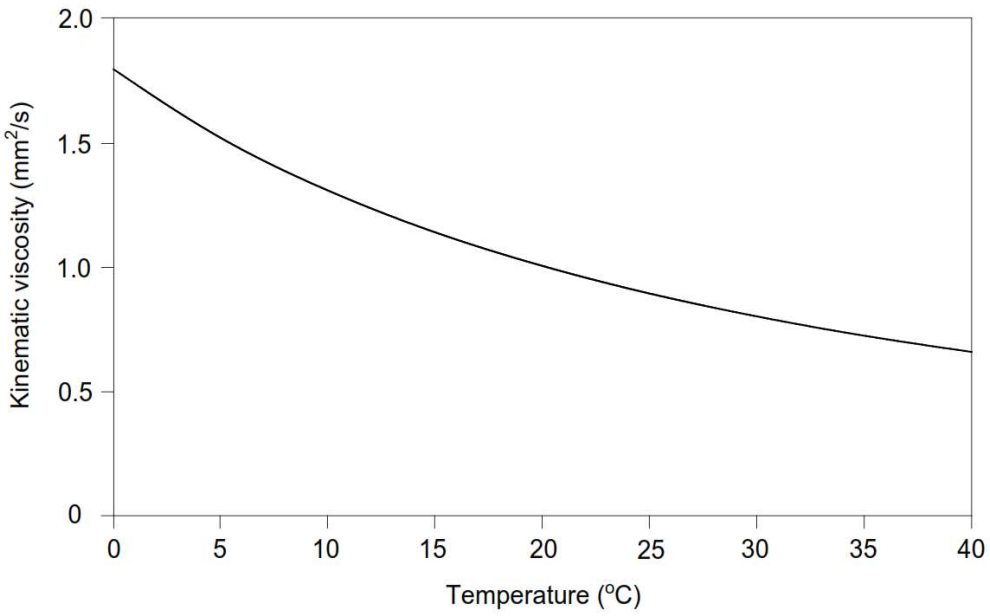

Figure 1.4: Kinematic viscosity of water in temperature (adapted from Kestin et al., 1978).

The low temperatures are always related to low biomass regeneration. It has been reported that at temperatures <15 °C the hydraulic washouts of psychroactive sludge can occur (Lettinga et al., 1999; Yamamoto-Ikemoto et al., 2000). The hydrolysis rate of entrapped organics in UASB reactor is also affected by temperature, decreasing from 58 % at 25 °C to 33 % at 10 °C, simultaneously reducing the methanogenic activity

and leading to granules autolysis (Uemura and Harada, 2000). Earlier granular sludge bed studies report that the granule diameter decreases under the psychrophilic conditions (10-12 ^{o}C) and it was argued as being related to the erosion phenomenon (Rebac et al., 1995). A more recent study reported that the settling velocity of granule increases around 1.7-1.8 times from 5 and 40 ^{o}C (Winkler et al., 2012). These observations may explain why the start-up of granular sludge reactors at low temperatures is long and troublesome. To overcome this limitation zeolite was used as a carrier material for enhancing the start-up process of autotrophic denitrification, shortening it by 50 %; the process was carried out at an uncontrolled temperature (Montalvo et al., 2016).

However, certain successful operations at low temperatures have been reported. The continuous operation of the EGSB reactor led to the efficient treatment of wastewater at 10 ^{o}C (Syutsubo et al., 2008). Some studies indicate that the anaerobic degradation can be possible even at 2 and 1 ^{o}C at reduced conversion rate (Scully et al., 2006; Zou et al., 2016).

The acclimation of mesophilic biomass to low temperatures may be achieved through successive changes in the community structure, showing a selective pressure of psychroactive microorganisms (McKeown et al., 2012). Psychrophiles can proliferate at low temperatures and higher water viscosity, overcoming the reduced enzyme activity, decreased membrane fluidity, altered nutrient and waste transport, decreased rates of transcription, translation, cell division, protein denaturation, inappropriate protein folding, and intracellular ice formation (D'Amico et al., 2006). The successive changes in community structure are slow; thus, the changes in temperature in engineered systems using granular sludge without carrier material should be imposed slowly.

1.3.3 pH

One of the most important factors considered during the design and operation of biological treatment reactors is pH. The biological processes are highly vulnerable to pH fluctuations affecting the reactor performance and even causing their failure; pH affects

the stability of enzymes, state of substrates, transport of substrate through the cell membrane, ATP synthesis, and other biological processes (J. Xu et al., 2016).

During the denitrification process, the pH value increases in systems without a good buffer capacity. Alkalinity savings can be obtained by using NO_2^- (Chung et al., 2014). HS^- as the electron donor source reduces the alkalinity requirements in comparison to S^0 where the protons need to be neutralized, e.g., using limestone (Yang et al., 2017). To ensure proper pH and an increase in alkalinity, the studies on effect of eggshell addition (consisting almost entirely of $CaCO_3$) to autotrophic denitrification with HS^- were reported (Y. Xu et al., 2016). Eggshells could maintain neutral conditions in a pH range of 7.05-7.74, revealing better properties than either the oyster shell or limestone. The combination of autotrophic and heterotrophic denitrification that produces CO_2 can positively influence the pH stability (Park and Yoo, 2009).

The optimum pH range for autotrophic denitrification was reported to be around 6.5-7.5 (Oh et al., 2000). Microorganisms involved in autotrophic denitrification like *Thiobacillus denitrificans* can grow in a wide pH range (4.0-9.5) with an optimum at pH between 6-7. However, even an alkaliphilic group performing autotrophic denitrification was found within *γ*-Proteobacteria (Shao et al., 2010; J. Xu et al., 2016). Other studies state that near-neutral pH (7.5-8.0) and a weak base (8.5-9.0) are efficient for desulfurization under NO_3^- presence (Krishnakumar and Manilal, 1999; J. Xu et al., 2016). Bacterial communities are more sensitive to acidic pH in comparison to alkaline pH. Mahmood et al. (2008) reported that the NO_3^- and HS^- removal dropped at acidic pH=3, while the highest performance was obtained at pH=8. Studies with O_2 as the electron acceptor for H_2S reveal the same phenomena.

The studies on autotrophic denitrification with HS^- shows a higher sensitivity to pH shocks than to the substrate shocks while the recovery from pH shocks was reported as faster than from the substrate shocks (Cai et al., 2010).

References

Allen, L.A., 1949. The effect of nitro-compounds and some other substances on production of hydrogen sulphide by sulphate-reducing bacteria in sewage. Proc. Soc. Appl. Bacteriol. 12, 26–38.

An, S., Tang, K., Nemati, M., 2010. Simultaneous biodesulphurization and denitrification using an oil reservoir microbial culture: Effects of sulphide loading rate and sulphide to nitrate loading ratio. Water Res. 44, 1531–1541.

Atlas, R.M., Bartha, R., 1981. Microbial ecology: fundamentals and applications. Addison-Wesley Publishing Company.

Auguet, O., Pijuan, M., Borrego, C.M., Gutierrez, O., 2016. Control of sulfide and methane production in anaerobic sewer systems by means of Downstream Nitrite Dosage. Sci. Total Environ. 550, 1116–1125.

Bayrakdar, A., Tilahun, E., Calli, B., 2016. Biogas desulfurization using autotrophic denitrification process. Appl. Microbiol. Biotechnol. 100, 939–948.

Bentzen, G., Smit, A.T., Bennett, D., Webster, N.J., Reinholt, F., Sletholt, E., Hobsont, J., 1995. Controlled dosing of nitrate for prevention of H_2S in a sewer network and the effects on the subsequent treatment processes. Water Sci. Technol. 31, 293–302.

Berg, J.S., Schwedt, A., Kreutzmann, A.-C., Kuypers, M.M.M., Milucka, J., 2014. Polysulfides as intermediates in the oxidation of sulfide to sulfate by Beggiatoa spp. Appl. Environ. Microbiol. 80, 629–636.

Bialek, K., Kumar, A., Mahony, T., Lens, P.N.L., O'Flaherty, V., 2012. Microbial community structure and dynamics in anaerobic fluidized-bed and granular sludge-bed reactors: Influence of operational temperature and reactor configuration. Microb. Biotechnol. 5, 738–752.

Borkenstein, C.G., Fischer, U., 2006. Sulfide removal and elemental sulfur recycling from a sulfide-polluted medium by Allochromatium vinosum strain 21D. Int. Microbiol. 9, 253–258.

Cai, J., Zheng, P., Mahmood, Q., 2010. Influence of transient pH and substrate shocks on simultaneous anaerobic sulfide and nitrate removal. J. Hazard. Mater. 174, 162–166.

Cai, J., Zheng, P., Mahmood, Q., 2008. Effect of sulfide to nitrate ratios on the simultaneous anaerobic sulfide and nitrate removal. Bioresour. Technol. 99, 5520–5527.

Cai, J., Zheng, P., Mahmood, Q., Islam, E., Hu, B., Wu, D., 2007. Effects of loading rate and hydraulic residence time on anoxic sulfide biooxidation. J. Zhejiang Univ. - Sci. A 8, 1149–1156.

Cai, J., Zheng, P., Mahmood, Q., Zhang, J., 2017. Elemental sulfur recovery of biological sulfide removal process from wastewater: A review. Crit. Rev. Environ. Sci. Technol. 47, 2079–2099.

Caldwell, D.E., Caldwell, S.J., Laycock, J.P., 1976. Thermothrix thioparus gen. et sp. nov. a facultatively anaerobic facultative chemolithotroph living at neutral pH and high temperature. Can. J. Microbiol. 22, 1509–1517.

Campos, J.L., Carvalho, S., Portela, R., Mosquera-Corral, A., Méndez, R., 2008. Kinetics of denitrification using sulphur compounds: effects of S/N ratio, endogenous and exogenous compounds. Bioresour. Technol. 99, 1293–1299.

Cardoso, R.B., Sierra-Álvarez, R., Rowlette, P., Flores, E.R., Gómez, J., Field, J.A., 2006. Sulfide oxidation under chemolithoautotrophic denitrifying conditions. Biotechnol. Bioeng. 95, 1148–1157.

Cardoso, R.B., Texier, A.C., Sierra-Álvarez, R., Field, J.A., Razo-Flores, E., Gómez, J., 2008. Simultaneous sulfide and acetate oxidation under denitrifying conditions using an inverse fluidized bed reactor. J. Chem. Technol. Biotechnol. 83, 1197–1203.

Carroll, J.J., Mather, A.E., 1989. The solubility of hydrogen sulphide in water from 0 to 90°C and pressures to 1 MPa. Geochim. Cosmochim. Acta 53, 1163–1170.

Chen, C., Ren, N., Wang, A., Yu, Z., Lee, D.J., 2008a. Microbial community of granules in expanded granular sludge bed reactor for simultaneous biological removal of sulfate, nitrate and lactate. Appl. Microbiol. Biotechnol. 79, 1071–1077.

Chen, C., Wang, A., Ren, N., Kan, H., Lee, D.J., 2008b. Biological breakdown of denitrifying sulfide removal process in high-rate expanded granular bed reactor. Appl. Microbiol. Biotechnol. 81, 765–770.

Chen, C., Wang, A., Ren, N., Zhao, Q., Liu, L., Adav, S.S., Lee, D.J., Chang, J.S., 2010. Enhancing denitrifying sulfide removal with functional strains under micro-aerobic condition. Process Biochem. 45, 1007–1010.

Chen, C., Xu, X.-J., Xie, P., Yuan, Y., Zhou, X., Wang, A.-J., Lee, D.-J., Ren, N.-Q., 2017. Pyrosequencing reveals microbial community dynamics in integrated simultaneous desulfurization and denitrification process at different influent nitrate concentrations. Chemosphere 171, 294–301.

Chen, F., Xia, Q., Ju, L.K., 2006. Competition between oxygen and nitrate respirations in continuous culture of Pseudomonas aeruginosa performing aerobic denitrification. Biotechnol. Bioeng. 93, 1069–1078.

Chen, J., Chen, R., Hong, M., 2015. Influence of pH on hexavalent chromium reduction by Fe(II) and sulfide compounds. Water Sci. Technol. 72, 22–28.

Chung, J., Amin, K., Kim, S., Yoon, S., Kwon, K., Bae, W., 2014. Autotrophic denitrification of nitrate and nitrite using thiosulfate as an electron donor. Water Res. 58, 169–178.

Cline, C., Hoksberg, A., Abry, R., Janssen, A., 2003. Biological process for H_2S removal from gas streams: The Shell-Paques/THIOPAQ^{TM} gas desulfurization process. Proc. Laurance Reid Gas Cond. Conf. 1–18.

Cohen, Y., Jorgensen, B.B., Revsbech, N.P., Poplawski, R., 1986. Adaptation to hydrogen sulfide of oxygenic and anoxygenic photosynthesis among cyanobacteria. Appl. Environ. Microbiol. 51, 398–407.

Colomer, F.L., Morató, H.E., Iglesias, E.M., 2012. Estimation of hydrogen sulfide emission rates at several wastewater treatment plants through experimental concentration measurements and dispersion modeling. J. Air Waste Manag. Assoc. 62, 758–766.

Costa, J.M., Rodriguez, R.P., Sancinetti, G.P., 2017. Removal sulfate and metals Fe^{+2}, Cu^{+2}, and Zn^{+2} from acid mine drainage in an anaerobic sequential batch reactor. J. Environ. Chem. Eng. 5, 1985–1989.

D'Amico, S., Collins, T., Marx, J.-C., Feller, G., Gerday, C., 2006. Psychrophilic microorganisms: challenges for life. EMBO Rep. 7, 385–389.

Dacey, J.W.H., Wakeham, S.G., 1986. Oceanic Dimethylsulfide: Production during Zooplankton Grazing on Phytoplankton. Science (80-.). 233, 1314–1316.

Dahl, C., Prange, A., 2006. Bacterial sulfur globules: occurrence, structure and metabolism, in: Inclusions in Prokaryotes. Springer, pp. 21–51.

De Gusseme, B., De Schryver, P., De Cooman, M., Verbeken, K., Boeckx, P., Verstraete, W., Boon, N., 2009. Nitrate-reducing, sulfide-oxidizing bacteria as microbial oxidants for rapid biological sulfide removal. FEMS Microbiol. Ecol. 67, 151–161.

Deng, L., Chen, H., Chen, Z., Liu, Y., Pu, X., Song, L., 2009. Process of simultaneous hydrogen sulfide removal from biogas and nitrogen removal from swine wastewater. Bioresour. Technol. 100, 5600–5608.

Di Capua, F., Ahoranta, S.H., Papirio, S., Lens, P.N.L., Esposito, G., 2016. Impacts of sulfur source and temperature on sulfur-driven denitrification by pure and mixed cultures of Thiobacillus. Process Biochem. 51, 1576–1584.

Di Capua, F., Milone, I., Lakaniemi, A.-M., Lens, P.N.L., Esposito, G., 2017. High-rate autotrophic denitrification in a fluidized-bed reactor at psychrophilic temperatures. Chem. Eng. J. 313, 591–598.

Di Capua, F., Papirio, S., Lens, P.N.L., Esposito, G., 2015. Chemolithotrophic denitrification in biofilm reactors. Chem. Eng. J. 280, 643–657.

Díaz, I., Fdz-Polanco, M., 2012. Robustness of the microaerobic removal of hydrogen sulfide from biogas. Water Sci. Technol. 65, 1368–1374.

Díaz, I., Lopes, A.C., Perez, S.I., Fdz-Polanco, M., 2010. Performance evaluation of oxygen, air and nitrate for the microaerobic removal of hydrogen sulphide in biogas from sludge digestion. Bioresour. Technol. 101, 7724–7730.

Díaz, I., Perez, S.I., Ferrero, E.M., Fdz-Polanco, M., 2011. Effect of oxygen dosing point and mixing on the microaerobic removal of hydrogen sulphide in sludge digesters. Bioresour. Technol. 102, 3768–3775.

Doğan, E.C., Türker, M., Dağaçsan, L., Arslan, A., 2012. Simultaneous sulfide and nitrite removal from industrial wastewaters under denitrifying conditions. Biotechnol. Bioprocess Eng. 17, 661–668.

Dolejs, P., Paclík, L., Maca, J., Pokorna, D., Zabranska, J., Bartacek, J., 2015. Effect of S/N ratio on sulfide removal by autotrophic denitrification. Appl. Microbiol. Biotechnol. 99, 2383–2392.

Fajardo, C., Mora, M., Fernández, I., Mosquera-Corral, A., Campos, J.L., Méndez, R., 2014. Cross effect of temperature, pH and free ammonia on autotrophic denitrification process with sulphide as electron donor. Chemosphere 97, 10–15.

Fales, A.L., 1929. Treatment of industrial wastes from paper mills and tannery on Neponset river. Ind. Eng. Chem. 21, 216–221.

Fernández, M., Ramírez, M., Gómez, J.M., Cantero, D., 2014. Biogas biodesulfurization in an anoxic biotrickling filter packed with open-pore polyurethane foam. J. Hazard. Mater. 264, 529–535.

Fernández, M., Ramírez, M., Pérez, R.M., Gómez, J.M., Cantero, D., 2013. Hydrogen sulphide removal from biogas by an anoxic biotrickling filter packed with Pall rings. Chem. Eng. J. 225, 456–463.

Fortuny, M., Baeza, J.A., Gamisans, X., Casas, C., Lafuente, J., Deshusses, M.A., Gabriel, D., 2008. Biological sweetening of energy gases mimics in biotrickling filters. Chemosphere 71, 10–17.

Fortuny, M., Gamisans, X., Deshusses, M.A., Lafuente, J., Casas, C., Gabriel, D., 2011. Operational aspects of the desulfurization process of energy gases mimics in biotrickling filters. Water Res. 45, 5665–5674.

Garcia de Lomas, J., Corzo, A., Gonzalez, J.M., Andrades, J.A., Iglesias, E., Montero, M.J., 2006. Nitrate promotes biological oxidation of sulfide in wastewaters: Experiment at plant-scale. Biotechnol. Bioeng. 93, 801–811.

Gayh, U., Stooß, A., Behrendt, J., Otterpohl, R., 2010. Desulphurisation of biogas analysis, evaluation and optimisation, in: Third International Symposium on Energy from Biomass and Waste, Venice, Italy. pp. 8–10.

Grady Jr, C.P.L., Daigger, G.T., Love, N.G., Filipe, C.D.M., 2011. Biological wastewater treatment. CRC press.

Guo, Q., Hu, H.Y., Shi, Z.J., Yang, C.C., Li, P., Huang, M., Ni, W.M., Shi, M.L., Jin, R.C., 2016. Towards simultaneously removing nitrogen and sulfur by a novel process: Anammox and autotrophic desulfurization-denitrification (AADD). Chem. Eng. J. 297, 207–216.

Hao, O.J., Chen, J.M., Huang, L., Buglass, R.L., 1996. Sulfate-reducing bacteria. Crit. Rev. Environ. Sci. Technol. 26, 155–187.

Heijnen, J.J., 2002. Bioenergetics of microbial growth, in: Encyclopedia of Bioprocess Technology. Wiley Online Library, pp. 267-291.

Hendrickson, R.G., Chang, A., Hamilton, R.J., 2004. Co-worker fatalities from hydrogen sulfide. Am. J. Ind. Med. 45, 346–350.

Holkenbrink, C., Barbas, S.O., Mellerup, A., Otaki, H., Frigaard, N.-U., 2011. Sulfur globule oxidation in green sulfur bacteria is dependent on the dissimilatory sulfite reductase system. Microbiology 157, 1229–1239.

Huang, C., Li, Z., Chen, F., Liu, Q., Zhao, Y., Gao, L., Chen, C., Zhou, J., Wang, A., 2016. Efficient regulation of elemental sulfur recovery through optimizing working height of upflow anaerobic sludge blanket reactor during denitrifying sulfide removal process. Bioresour. Technol. 200, 1019–1023.

Huang, C., Liu, Q., Chen, C., Chen, F., Zhao, Y.-K., Gao, L.-F., Liu, W.-Z., Zhou, J.-Z., Li, Z.-L., Wang, A.-J., 2017. Elemental sulfur recovery and spatial distribution of functional bacteria and expressed genes under different carbon/nitrate/sulfide loadings in up-flow anaerobic sludge blanket reactors. J. Hazard. Mater. 324, 48–53.

Huber, B., Herzog, B., Drewes, J.E., Koch, K., Müller, E., 2016. Characterization of sulfur oxidizing bacteria related to biogenic sulfuric acid corrosion in sludge digesters. BMC Microbiol. 16, 153.

Hubert, C., Voordouw, G., Mayer, B., 2009. Elucidating microbial processes in nitrate- and sulfate-reducing systems using sulfur and oxygen isotope ratios: The example of oil reservoir souring control. Geochim. Cosmochim. Acta 73, 3864–3879.

Ibañez, J.G., Hernandez-Esparza, M., Doria-Serrano, C., Fregoso-Infante, A., Singh, M.M., 2010. Environmental chemistry: fundamentals. Springer Science & Business Media.

Janssen, A.J.H., Lens, P.N.L., Stams, A.J.M., Plugge, C.M., Sorokin, D.Y., Muyzer, G., Dijkman, H., Van Zessen, E., Luimes, P., Buisman, C.J.N., 2009. Application of bacteria involved in the biological sulfur cycle for paper mill effluent purification. Sci. Total Environ. 407, 1333–1343.

Janssen, A.J.H., Meijer, S., Bontsema, J., Lettinga, G., 1998. Application of the redox potential for controlling a sulfide oxidizing bioreactor. Biotechnol. Bioeng. 60, 147–155.

Jiang, G., Sharma, K.R., Guisasola, A., Keller, J., Yuan, Z., 2009. Sulfur transformation in rising main sewers receiving nitrate dosage. Water Res. 43, 4430–4440.

Jin, R.-C., Yang, G.-F., Zhang, Q.-Q., Ma, C., Yu, J.-J., Xing, B.-S., 2013. The effect of sulfide inhibition on the ANAMMOX process. Water Res. 47, 1459–1469.

Joye, S.B., Hollibaugh, J.T., 1995. Influence of sulfide inhibition of nitrification on nitrogen regeneration in sediments. Science (80-.). 270, 623–625.

Kampschreur, M.J., Temmink, H., Kleerebezem, R., Jetten, M.S., van Loosdrecht, M.C., 2009. Nitrous oxide emission during wastewater treatment. Water Res. 43, 4093–4103.

Kelly, D.P., Wood, A.P., 2000. Confirmation of Thiobacillus denitrificans as a species of the genus Thiobacillus, in the β-subclass of the Proteobacteria, with strain NCIMB 9548 as the type strain. Int. J. Syst. Evol. Microbiol. 50, 547–550.

Keränen, A., Leiviskä, T., Hormi, O., Tanskanen, J., 2015. Removal of nitrate by modified pine sawdust: Effects of temperature and co-existing anions. J. Environ. Manage. 147, 46–54.

Kestin, J., Sokolov, M., Wakeham, W.A., 1978. Viscosity of liquid water in the range −8°C to 150°C. J. Phys. Chem. Ref. Data 7, 941–948.

Kleerebezem, R., Mendez, R., 2002. Autotrophic denitrification for combined hydrogen sulfide removal from biogas and post-denitrification. Water Sci. Technol. 45, 349–356.

Knobeloch, L., Salna, B., Hogan, A., Postle, J., Anderson, H., 2000. Blue babies and nitrate-contaminated well water. Environ. Health Perspect. 108, 675–678.

Knowles, R., 1982. Denitrification. Microbiol. Rev. 46, 43–70.

Kodama, Y., Watanabe, K., 2004. Sulfuricurvum kujiense gen. nov., sp. nov., a facultatively anaerobic, chemolithoautotrophic, sulfur-oxidizing bacterium isolated from an underground crude-oil storage cavity. Int. J. Syst. Evol. Microbiol. 54, 2297–2300.

Korner, H., Zumft, W.G., 1989. Expression of denitrification enzymes in response to the dissolved oxygen levels and respiratory substrate in continuous culture of Pseudomonas stutzeri. Appl. Environ. Microbiol. 55, 1670–1676.

Krayzelova, L., Bartacek, J., Kolesarova, N., Jenicek, P., 2014. Microaeration for hydrogen sulfide removal in UASB reactor. Bioresour. Technol. 172, 297–302.

Krishnakumar, B., Majumdar, S., Manilal, V.B., Haridas, A., 2005. Treatment of sulphide containing wastewater with sulphur recovery in a novel reverse fluidized loop reactor (RFLR). Water Res. 39, 639–647.

Krishnakumar, B., Manilal, V.B., 1999. Bacterial oxidation of sulphide under denitrifying conditions. Biotechnol. Lett. 21, 437–440.

Kuenen, J.G., Robertson, L.A., 1992. The use of natural bacterial populations for the treatment of sulphur-containing wastewater. Biodegradation 3, 239–254.

Lebrero, R., Toledo-Cervantes, A., Muñoz, R., del Nery, V., Foresti, E., 2016. Biogas upgrading from vinasse digesters: a comparison between an anoxic biotrickling filter and an algal-bacterial photobioreactor. J. Chem. Technol. Biotechnol. 91, 2488–2495.

Lee, C.-Y., Ho, K.-L., Lee, D.-J., Su, A., Chang, J.-S., 2012. Electricity harvest from nitrate/sulfide-containing wastewaters using microbial fuel cell with autotrophic denitrifier, Pseudomonas sp. C27. Int. J. Hydrogen Energy 37, 15827–15832.

Lettinga, G., Rebac, S., Parshina, S., Nozhevnikova, A., van Lier, J.B., Stams, A.J., 1999. High-rate anaerobic treatment of wastewater at low temperatures. Appl. Environ. Microbiol. 65, 1696–1702.

Lettinga, G., Van Velsen, A.F.M., Hobma, S.W., De Zeeuw, W., Klapwijk, A., 1980. Use of the upflow sludge blanket (USB) reactor concept for biological wastewater treatment, especially for anaerobic treatment. Biotechnol. Bioeng. 22, 699–734.

Li, W., Zhao, Q., Liu, H., 2009. Sulfide removal by simultaneous autotrophic and heterotrophic desulfurization-denitrification process. J. Hazard. Mater. 162, 848–853.

Li, X., Jiang, X., Zhou, Q., Jiang, W., 2016. Effect of S/N ratio on the removal of hydrogen sulfide from biogas in anoxic bioreactors. Appl. Biochem. Biotechnol. 180, 930–944.

Liu, B., Zhang, F., Feng, X., Liu, Y., Yan, X., Zhang, X., Wang, L., Zhao, L., 2006. Thauera and Azoarcus as functionally important genera in a denitrifying quinoline-removal bioreactor as revealed by microbial community structure comparison. FEMS Microbiol. Ecol. 55, 274–286.

Liu, C., Zhao, D., Ma, W., Guo, Y., Wang, A., Wang, Q., Lee, D.J., 2016. Denitrifying sulfide removal process on high-salinity wastewaters in the presence of Halomonas sp. Appl. Microbiol. Biotechnol. 100, 1421–1426.

Liu, C., Zhao, D., Yan, L., Wang, A., Gu, Y., Lee, D.-J., 2015. Elemental sulfur formation and nitrogen removal from wastewaters by autotrophic denitrifiers and anammox bacteria. Bioresour. Technol. 191, 332–336.

Liu, Y., Ngo, H.H., Guo, W., Zhou, J., Peng, L., Wang, D., Chen, X., Sun, J., Ni, B.J., 2017. Optimizing sulfur-driven mixotrophic denitrification process: System performance and nitrous oxide emission. Chem. Eng. Sci. 172, 414–422.

Lu, H., Chandran, K., Stensel, D., 2014. Microbial ecology of denitrification in biological wastewater treatment. Water Res. 64, 237–254.

Ma, Y., Zhao, J., Yang, B.L., 2006. Removal of H_2S in waste gases by an activated carbon bioreactor. Int. Biodeterior. Biodegrad. 57, 93–98.

Madigan, M.T., Martinko, J.M., Parker, J., 1997. Brock biology of microorganisms. Prentice Hall Upper Saddle River, NJ.

Mahmood, Q., Zheng, P., Hayat, Y., Islam, E., Wu, D., Ren-cun, J., 2008. Effect of pH on anoxic sulfide oxidizing reactor performance. Bioresour. Technol. 99, 3291–3296.

Mas, J., van Gemerden, H., 1987. Influence of sulfur accumulation and composition of sulfur globule on cell volume and buoyant density of Chromatium vinosum. Arch. Microbiol. 146, 362–369.

McIsaac, G.F., David, M.B., Gertner, G.Z., Goolsby, D.A., 2001. Eutrophication: Nitrate flux in the Mississippi River. Nature 414, 166–167.

McKeown, R.M., Hughes, D., Collins, G., Mahony, T., O'Flaherty, V., 2012. Low-temperature anaerobic digestion for wastewater treatment. Curr. Opin. Biotechnol. 23, 444–451.

Midha, V., Jha, M.K., Dey, A., 2012. Sulfide oxidation in fluidized bed bioreactor using nylon support material. J. Environ. Sci. 24, 512–519.

Mohseni-Bandpi, A., Elliott, D.J., Zazouli, M.A., 2013. Biological nitrate removal processes from drinking water supply-a review. J. Environ. Heal. Sci. Eng. 11, 35.

Montalvo, S., Huiliñir, C., Gálvez, D., Roca, N., Guerrero, L., 2016. Autotrophic denitrification with sulfide as electron donor: Effect of zeolite, organic matter and temperature in batch and continuous UASB reactors. Int. Biodeterior. Biodegrad. 108, 158–165.

Montebello, A.M., Bezerra, T., Rovira, R., Rago, L., Lafuente, J., Gamisans, X., Campoy, S., Baeza, M., Gabriel, D., 2013. Operational aspects, pH transition and microbial shifts of a H_2S desulfurizing biotrickling filter with random packing material. Chemosphere 93, 2675–2682.

Moon, H.S., Ahn, K.-H., Lee, S., Nam, K., Kim, J.Y., 2004. Use of autotrophic sulfur-oxidizers to remove nitrate from bank filtrate in a permeable reactive barrier system. Environ. Pollut. 129, 499–507.

Moosa, S., Harrison, S.T.L., 2006. Product inhibition by sulphide species on biological sulphate reduction for the treatment of acid mine drainage. Hydrometallurgy 83, 214–222.

Muyzer, G., Stams, A.J.M., 2008. The ecology and biotechnology of sulphate-reducing bacteria. Nat. Rev. - Microbiol. 6, 441–454.

Odintsova, E. V, Jannasch, H.W., Mamone, J.A., Langworthy, T.A., 1996. Thermothrix azorensis sp. nov., an obligately chemolithoautotrophic, sulfur-oxidizing, thermophilic bacterium. Int. J. Syst. Evol. Microbiol. 46, 422–428.

Oh, J., Silverstein, J., 1999. Oxygen inhibition of activated sludge denitrification. Water Res. 33, 1925–1937.

Oh, S.-E., Kim, K.-S., Choi, H.-C., Cho, J., Kim, I.S., 2000. Kinetics and physiological characteristics of autotrophic dentrification by denitrifying sulfur bacteria. Water Sci. Technol. 42, 59–68.

Ontiveros-Valencia, A., Tang, Y., Zhao, H.-P., Friese, D., Overstreet, R., Smith, J., Evans, P., Rittmann, B.E., Krajmalnik-Brown, R., 2014. Pyrosequencing analysis yields comprehensive assessment of microbial communities in pilot-scale two-stage membrane biofilm reactors. Environ. Sci. Technol. 48, 7511–7518.

Oyarzún, P., Arancibia, F., Canales, C., Aroca, G.E., 2003. Biofiltration of high concentration of hydrogen sulphide using Thiobacillus thioparus. Process Biochem. 39, 165–170.

Pan, Y., Ye, L., Yuan, Z., 2013. Effect of H_2S on N_2O reduction and accumulation during denitrification by methanol utilizing denitrifiers. Environ. Sci. Technol. 47, 8408–8415.

Park, J.Y., Yoo, Y.J., 2009. Biological nitrate removal in industrial wastewater treatment: which electron donor we can choose. Appl. Microbiol. Biotechnol. 82, 415–429.

Parkin, G.F., Lynch, N.A., Kuo, W.-C., Van Keuren, E.L., Bhattacharya, S.K., 1990. Interaction between sulfate reducers and methanogens fed acetate and propionate. Res. J. Water Pollut. Control Fed. 62, 780–788.

Pikaar, I., Rozendal, R.A., Yuan, Z., Keller, J., Rabaey, K., 2011. Electrochemical sulfide removal from synthetic and real domestic wastewater at high current densities. Water Res. 45, 2281–2289.

Pokorna, D., Zabranska, J., 2015. Sulfur-oxidizing bacteria in environmental technology. Biotechnol. Adv. 33, 1246–1259.

Rabaey, K., Van de Sompel, K., Maignien, L., Boon, N., Aelterman, P., Clauwaert, P., De Schamphelaire, L., Pham, H.T., Vermeulen, J., Verhaege, M., 2006. Microbial fuel cells for sulfide removal. Environ. Sci. Technol. 40, 5218–5224.

Ramos, I., Pérez, R., Fdz-Polanco, M., 2013. Microaerobic desulphurisation unit: A new biological system for the removal of H_2S from biogas. Bioresour. Technol. 142, 633–640.

Rasi, S., Läntelä, J., Rintala, J., 2011. Trace compounds affecting biogas energy utilisation - A review. Energy Convers. Manag. 52, 3369–3375.

Ravichandra, P., Gopal, M., Annapurna, J., 2009. Biological sulfide oxidation using autotrophic Thiobacillus sp.: Evaluation of different immobilization methods and bioreactors. J. Appl. Microbiol. 106, 1280–1291.

Rebac, S., Ruskova, J., Gerbens, S., van Lier, J.B., Stams, A.J.M., Lettinga, G., 1995. High-rate anaerobic treatment of wastewater under psychrophilic conditions. J. Ferment. Bioeng. 80, 499–506.

Reyes-Avila, J., Razo-Flores, E., Gómez, J., 2004. Simultaneous biological removal of nitrogen, carbon and sulfur by denitrification. Water Res. 38, 3313–3321.

Rittmann, B.E., McCarty, P.L., 2001. Environmental biotechnology: principles and applications. McGraw-Hill.

Saad, S.A., Welles, L., Lopez-Vazquez, C.M., van Loosdrecht, M.C.M., Brdjanovic, D., 2017. Sulfide effects on the anaerobic metabolism of polyphosphate-accumulating organisms. Chem. Eng. J. 326, 68–77.

Sahinkaya, E., Kilic, A., Duygulu, B., 2014. Pilot and full scale applications of sulfur-based autotrophic denitrification process for nitrate removal from activated sludge process effluent. Water Res. 60, 210–217.

Schedel, M., Trüper, H.G., 1980. Anaerobic oxidation of thiosulfate and elemental sulfur in Thiobacillus denitrificans. Arch. Microbiol. 124, 205–210.

Schicho, R.N., Ma, K., Adams, M.W.W., Kelly, R.M., 1993. Bioenergetics of sulfur reduction in the hyperthermophilic archaeon Pyrococcus furiosus. J. Bacteriol. 175, 1823–1830.

Scully, C., Collins, G., O'Flaherty, V., 2006. Anaerobic biological treatment of phenol at 9.5-15 °Cin an expanded granular sludge bed (EGSB)-based bioreactor. Water Res. 40, 3737–3744.

Shao, M.F., Zhang, T., Fang, H.H.P., 2010. Sulfur-driven autotrophic denitrification: Diversity, biochemistry, and engineering applications. Appl. Microbiol. Biotechnol. 88, 1027–1042.

Shinabe, K., Oketani, S., Ochi, T., Kanchanatawee, S., Matsumura, M., 2000. Characteristics of hydrogen sulfide removal in a carrier-packed biological deodorization system. Biochem. Eng. J. 5, 209–217.

Shively, J.M., 1974. Inclusion bodies of prokaryotes. Annu. Rev. Microbiol. 28, 167–188.

Siegel, L.M., 1975. Biochemistry of the sulfur cycle, in: Metabolism of Sulfur Compounds. Academic Press, pp. 217–286.

Sublette, K.L., Sylvester, N.D., 1987. Oxidation of hydrogen sulfide by continuous cultures of Thiobacillus denitrificans. Biotechnol. Bioeng. 29, 753–758.

Sumino, H., Murota, R., Miyashita, A., Imachi, H., Ohashi, A., Harada, H., Syutsubo, K., 2012. Treatment of low-strength wastewater in an anaerobic down-flow hanging sponge (AnDHS) reactor at low temperature. J. Environ. Sci. Heal. Part A 47, 1803–8.

Syed, M., Soreanu, G., Falletta, P., Béland, M., 2006. Removal of hydrogen sulfide from gas streams using biological processes - A review. Can. Biosyst. Eng. 48, 1–14.

Syutsubo, K., Yoochatchaval, W., Yoshida, H., Nishiyama, K., Okawara, M., Sumino, H., Araki, N., Harada, H., Ohashi, A., 2008. Changes of microbial characteristics of retained sludge during low-temperature operation of an EGSB reactor for low-strength wastewater treatment. Water Sci. Technol. 57, 277–281.

Takai, K., Suzuki, M., Nakagawa, S., Miyazaki, M., Suzuki, Y., Inagaki, F., Horikoshi, K., 2006. Sulfurimonas paralvinellae sp. nov., a novel mesophilic, hydrogen- and sulfur-oxidizing chemolithoautotroph within the Epsilonproteobacteria isolated from a deep-sea hydrothermal vent polychaete nest, reclassification of Thiomicrospira denitrificans as S. Int. J. Syst. Evol. Microbiol. 56, 1725–1733.

Takeuchi, T.L., Suzuki, I., 1997. Cell hydrophobicity and sulfur adhesion of Thiobacillus thiooxidans. Appl. Environ. Microbiol. 63, 2058–2061.

Tan, W., Huang, C., Chen, C., Liang, B., Wang, A., 2016. Bioaugmentation of activated sludge with elemental sulfur producing strain Thiopseudomonas denitrificans X2 against nitrate shock load. Bioresour. Technol. 220, 647–650.

Taylor, J., Parkes, R.J., 1983. The cellular fatty-acids of the sulfate-reducing bacteria, Desulfobacter sp., Desulfobulbus sp. and Desulfovibrio desulfuricans. J. Gen. Microbiol. 129, 3303–3309.

Tchobanoglous, G., Burton, F.L., Stensel, H.D., 2003. Wastewater Engineering: Treatment and Reuse (Fourth Edition). McGraw-Hill.

Trouve, C., Chazal, P.M., Gueroux, B., Sauvaitre, N., 1998. Denitrification by new strains of Thiobacillus denitrificans under non-standard physicochemical conditions. Effect of temperature, pH, and sulphur source. Environ. Technol. 19, 601–610.

Uemura, S., Harada, H., 2000. Treatment of sewage by a UASB reactor under moderate to low temperature conditions. Bioresour. Technol. 72, 275–282.

Ullah, I., Jilani, G., Khan, K.S., Akhtar, M.S., Rasheed, M., 2014. Sulfur oxidizing bacteria from sulfur rich ecologies exhibit high capability of phosphorous solubilization. Int. J. Agric. Biol. 16, 550–556.

Vaiopoulou, E., Provijn, T., Prévoteau, A., Pikaar, I., Rabaey, K., 2016. Electrochemical sulfide removal and caustic recovery from spent caustic streams. Water Res. 92, 38–43.

van der Zee, F.P., Villaverde, S., García, P.A., Fdz-Polanco, F., 2007. Sulfide removal by moderate oxygenation of anaerobic sludge environments. Bioresour. Technol. 98, 518–524.

Visser, A., Beeksma, I., van der Zee, F., Stams, A.J.M., Lettinga, G., 1993. Anaerobic degradation of volatile fatty acids at different sulphate concentrations. Appl. Microbiol. Biotechnol. 40, 549–556.

Viviantira, E., Wan, C., Wong, B.T., Lee, D.J., 2012. Denitrifying sulfide removal with methanogenic culture. J. Taiwan Inst. Chem. Eng. 43, 374–385.

Wang, A., Liu, C., Ren, N., Han, H., Lee, D., 2010. Simultaneous removal of sulfide, nitrate and acetate: Kinetic modeling. J. Hazard. Mater. 178, 35–41.

Wang, J., Lu, H., Chen, G.H., Lau, G.N., Tsang, W.L., van Loosdrecht, M.C.M., 2009. A novel sulfate reduction, autotrophic denitrification, nitrification integrated (SANI) process for saline wastewater treatment. Water Res. 43, 2363–2372.

Wang, X., Zhang, Y., Zhou, J., Zhang, T., Chen, M., 2015. Regeneration of elemental sulfur in a simultaneous sulfide and nitrate removal reactor under different dissolved oxygen conditions. Bioresour. Technol. 182, 75–81.

Wang, Y., Pavissich, J.P., Sabba, F., Bott, C., Nerenberg, R., 2011. Elemental sulfur (S^0) as a supplemental electron donor for wastewater denitrification. Proc. Water Environ. Fed. 2011, 1590–1597.

Wei, C., Wei, L., Li, C., Wei, D., Zhao, Y., 2018. Effects of salinity, C/S ratio, S/N ratio on the BESI process, and treatment of nanofiltration concentrate. Environ. Sci. Pollut. Res. 25, 5129–5139.

Wei, Y., Dai, J., Mackey, H.R., Chen, G.-H., 2017. The feasibility study of autotrophic denitrification with iron sludge produced for sulfide control. Water Res. 122, 226–233.

Winkler, M.K.H., Bassin, J.P., Kleerebezem, R., van der Lans, R.G.J.M., van Loosdrecht, M.C.M., 2012. Temperature and salt effects on settling velocity in granular sludge technology. Water Res. 46, 5445–5451.

Wong, B.T., Lee, D.J., 2011. Sulfide enhances methanogenesis in nitrate-containing methanogenic cultures. Bioresour. Technol. 102, 2427–2432.

Xu, G., Yin, F., Chen, S., Xu, Y., Yu, H.-Q., 2016. Mathematical modeling of autotrophic denitrification (AD) process with sulphide as electron donor. Water Res. 91, 225–234.

Xu, J., Ding, K., Yang, C., Huang, T., 2018. Regulation of influent sulfide concentration on anaerobic denitrifying sulfide removal. Environ. Technol. 1–21.

Xu, J., Fan, Y., Li, Z., 2016. Effect of pH on elemental sulfur conversion and microbial communities by autotrophic simultaneous desulfurization and denitrification. Environ. Technol. 37, 3014–3023.

Xu, X.-J., Chen, C., Guan, X., Yuan, Y., Wang, A.-J., Lee, D.-J., Zhang, Z.-F., Zhang, J., Zhong, Y.-J., Ren, N.-Q., 2017. Performance and microbial community analysis of a microaerophilic sulfate and nitrate co-reduction system. Chem. Eng. J. 330, 63–70.

Xu, Y., Chen, N., Feng, C., Hao, C., Peng, T., 2016. Sulfur-based autotrophic denitrification with eggshell for nitrate-contaminated synthetic groundwater treatment. Environ. Technol. 37, 3094–3103.

Yamamoto-Ikemoto, R., Komori, T., Nomuri, M., Ide, Y., Matsukami, T., 2000. Nitrogen removal from hydroponic culture wastewater by autotrophic denitrification using thiosulfate. Water Sci. Technol. 42, 369–376.

Yang, W., Zhao, Q., Lu, H., Ding, Z., Meng, L., Chen, G.-H., 2016. Sulfide-driven autotrophic denitrification significantly reduces N2O emissions. Water Res. 90, 176–184.

Yang, Y., Chen, T., Sumona, M., Gupta, B. Sen, Sun, Y., Hu, Z., Zhan, X., 2017. Utilization of iron sulfides for wastewater treatment: a critical review. Rev. Environ. Sci. Biotechnol. 16, 289–308.

Zehnder, A.J.B., 1988. Biology of anaerobic microorganisms. John Wiley and Sons Inc.

Zhang, L., De Schryver, P., De Gusseme, B., De Muynck, W., Boon, N., Verstraete, W., 2008.

Chemical and biological technologies for hydrogen sulfide emission control in sewer systems: A review. Water Res. 42, 1–12.

Zhang, Y., Angelidaki, I., 2015. Recovery of ammonia and sulfate from waste streams and bioenergy production via bipolar bioelectrodialysis. Water Res. 85, 177–184.

Zheng, M., Zuo, Z., Zhang, Y., Cui, Y., Dong, Q., Liu, Y., Huang, X., Yuan, Z., 2017. Nitrite production from urine for sulfide control in sewers. Water Res. 122, 447–454.

Zhou, W., Li, Y., Liu, X., He, S., Huang, J.C., 2017. Comparison of microbial communities in different sulfur-based autotrophic denitrification reactors. Appl. Microbiol. Biotechnol. 101, 447–453.

Zhou, W., Liu, X., Dong, X., Wang, Z., Yuan, Y., Wang, H., He, S., 2016. Sulfur-based autotrophic denitrification from the micro-polluted water. J. Environ. Sci. 44, 180–188.

Zhou, Z., Yu, Z., Meng, Q., 2012. Effects of nitrate on methane production, fermentation, and microbial populations in vitro ruminal cultures. Bioresour. Technol. 103, 173–179.

Zou, G., Papirio, S., Lakaniemi, A.M., Ahoranta, S.H., Puhakka, J.A., 2016. High rate autotrophic denitrification in fluidized-bed biofilm reactors. Chem. Eng. J. 284, 1287–1294.

Zytoon, M.A.-M., AlZahrani, A.A., Noweir, M.H., El-Marakby, F.A., 2014. Bioconversion of high concentrations of hydrogen sulfide to elemental sulfur in airlift bioreactor. Sci. World J. 2014.

Ødegård, H., 1992. Fjerning av næringsstoffer ved rensing av avløpsvann. Tapir.

2 Aim, objectives, and approach

The experimental studies concerning the biological oxidation of H_2S with NO_3^- are discussed in this thesis. The main aim of this work is to better understand the process conditions and mechanisms to increase the robustness of autotrophic microbial H_2S oxidation.

The objective of these investigations was to evaluate the temperature (25-10 °C) and N/S ratio influence on the simultaneous NO_3^- and H_2S removal. Additionally, the dynamics of microbial communities under temperature stress were examined, and a method for indirect H_2S measurements was developed.

The scope included literature studies related to the biological H_2S removal, construction and operation of the EGSB reactor, and statistical analysis of obtained data.

In Article I, the short-term temperature impact was evaluated including the scanning electron microscopy (SEM) investigations. The temperature impact in the long-term experiment and description of microbial community dynamics is described in Articles II and III. Article IV focuses on the N/S ratio impact on the process under psychrophilic conditions. Temperature and N/S ratio impacts were modeled in Article V. In addition, unpublished results give a more detailed description of the developed method for H_2S measurements used in these investigations.

3 Materials and methods

A brief overview of the research strategy, organization, materials and methods is included here. More detailed descriptions can be found in the attached Articles.

3.1 Research strategy and organization

The study began with a literature review on H_2S removal methods. From a multitude of removal methods, the research was focused on the biological methods where the NO_3^- is supplied as the electron acceptor for H_2S removal. Before the experimental studies on temperature and N/S ratio started, the analytical methods and experimental setup had to be designed, developed, and built. A flow diagram of the research strategy is provided in Figure 3.1.

The experimental work, along with the majority of analytical work, was conducted at University of South-Eastern Norway (USN), campus Porsgrunn. Part of the analytical work was performed in cooperation with external partners. The microbial community analyses were performed at the University of Warmia and Mazury (Poland), while the SEM analyses were carried out at the Lublin University of Technology (Poland).

The experimental work was performed in an expanded granular sludge bed (EGSB) reactor in two trials. Each trial was preceded with the acclimatization period of around 1 month.

The first short-term trial was focused on the evaluation whether the process can run at frequent temperature changes (25-10 °C) and S^0 can be stored on granular sludge. The results are described in Article I.

The main trial was performed over the 150 days (excluding acclimatization period). During this trial, the temperature impact (25-10 °C) in a longer time span and different N/S ratios (0.35-1.30) were studied. Obtained results were analyzed based on chemical markers and by using Gibbs free energy and electron balance. The microbial communities in biomass samples at different temperatures were examined. The results from the main trial are included in Articles II-IV.

Additionally, the preliminary attempt to the mathematical modeling of the data obtained from the main trial is described in Article V.

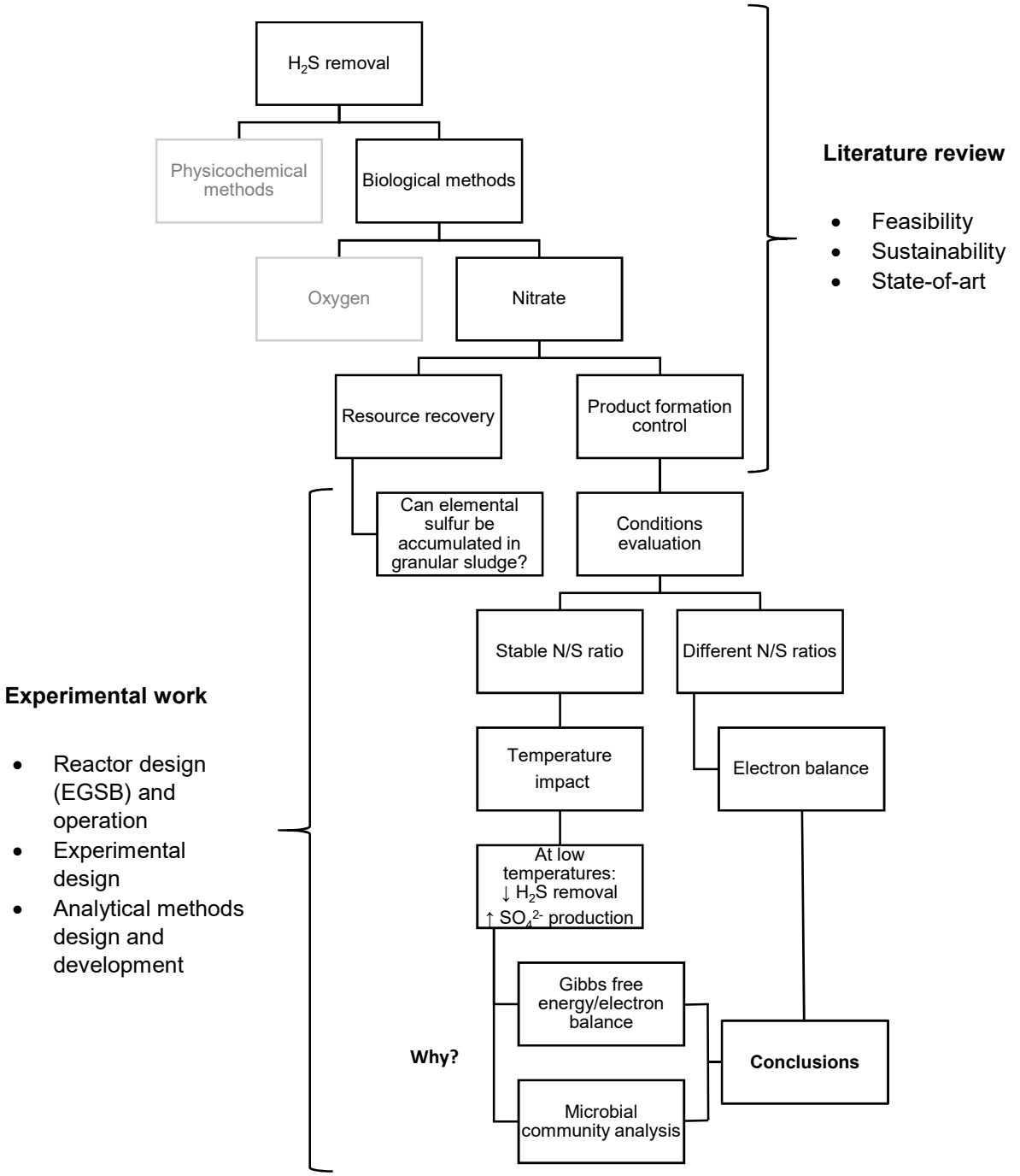

Figure 3.1: Research strategy flow diagram.

3.2 Reactor configuration

The EGSB reactor used in this research was designed and built at USN. The laboratory-scale reactor made of polycarbonate had an effective volume of 0.5 L with 32 mm inner diameter and 620 mm effective height (Figure 3.2). The reactor was equipped with gas, sample, and sludge removal valves. A recirculation loop, effluent, and feed were connected to the reactor; the recirculation loop and feed were equipped with peristaltic pumps. Due to the focus on the temperature impact, the reactor temperature was maintained by a cold plate cooler (TE Technology, Inc., Traverse City, MI, USA) attached before the reactor inlet. Additionally, the recirculation loop was equipped with a pH meter for continuous measurements. The detailed overview of the reactor working parameters is given in Articles.

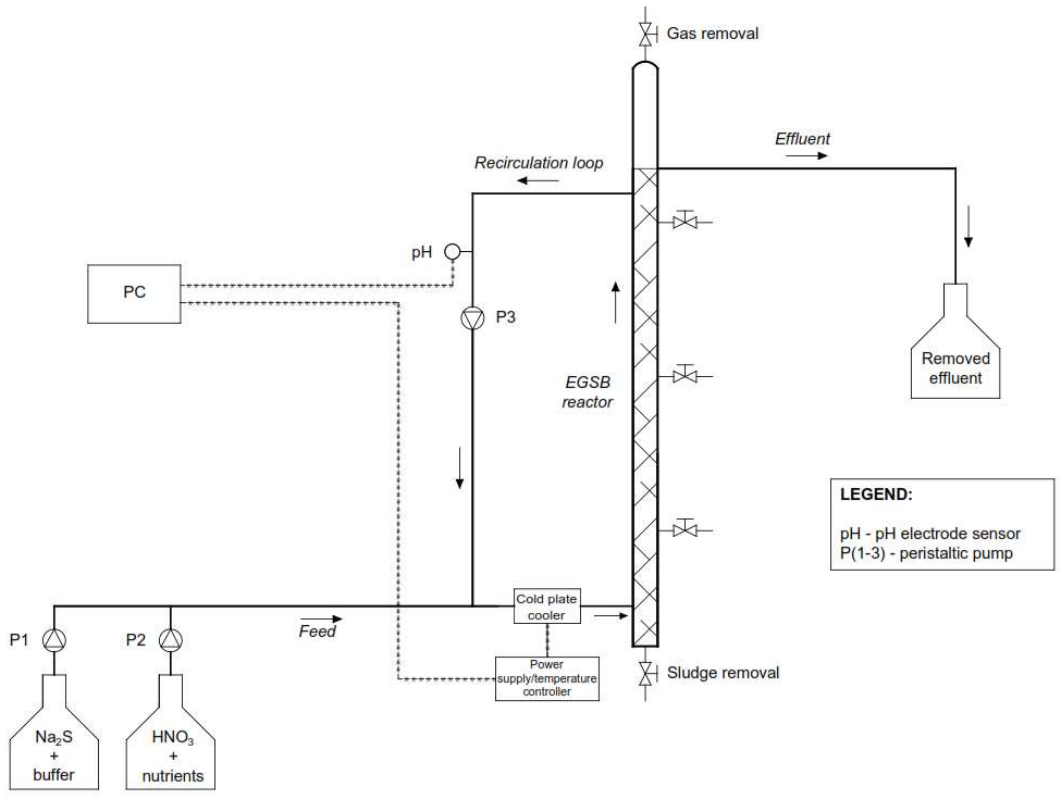

Figure 3.2: Experimental setup.

3.3 Influent and analytical methods

The reactor was continuously fed with laboratory-prepared synthetic wastewater that consisted of nitric acid (HNO_3) as the electron acceptor and sodium sulfide nonahydrate ($Na_2S{\cdot}9H_2O$) as the electron donor. Sources of the electron acceptor and donor were prepared and supplied in separate tanks. The pH buffer, macro-, microelements, and vitamins were supplied. The detailed feeding parameters are given in Articles.

Samples obtained from experiments were analyzed immediately for nitrate (NO_3^-), sulfate (SO_4^{2-}), sulfide (HS^-), and thiosulfate ($S_2O_3^{2-}$). The presence of nitrite (NO_2^-) was only qualified, however, during the experimental periods its presence was not detected. Before analysis, samples were filtered and diluted.

The analyses were performed by ion chromatography (Dionex ICS-5000) using potassium hydroxide (KOH) as the eluent. The used method was developed prior to the experimental period and was improved between the trials. Sample separation and elution in the main trial was performed by using an IonPac AS11-HC 2mm analytical column. Analysis started at 22 mM KOH, gradient started at 6 min, ramped up in 3 min to 45 mM and kept at that concentration for another 4 min. The data acquisition time was 13 min, while the injection volume was 10 µL and the flow rate 0.3 mL/min. A chromatogram is presented in Figure 3.3.

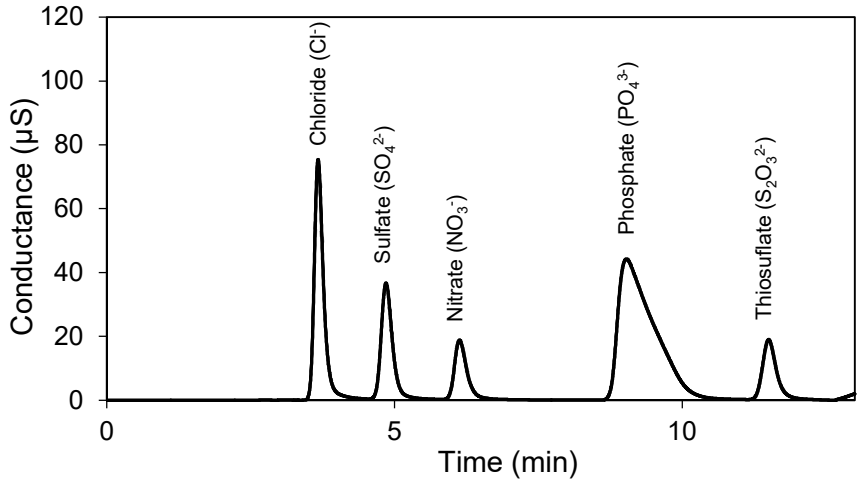

Figure 3.3: Chromatogram of the employed analytical method.

The developed method for anions analysis was expanded to build an indirect method for HS^- determination described in Chapter 4.6 (Unpublished results – Indirect analysis of sulfide in environmental samples).

Anion analysis was the key measurement method used during these studies. However, other analytical methods and measurements like total solids (TS), volatile solids (VS), microbial community analysis, and SEM were also used. The detailed description of microbial community analysis and SEM is given in Articles.

4 Summary of results

In this section, the research leading to the five papers, key findings, and method development are summarized.

4.1 Article I – Short-term temperature impact on simultaneous biological nitrogen-sulphur treatment in EGSB reactor

This study is focused on the short-term temperature effect (25-10 °C) on an expanded granular sludge bed (EGSB) reactor for HS^- removal using NO_3^- as an electron acceptor. The reactor was run at N/S ratio of 0.35 and pH of 8.5-9.0. Temperature variations had an impact on the product distribution. The $S_2O_3^{2-}$ and SO_4^{2-} increased with decreasing temperature. HS^- conversion to S^0 amounted up to 76 %. At the temperature range of 15-10 °C, the effluent sulfur concentration exceeded the influent sulfur concentration, suggesting the loss of earlier accumulated sulfur from the granular sludge bed.

Sulfur and iron were found on the granular sludge surface by using SEM. It was hypothesized that FeS and S^0 are present on the granular sludge surface, confirming S^0 accumulation. Additionally, struvite was found inside the granules.

4.2 Article II – Metabolic divergence in simultaneous biological removal of nitrate and sulfide for elemental sulfur production under temperature stress

In this article, the simultaneous removal of NO_3^- and HS^- at temperature stress (25-10 °C) in EGSB reactor in the longer timespan was evaluated. The EGSB reactor was run over 120 days at N/S molar ratio of 0.35 (for S^0 production) under constant sulfur loading rate of 0.4 kg S/m^3d.

The simultaneous removal of NO_3^- and HS^- was achieved under the applied conditions. Average HS^--S removal varied from 98 % at 25 °C to 89.2 % at 10 °C, with complete NO_3^- removal. The temperature changes did not have a strong impact on substrates removal, while the relative presence of effluent sulfur components was more affected.

The temperature drops caused a decrease in the granular sludge S^0 accumulation by nearly 2.5 times from 45.2 % at 25 °C to 18.3 % at 10 °C. Simultaneously, the SO_4^{2-} production increased from 14.4 % at 25 °C to 22.1 % at 10 °C.

Changes in products distribution with temperature decrease leading to lower S^0 and higher SO_4^{2-} production were explained as metabolic divergence. At lower temperatures, the more exergonic reaction (SO_4^{2-} production) was increasing its share. On the basis of the substrate metabolism analysis and Gibbs free energy calculations, it was observed that the changes in metabolism allowed the microbial communities to obtain more energy per HS^- consumed.

The overall Gibbs free energy, including the removal rate of substrates remained nearly constant over the whole temperature range due to the decreasing HS^- removal, complete NO_3^- removal and increasing SO_4^{2-} production. It is hypothesized that the metabolic shift is a natural response of microorganisms to compensate for the temperature-induced changes in energy requirements. It is also hypothesized that the temperature drop induced the changes in microbial community structure, which influenced changes in products distribution and substrates removal.

4.3 Article III – Temperature-induced changes in microbial community under autotrophic denitrification with sulfide

The objective of this study was a further investigation of the temperature impact on simultaneous NO_3^- and HS^- removal with focus on changes in microbial communities.

High throughput sequencing indicated that the transition from methanogenic conditions (inoculum sludge) to the imposed experimental conditions led to the development of Proteobacteria share in microbial community. Proteobacteria comprised 72.1 and 71.0 % of all sequences obtained from the biomass at 25 and 10 °C, respectively, while the share of Proteobacteria in the inoculum was minor (4.8 %). Changes in temperature reveal that the Shannon-Wiener diversity index of biomass was highest in the inoculum (7.19), lower at 25 °C (6.60) and the lowest at 10 °C (6.19). A similar tendency was observed for

evenness index. Even with lower diversity, the bacterial community was evidently capable of utilizing the supplied inorganic feed throughout the studied temperature range.

The *β*-Proteobacteria (mainly *Thauera* sp. and *Alicycliphilus* sp.) predominated at 25 °C (64 %) when the S^0 accumulation was the highest (45 %). Decreasing the temperature to 10 °C reduced both the abundance of *β*-Proteobacteria (to 28 %) and the accumulation of S^0 (to 18 %). At 10 °C, chemolithoautotrophic sulfide-oxidizing bacteria belonging mainly to *ε*-Proteobacteria (*Sulfurimonas* sp.) were abundant in the biomass (over 31 % of all sequences) and SO_4^{2-} production increased slightly. Increased presence of *ε*-Proteobacteria implies their competitive advantage at low temperatures.

Based on the comparison of the most abundant Proteobacteria classes and effluent sulfur compounds, the reactor effluent characteristics, especially in S^0 accumulation, appeared to be associated with the microbial community. The 2.5 times lower S^0_{acc} at 10 °C (compared to 25 °C) was reflected in the *β*-Proteobacteria presence that diminished to a similar degree as S^0_{acc} (nearly 2.3 times) from 64 % at 25 to 28 % at 10 °C.

4.4 Article IV – Effects of N/S molar ratio on products formation in psychrophilic autotrophic biological removal of sulfide

This study aimed to evaluate the effects of different N/S molar ratios as a strategy to control sulfur products distribution in an EGSB reactor at 10 °C.

Four different N/S molar ratios (0.35, 0.40, 0.60, and 1.30) were tested through the 60 days of the experiment. Efficient psychrophilic HS^- removal with sulfur products oxidation control by NO_3^- supply is documented.

The highest HS^- removal was obtained at N/S=0.35 and 1.30 (89.1 ± 2.2 and 89.6 ± 2.9 %). Removal of HS^- was lesser at mid-N/S with the lowest value (76.9 ± 2.6 %) at N/S=0.60. NO_3^- removal remained high for all N/S ratios (98.7 ± 2.8 %). N/S molar ratio influenced the sulfur products distribution. Each increase in NO_3^- resulted in a SO_4^{2-} concentration rise, depletion of S^0 fractions and pH drop, even in case of N/S=0.40 (based on a catabolic reaction, Eq. 1.8). Results clearly indicate that the

appropriate N/S ratio for S^0 production is lower than that reflected in the catabolic reaction.

At the highest studied N/S ratio (1.30), the sum of sulfur components in the effluent was 22 % higher than in the influent during this period. The excess of effluent sulfur is explained by the oxidation of previously accumulated elemental sulfur (S^0_{acc}). The observed phenomena must have a temporary nature until the S^0_{acc} in the granules is exhausted. Oxidation of accumulated S^0 under the presence of unreacted HS^- can be explained by culture flexibility in utilizing the available resources for energy gain.

Obtained experimental results show the offset form theoretical values with good match only at N/S=1.30.

4.5 Article V – Modeling N/S ratio and temperature effects in simultaneous biological denitrification and sulfide oxidation

This article was focused on N/S ratio and temperature modeling based on the obtained experimental results. Modeling can facilitate further understanding and optimization of simultaneous biological NO_3^- and HS^- removal. So far, models related to autotrophic denitrification are based on fixed stoichiometry or yield values.

The developed model, which includes variable process stoichiometry, attempts to predict the distribution of sulfur oxidation products. Stoichiometric coefficients are based on combined experimental results from temperature (25-10 °C) and N/S ratio (0.35-1.30) studies. The model can be used as a prediction tool for autotrophic denitrification with HS^-. S^0 production is included in the mathematical model, however, its accumulation and release (as SO_4^{2-}) with increasing N/S ratio (e.g., leading to higher effluent than feed total sulfur mass at N/S=1.30) is not simulated. A conceptual model accounting for the biological accumulation and release of elemental sulfur is proposed here as a next step in refining the model.

4.6 Unpublished results – Indirect analysis of sulfide in environmental samples

Sulfides generation in natural waters and wastewaters is mainly related to sulfate reduction by sulfate reducing bacteria (SRB). Hydrogen sulfide (H_2S) is characterized by a strong odor of rotten eggs, lipophilicity, and toxic properties (Whiteman et al., 2011). Due to the adverse impact of sulfide and their gaseous derivatives, the measurements of sulfide are of great interest. Many dissolved inorganic forms of sulfur exist in natural waters. Sulfates (SO_4^{2-}), sulfides (H_2S, HS^-, and S^{2-}), elemental sulfur (S^0), and thiosulfates ($S_2O_3^{2-}$) seem to prevail in aquatic systems (Hurse and Abeydeera, 2002). Substrates of sulfur oxidation, such as S^{2-} and $S_2O_3^{2-}$ exhibit high reactivity and instability that leads to their decomposition or oxidation. Due to these properties, determination of S^{2-} and $S_2O_3^{2-}$ is difficult. Analytical methods for S^{2-} determination include classical, chromatographic, electrochemical, and spectrophotometric techniques (Lawrence et al., 2000). Currently, the common methods for S^{2-} determination in environmental analyses are the iodometric method and the methylene blue method, which represent classical and spectrophotometric methods, respectively (Patnaik, 2010). Both of these methods face problems related to their standardization procedure, where for classical titration losses of sulfur during the titration process are significant and the potential presence of $S_2O_3^{2-}$ can lead to overestimation of the final result (Florence and Farrar, 1980). Additionally, the spectrophotometric method gives inappropriate results in the presence of PO_4^{3-} and in case of colored samples (Percheron et al., 1996). The EPA does not recommend any method for dissolved S^{2-} measurements (Reese et al., 2011).

Chromatographic methods like ion chromatography (IC) allow for S^{2-} measurements by means of a UV detector, where the usage of conductivity detector is not possible. To detect and quantify S^{2-} with a conductivity detector, it is necessary to transform S^{2-} into a stable form which would prevent losses to the gas phase or other transformations. Complete oxidation of S^{2-} present in the liquid sample will result in the formation of SO_4^{2-} that is an equivalent to S^{2-}. Among the common oxidizing agents, we can distinguish

chromate (CrO_4^{2-}), hydrogen peroxide (H_2O_2), perchlorate (ClO_4^-), and manganate (VII) (MnO_4^-).

Potassium manganate (VII) ($KMnO_4$) is used to remove iron and H_2S from wastewater through manganese filters (Jang et al., 2003; Zhang et al., 2015). The potential of $KMnO_4$ can also be adapted in analytical methods. The reaction of unstable forms of sulfur (S^{2-} and $S_2O_3^{2-}$) with $KMnO_4$ leads to the oxidation of sulfur species to SO_4^{2-} (Eqs. 4.1, 4.2).

$$4H_2O + 3S^{2-} + 8MnO_4^- \rightarrow 8MnO_2 + 3SO_4^{2-} + 8OH^- \quad (4.1)$$

$$H_2O + 3S_2O_3^{2-} + 8MnO_4^- \rightarrow 8MnO_2 + 6SO_4^{2-} + 2OH^- \quad (4.2)$$

In this work, ion chromatography with conductivity detector was proposed for determination of S^{2-}, $S_2O_3^{2-}$, and SO_4^{2-}, where S^{2-} is measured indirectly as an increase in the SO_4^{2-} concentration caused by the oxidation with $KMnO_4$.

4.6.1 Materials and methods

Reagents

All reagents were prepared from analytical-reagent grade chemicals. Deionized water with a specific resistance of 18.2 mΩ was used to prepare the solutions (Thermo Smart2Pure, USA). All stock solutions were prepared on a daily basis.

Stock solutions preparation

Calibration solutions were prepared for SO_4^{2-} and $S_2O_3^{2-}$ by dilution in deionized water. Solutions for SO_4^{2-} calibration (9.38-150 mg/L) were prepared by dilution of a standard solution, which contains 1000 mg/L of SO_4^{2-} (as Na_2SO_4) (Merck Millipore, Germany). $S_2O_3^{2-}$ calibration solutions (6.25-100 mg/L) were prepared by diluting 0.0113 N of the $Na_2S_2O_3$ standard solution (Hach Lange, Germany).

A stock solution containing 100 mg/L of S^{2-} was prepared by dissolving 0.749 g of $Na_2S{\cdot}9H_2O$ (Alfa Aesar, Germany) with deionized water to 1000 mL in the nitrogen-

sparked volumetric flask. The working standards (6.25-50 mg/L) were carefully diluted and mixed with deionized water.

The working standards of $S_2O_3^{2-}$ (10-40 mg/L) were made by diluting the 0.0113 N of $Na_2S_2O_3$ standard solution (Hach Lange, Germany).

Solutions of $KMnO_4$ (Merck Millipore, Germany) were prepared by dissolving in deionized water. Their concentrations depended on the concentration of S^{2-} and $S_2O_3^{2-}$ in the working solution, in accordance to Eqs. 4.1 and 4.2 with 5 % excess.

Working standards were oxidized by addition of $KMnO_4$ solution. It resulted in blackish manganese dioxide (MnO_2) solids precipitate that was removed with 0.45 µL filter (first 2 mL of filtrate was removed) and subsequently transferred to 1.5 mL PP vials to be measured immediately.

Instrumentation

Dionex ICS-5000 ion chromatograph equipped with a Dionex IonPac AG11-HC (2x50 mm) guard, IonPac AS11-HC (2x250 mm) separating column (23 °C) and a conductivity detector (30 °C) was used in the experiment. Dionex ASRS 300 2mm suppressor (17 mA) was attached in front of the conductivity detector. The samples were injected with a Dionex AS-AP autosampler. The data processing was done with Chromeleon 7.1 software (Thermo Scientific Dionex, USA). A potassium hydroxide (KOH) gradient was applied with automatic eluent generator using an EluGen cartridge (EGC II KOH, Dionex, USA).

Experimental design

Working solutions of S^{2-} (6.25, 12.5, 25, and 50 mg/L) and $S_2O_3^{2-}$ (10, 20, 40, and 80 mg/L) were measured after oxidation in 3 replications. Analysis started at 22 mM KOH, gradient began after 6 minutes and within the following 4 minutes, it increased to 45 mM, maintaining this concentration for another 4 minutes. The data acquisition time was 13 minutes. The injection volume was 10 µl and the flow rate 0.3 mL/min. Obtained SO_4^{2-} concentrations were recalculated on the S^{2-} and $S_2O_3^{2-}$ equivalents.

4.6.2 Results and discussion

The direct measurements of S^{2-} on an IC equipped with a conductivity detector are not possible, as no signal is obtained during S^{2-} analysis. Suppressor converts S^{2-} to H_2S and consequently, the analyte is not charged when it passes through the conductivity detector (Keller-Lehmann et al., 2006). However, the determination of SO_4^{2-} and $S_2O_3^{2-}$ on IC equipped with a conductivity detector is possible. The oxidation process was adapted for the detection of S^{2-} using an IC equipped with a conductivity detector.

Sulfide and thiosulfate oxidation – method evaluation

Oxidation of S^{2-} and $S_2O_3^{2-}$ by $KMnO_4$ was performed in the presented studies. During the experiment preparation, hydrogen peroxide (H_2O_2) was briefly tested as an oxidizing agent. The obtained results (under the excess of H_2O_2) have shown the problems associated with H_2O_2 excess decomposition ($H_2O_2 \rightarrow H_2O + ½O_2$) which led to sample concentrating and pressurizing in sample vials. Possible further H_2O_2 decomposition after sample injection can cause problems in a detector cell. The above-mentioned adverse effects do not occur with $KMnO_4$ excess. The result of the reaction between $KMnO_4$ and S^{2-} or $S_2O_3^{2-}$ is MnO_2 precipitate ($Mn^{+VII} \rightarrow Mn^{+IV}$) and SO_4^{2-} ($S^{-II} \rightarrow S^{+VI}$) which act as the equivalent of the oxidized sulfur compounds (Fig. 4.1).

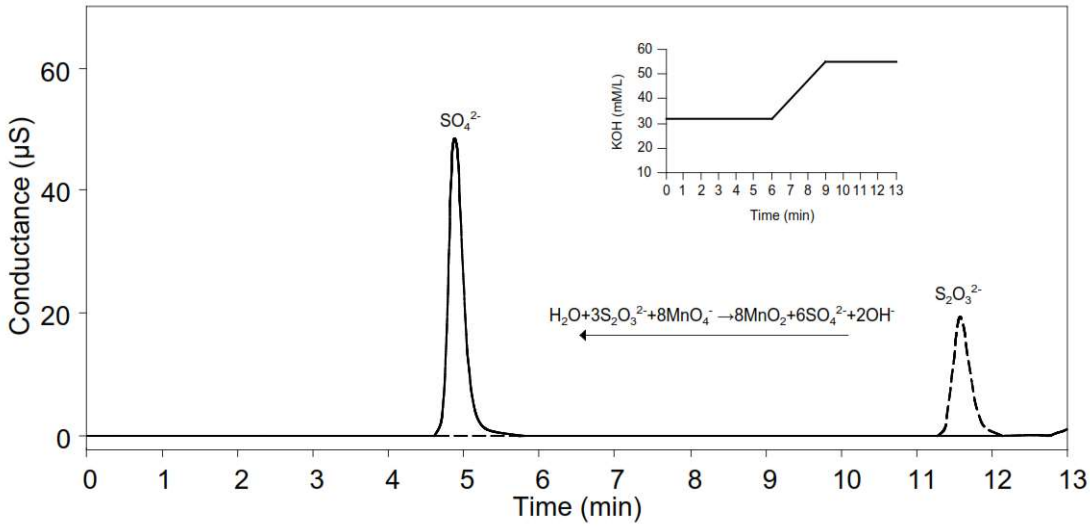

Figure 4.1: Standard solution chromatogram of $S_2O_3^{2-}$ (dashed line) and $S_2O_3^{2-}$ oxidized to SO_4^{2-} (solid line).

The chromatograms of the same $S_2O_3^{2-}$ concentration (20 mg/L) with and without oxidation show that peak height and peak area representing $S_2O_3^{2-}$ after oxidation (as SO_4^{2-}) is nearly two times larger ($Area_{SULFATE}/Area_{THIOSULFATE}$=1.81) than before oxidation. This feature can positively influence the method sensitivity.

Additionally, the presented method allows a simultaneous elution of Cl^-, NO_2^-, NO_3^- and PO_4^{3-} (data not shown). The presence of carbonate (CO_3^{2-}) and high concentration of Cl^- may induce a modification in SO_4^{2-} peak shape due to the close elution of CO_3^{2-} between Cl^- and SO_4^{2-} peaks (Giuriati et al., 2003). It may lead to difficulties with proper quantification. However, appropriate dilution of a particular sample may overcome this adverse impact of adjacent peaks.

Retention time for SO_4^{2-} equaled 4.9 min, whereas, for $S_2O_3^{2-}$, it was 11.5 min. The use of gradient allowed shortening the $S_2O_3^{2-}$ retention time.

Oxidation process with 5 % excess of oxidizing agent proceeded satisfactorily, confirming the theoretical assumptions. A linear correlation was obtained between the expected and found concentration of SO_4^{2-} with a determination coefficient 0.9998 (S^{2-}) and 0.9999 ($S_2O_3^{2-}$) (Fig. 4.2; Table 4.1 and 4.2).

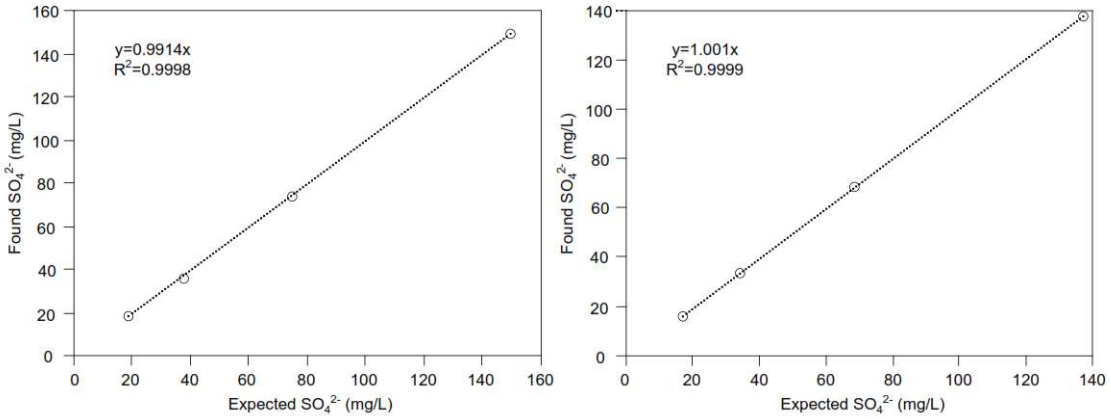

Figure 4.2: Expected vs. found SO_4^{2-} concentration after HS^- oxidation (left), after $S_2O_3^{2-}$ oxidation (right).

Table 4.1: Results of S^{2-} determination after $KMnO_4$ oxidation.

Sample spiked (mg/L)		Found (mg/L)	Recovery (%)
S^{2-}	$KMnO_4$	S^{2-}	
50	197.32	49.77	99.54
		49.67	99.33
		49.74	99.47
25	98.66	24.64	98.58
		24.68	98.71
		24.75	99.02
12.5	44.33	11.99	95.95
		12.02	96.13
		12.01	96.05
6.25	24.66	6.23	99.66
		6.21	99.28
		6.21	99.28

Table 4.2: Results of $S_2O_3^{2-}$ determination after $KMnO_4$ oxidation.

Sample spiked (mg/L)		Found (mg/L)	Recovery (%)
$S_2O_3^{2-}$	$KMnO_4$	$S_2O_3^{2-}$	
80	315.71	81.39	101.74
		80.48	100.61
		78.65	98.31
40	157.85	40.28	100.7
		40.08	100.2
		39.98	99.94
20	78.93	19.74	98.72
		19.70	98.48
		19.67	98.37
10	39.46	9.63	96.29
		9.58	95.83
		9.57	95.65

S^{2-} recovery was between 95.95-99.66 %, the lowest recovery was obtained for 12.5 mg S^{2-}/L. $S_2O_3^{2-}$ recovery ranged between 95.65-101.74 %, with the lowest recovery for 10 mg/L of $S_2O_3^{2-}$. Obtained deviation in recovery (<98 %) may be caused by manual preparation and dilution of samples.

Recommended procedure

The application of the presented method in liquid environmental samples containing several forms of dissolved sulfur and S^{2-} should be based on a dual procedure (Fig. 4.3).

A sample should be divided into two sub-samples. The first sub-sample ought to be oxidized ($KMnO_4$). Obtained result would represent the total sulfur concentration (as $SO_4^{2-}{}_{OX}$), whereas the second sub-sample ought to be analyzed without oxidation (SO_4^{2-}, $S_2O_3^{2-}$). The utmost diligence should be maintained in connection with the rapid oxidation of S^{2-} and possible transfer to the gas phase as H_2S. Data obtained from two

sub-samples can be recalculated regarding S^{2-} concentration based on Eqs. 4.3 and 4.4.

$$[SO_4^{2-}\text{-}S_{OX}] = [SO_4^{2-}\text{-}S] + [S_2O_3^{2-}\text{-}S] + [S^{2-}] \quad (4.3)$$

$$[S^{2-}] = [SO_4^{2-}\text{-}S_{OX}] - [SO_4^{2-}\text{-}S] - [S_2O_3^{2-}\text{-}S] \quad (4.4)$$

The examples of sulfide-containing samples preservation have been previously described (García-Calzada et al., 1999, Keller-Lehmann et al., 2006). Sulfide antioxidation buffer (SAOB) usually comprises an alkaline solution (NaOH) and complexing agents (EDTA, citric acid, ascorbic acid). In anion exchange chromatography, hydroxides (OH^-) are used as eluents; thus, the addition of OH^- would lead to peak overlapping and differences in peak area, peak shape, and retention time in accordance to the calibration procedure excluding SAOB impact (Fritz et al., 1987). The composition of universal SAOB is difficult to determine due to the varying characteristic of environmental samples. Therefore, while using this method on environmental samples, an emphasis should be placed on the mentioned aspect, especially when the time between sampling and analysis is extended. Uncontrolled sample oxidation may cause overestimation of SO_4^{2-} and $S_2O_3^{2-}$, while the S^{2-} will be underestimated.

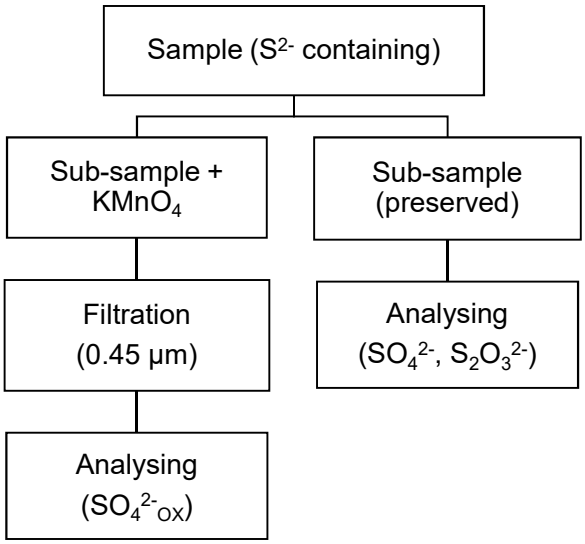

Figure 4.3: Recommended procedure for S^{2-} and $S_2O_3^{2-}$ determination.

References

Florence, T.M., Farrar, Y.J., 1980. Titration of microgram amounts of sulphide with a sulphide-selective electrode. Anal. Chim. Acta 116, 175–179.

Fritz, J.S., 1987. Ion Chromatography, Analytical Chemistry. John Wiley & Sons.

García-Calzada, M., Marbán, G., Fuertes, A.B., 1999. Potentiometric determination of sulphur in solid samples with a sulphide selective electrode. Anal. Chim. Acta 380, 39–45.

Giuriati, C., Cristofori, M.C., Gorni, A., Abballe, F., 2003. Ion chromatography applications in the determination of HF, HCl, NOx, SOx on stationary emissions. Ann. Dellistituto Super. Di Sanità 39, 223–228.

Hurse, T.J., Abeydeera, W.P.P., 2002. Quantification of sulfur and sulfur-containing compounds in wastewaters by means of a combination of liquid chromatographic methods. J. Chromatogr. A 942, 201–210.

Jang, H.T., Sang, B.K., Dong, S.D., 2003. The removal of hydrogen sulfide with manganic sorbent in a high-temperature fluidized-bed reactor. Korean J. Chem. Eng. 20, 116–120.

Keller-Lehmann, B., Corrie, S., Ravn, R., Yuan, Z., Keller, J., 2006. Preservation and simultaneous analysis of relevant soluble sulfur species in sewage samples. Proc. Second Int. IWA Conf. Sewer Oper. Maint. 26, 28.

Lawrence, N.S., Davis, J., Compton, R.G., 2000. Analytical strategies for the detection of sulfide: A review. Talanta. 52, 771-784.

Patnaik, P., 2010. Handbook of environmental analysis: chemical pollutants in air, water, soil, and solid wastes. CRC Press.

Percheron, G., Bernet, N., Moletta, R., 1996. A new method for the determination of dissolved sulfide in strongly colored anaerobically treated effluents. Bioprocess Eng. 15, 317–322.

Reese, B.K., Finneran, D.W., Mills, H.J., Zhu, M.X., Morse, J.W., 2011. Examination and refinement of the determination of aqueous hydrogen sulfide by the methylene blue method. Aquat. Geochemistry 17, 567–582.

Whiteman, M., Le Trionnaire, S., Chopra, M., Fox, B., Whatmore, J., 2011. Emerging role of hydrogen sulfide in health and disease: critical appraisal of biomarkers and pharmacological tools. Clin. Sci. 121, 459–488.

Zhang, J., Wang, L., Song, H., Song, H., 2015. Adsorption of low-concentration H_2S on manganese dioxide-loaded activated carbon. Res. Chem. Intermed. 41, 6087–6104.

5 Conclusions

The biological method for autotrophic hydrogen sulfide removal using nitrate as an electron acceptor in a granular sludge bed reactor, established and investigated in this study, proved to be efficient and controllable. The experimental work was performed in a high rate reactor, demonstrating the efficiency of the approach compared to standard industrial methods. This chapter summarises the overall research findings regarding the two critical parameters: temperature and N/S ratio, their significance, implications and future aspects.

5.1 Temperature

The temperature impact studies are usually limited to the most favorable temperature range for SOB. Here, the temperature effects were studied in a high rate continuous flow reactor in the 25-10 ^{o}C temperature range and invariable feeding properties. High HS^- removal rates at the range from 98 % (25 ^{o}C) to 89.2 % (10 ^{o}C) were obtained at both meso- and psychrophilic conditions. The decreasing temperature did not affect the NO_3^- removal (not detected in the effluent samples). Thus, the autotrophic HS^- removal can be performed with satisfactory results at temperatures often encountered in colder climates. Consequently, the temperature maintenance costs can be reduced.

The temperature influenced the products distribution more than substrates removal. A step-wise temperature decrease caused a change towards more oxidized products. At lower temperatures SO_4^{2-} production increased while the S^0 accumulation decreased. The average S^0 yield ranged from 83.7 % at 25 ^{o}C to 67 % at 10 ^{o}C while the SO_4^{2-} presence increased from 14.4 % (25 ^{o}C) to 22.1 % (10 ^{o}C).

Further evaluation of the obtained results was focused on Gibbs free energy analysis and microbial community analysis at different temperature levels. The goal of these analyses was to explain the changes in products composition and HS^- removal. The Gibbs free energy analysis revealed that the changes in removal rate and product characteristics allowed microorganisms to maintain a similar reaction energy (for catabolism) at each temperature. This metabolic shift allowed the biomass to obtain

more energy per HS^- consumed by higher production of SO_4^{2-}. That is hypothesized to be a natural response of microbiota to compensate for the temperature-induced changes.

5.2 Microbial communities

The observed metabolic shift as an adaptation to psychrophilic conditions is supported by the microbial community analysis. The microbial communities analyzed at 25 and 10 °C differed significantly. *Thauera* sp. and *Alicycliphilus* sp. (both *β*-Proteobacteria) prevailed and comprised over 57 % of all identified sequences under mesophilic conditions (25 °C). *ε*-Proteobacteria (mostly *Sulfurimonas* sp., 31.3 %) dominated under psychrophilic conditions (10 °C).

Changes in the relative abundance of these Proteobacteria classes were similar to the changes in product composition. Especially, in case of S^0_{acc}, which production decreased 2.5 times from 25 to 10 °C while the presence of *β*-Proteobacteria (*Thauera* sp. and *Alicycliphilus* sp.) decreased by 2.3 times. This suggests that their presence is related to the HS^- oxidation to S^0 and its accumulation.

5.3 N/S molar ratio

The different N/S ratios (0.35, 0.40, 0.60, and 1.30) were examined under psychrophilic conditions (10 °C) after the temperature studies. The HS^- removal was influenced more by the N/S ratio changes than by the temperature changes. The highest HS^- removal was obtained at the lowest and highest studied N/S ratios, 89.2 and 89.6 %, respectively. Lower HS^- removal was obtained at intermediate N/S ratios with the lowest, 76.9 % obtained at N/S=0.60. Products distribution followed the general stoichiometric trend with more oxidized products as more NO_3^- was available. The concentrations deviated from theoretical predictions, implying that the reactions in continuous flow sludge bed bioreactors are more complicated than accounted for in stoichiometric models.

Increasing N/S feed ratio caused, as expected, an increase in SO_4^{2-} production. Depletion of stored S^0 was, however, also observed during this change even though literature claims that such oxidation occurs only when reduced sulfur compounds are depleted.

Apparently, the S^0 accumulated during the low N/S feed ratio was utilized at higher N/S, serving as an electron donor reserve. This utilization of stored energy led to SO_4^{2-} production and total effluent S concentration higher than total influent S. This can explain the lower removal of HS^- at mid-N/S ratios and high sulfur concentration obtained in the effluent at N/S=1.30.

Loss of the earlier accumulated S^0 (observed as higher effluent than feed sulfur concentration) emphasizes the importance of feed N/S ratio control in continuous process performance with variable inlet HS^- and NO_3^-. The presence of S^0 was confirmed by SEM analysis where sulfur and iron on the granular sludge surface (as FeS and S^0) were observed. Struvite was also found, implying that the investigated process can combine efficient sulfide removal with minerals precipitation where electron acceptor supply has a strong impact on product quality.

5.4 Future aspects

On the basis of the experience from the presented work, a few future aspects can be addressed enabling to further develop practical applications and give deeper insight into the biological HS^- oxidation with NO_3^-.

Further investigations related to the studied process ought to be focused on the product quality/purity. The investigations focused on the decrease of SO_4^{2-} production at N/S ratios referring to S^0 production and increasing the S^0 accumulation both under mesophilic and psychrophilic conditions should be performed. To achieve this goal, the working parameters like HRT, vertical velocity, slight N/S ratio corrections and reactor design should be investigated. Investigations ought to be followed with microbial community analysis, such as the relationship with S^0 accumulation and specific microorganisms can be found as in this study. Naturally, the scaling up from laboratory scale to, e.g., pilot scale is necessary for the process development.

The oxidation of accumulated S^0 was observed during this work. However, the mechanisms of this oxidation remain unknown. It occurs in contradiction

to the literature stating that oxidation of accumulated S^0 occurs only when reduced sulfur compounds are depleted. Here, it was observed that the bacteria oxidized accumulated S^0 in the presence of reduced sulfur compounds, probably to recover energy stored as sulfur. Further experiments focused on S^0 oxidation shall be performed to better understand this phenomenon. Such investigations should also lead to an improved mathematical model and process simulations since such S^0 release is not accounted for in the current models.

Since granular SOB sludge can accumulate S^0, such granular sludge can be harvested to maintain a stable sludge bed should be investigated in the future. Struvite was also observed to accumulate in the granules. Minerals precipitated in such granules may have a certain value and improve the environmental and economical attractiveness of the studied process, and should, therefore, be studied further. The obtained granular sludge consisting of S^0 and struvite may even serve as a fertilizer without further processing.

Part II

Article II

Metabolic divergence in simultaneous biological removal of nitrate and sulfide for elemental sulfur production under temperature stress

Michal Sposob, Rune Bakke, & Carlos Dinamarca

Published in *Bioresource Technology*, 233, 209-215, 2017.

Bioresource Technology 233 (2017) 209–215

Contents lists available at ScienceDirect

Bioresource Technology

journal homepage: www.elsevier.com/locate/biortech

Metabolic divergence in simultaneous biological removal of nitrate and sulfide for elemental sulfur production under temperature stress

Michal Sposob *, Rune Bakke, Carlos Dinamarca

University College of Southeast Norway, Kjølnes Ring 56, Porsgrunn 3918, Norway

HIGHLIGHTS

- Simultaneous biological nitrate and sulfide removal at 25–10 °C was documented.
- Sulfide removal was from 98 (25 °C) to 89.2% (10 °C) with complete nitrate removal.
- Elemental sulfur yield ranged from 83.7% at 25 °C to 67% at 10 °C.
- Accumulation of elemental sulfur decreased with temperature.
- Metabolic shift at lower temperature was indicated by increased sulfate production.

GRAPHICAL ABSTRACT

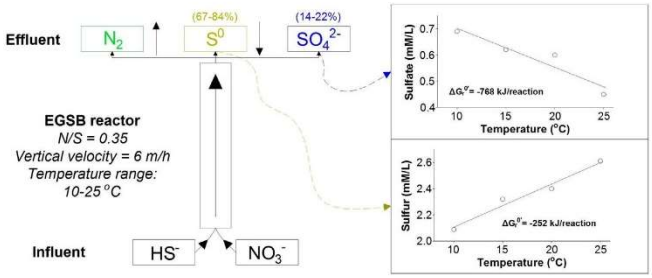

ARTICLE INFO

Article history:
Received 15 December 2016
Received in revised form 24 February 2017
Accepted 26 February 2017
Available online 28 February 2017

Keywords:
Autotrophic denitrification
Elemental sulfur recovery
Sulfate production
Sulfide removal
Temperature impact

ABSTRACT

The simultaneous removal of NO_3^- and HS^- at temperature stress (25–10 °C) is evaluated here. An expanded granular sludge bed (EGSB) reactor was run over 120 days at N/S molar ratio of 0.35 (for S^0 production) under constant sulfur loading rate of 0.4 kg S/m^3 d. The simultaneous removal of NO_3^- and HS^-, was achieved at applied conditions. Average HS^--S removal varied from 98 (25 °C) to 89.2% at 10 °C, with almost complete NO_3^- removal. Average S^0 yield ranged from 83.7 at 25 °C to 67% at 10 °C. The temperature drop caused a decrease in granular sludge accumulated S^0 fraction by nearly 2.5 times. Decreased temperature caused metabolic pathway change observed as higher SO_4^{2-} production, apparently allowing the biomass to obtain more energy per HS^- consumed. It is hypothesized that the metabolic shift is a natural response to compensate for temperature-induced changes in energy requirements.

1. Introduction

Hydrogen sulfide (H_2S) is commonly present in biogas, septic tanks, domestic and industrial wastewaters. Wastewaters rich in organic matter and sulfate (SO_4^{2-}) are providing the ideal conditions for active growth of sulfate reducing bacteria (SRB), leading to H_2S production. Typically, domestic wastewater consists around 10 mg HS^-/L (Pikaar et al., 2011). H_2S is characterized by its adverse impact, even at low concentrations, such as corrosion, odor release and toxicity, thus, H_2S removal is deemed to be necessary (Reyes-Avila et al., 2004). Many methods have been employed for H_2S removal from both gas and liquid phase. Physicochemical methods are effective and widely used for this purpose, however at considerable energy and catalyst costs and great amount of produced sludge (Li et al., 2009).

Biological methods are attractive alternatives to physicochemical methods due to lower operational and environmental costs. Commercially applied biological methods for H_2S removal use mainly oxygen (O_2) as electron acceptor. Alternative electron acceptors for biological H_2S removal are nitrate (NO_3^-) and nitrite

* Corresponding author.
E-mail address: michal.sposob@usn.no (M. Sposob).

http://dx.doi.org/10.1016/j.biortech.2017.02.122
0960-8524/

(NO_2^-) which can be easily added without system modifications. This property makes it easily applicable for sewer systems where NO_3^- or NO_2^- can be supplied at any place in the network (Auguet et al., 2016). NO_3^- and NO_2^- serve as electron acceptors for sulfide oxidizing bacteria (SOB) growth. Such impact of NO_2^- on H_2S production was highlighted already by Allen (1949) who found that the addition of nitrobenzene, dinitrobenzene or T.N.T. to sewage sludge inhibited H_2S production for prolonged periods. Autotrophic denitrification does not require organic substrates for bacterial growth so biomass production and operational costs are low (Sahinkaya and Dursun, 2012). Sulfide (HS^-) can be oxidized to elemental sulfur (S^0) and/or SO_4^{2-} depending on the relative presence of electron donor and acceptor as in Eqs. (1) and (2) (Kleerebezem and Mendez, 2002).

$$3HS^- + 3.9NO_3^- + 0.2NH_4^+ + HCO_3^- + 1.7H^+ \rightarrow CH_{1.8}O_{0.5}N_{0.2} + 1.95N_2 + 3SO_4^{2-} + 2.3H_2O \quad (1)$$

$$14.5HS^- + 5NO_3^- + 0.2NH_4^+ + HCO_3^- + 20.3H^+ \rightarrow CH_{1.8}O_{0.5}N_{0.2} + 2.5N_2 + 14.5S^0 + 17.4H_2O \quad (2)$$

Oxidation to S^0 can prevent the secondary pollution by SO_4^{2-}. NO_3^- and HS^- can be removed at their relative ratio corresponding to S^0 production according to Eq. (2). The combination of NO_3^- and O_2 as electron acceptors can enhance the S^0 production (Wang et al., 2015). S^0 obtained by such biological conversion is characterized by lower density and different crystalline structure than orthorhombic sulfur (Berg et al., 2014). Hydrophobic S^0 can be recovered by gravity sedimentation and its purity can be increased to above 99.9% (w/w) by applying a melting step (Janssen et al., 2001). Oxidation of HS^- to S^0 is convenient in terms of effluent quality and energy consumption since the lower amount of electron acceptor is used Eqs. (2) vs. (1). Biologically produced S^0 can be used as soil fertilizer or fungicide (Tan et al., 2016).

Factors evaluated in previous studies are C/N/S ratios, hydraulic retention time, load, pH, reactor configuration and stimulation of process startup (Guo et al., 2016; Huang et al., 2016; Mahmood et al., 2007; Montalvo et al., 2016; Reyes-Avila et al., 2004). However, temperature impact can be of utmost importance especially in cold climates. Sulfur-based denitrification under different temperatures has been evaluated in batch assays, where it showed that at 15 °C the denitrification efficiency ranged from 36 to 59% (Fajardo et al., 2014). Another study showed that a process operated at 15 °C can completely remove NO_3^- (Xu et al., 2016). Autotrophic denitrification driven by thiosulfate ($S_2O_3^{2-}$) even at 3 °C in a *Thiobacillus denitrificans* inoculated fluidized bed reactor has been reported (Di Capua et al., 2017). This report is a continuation of a preliminary study of temperature impact (Sposob et al., 2016), now with a longer experimental investigation and a thermodynamic evaluation of observations. Sposob et al. (2016) observed simultaneous NO_3^- and HS^- removal at 10 °C in a fluidized bed reactor.

In the present work, a laboratory-scale expanded granular sludge bed (EGSB) reactor was used to measure temperature effects on sulfide oxidation products distribution. The objective of this study was to evaluate the temperature impact (25–10 °C) on simultaneous NO_3^- and HS^- removal at N/S = 0.35 according to Eq. (2), constant sulfur loading rate of 0.4 kg S/m^3 d and continuous flow with focus on S^0 recovery.

2. Materials and methods

2.1. Inoculum and enrichment

The inoculum was taken from an up-flow anaerobic sludge blanket (UASB) methane generating reactor treating pulp and paper industry wastewater at Norske Skog Saugbrugs, Halden, Norway. The EGSB reactor was inoculated with 0.25 L of sludge, with a total solid content of 59.9 g/L and 86% organic fraction. The reactor was fed continuously with the same influent composition for one month at 25 ± 0.1 °C in order to condition and enrich the sludge prior to the experimental period reported here. The imposed lithoautotrophic conditions caused no methane production and the presence of sulfur components was observed during the conditioning stage.

2.2. Synthetic wastewater

The EGSB reactor synthetic feed contained $Na_2S{\cdot}9H_2O$ (3.12 mM S/L) with $NaHCO_3$ at concentration equivalent to Eq. (2). Potassium phosphate was used as buffer. Nitric acid (HNO_3) was used as a source of electron acceptor at N/S ratio of 0.35 according to Eq. (2). Electron acceptor feed contained the following stock solutions: (A) NH_4Cl (10 g/L), $MgCl_2{\cdot}6H_2O$ (10 g/L), $CaCl_2{\cdot}2H_2O$ (10 g/L); (B) K_2HPO_4 (300 g/L); (C) $MnSO_4{\cdot}H_2O$ (0.04 g/L), $FeSO_4{\cdot}7H_2O$ (2.7 g/L), $CuSO_4{\cdot}5H_2O$ (0.055 g/L), $NiCl_2{\cdot}6H_2O$ (0.1 g/L), $ZnSO_4{\cdot}7H_2O$ (0.088 g/L), $CoCl_2{\cdot}6H_2O$ (0.05 g/L), H_3BO_3 (0.05 g/L); (D) vitamin solution (Wolin et al., 1963), 10 times concentrated. HNO_3, stock solutions A (10 ml/L), B (2 ml/L), C (2 ml/L) and D (1 ml/L) were dissolved in distilled water. Electron donor ($Na_2S{\cdot}9H_2O$) and acceptor (HNO_3) were fed from separate bottles to prevent contamination and reactions in the feed bottles (Fig. 1).

2.3. Experimental setup

The laboratory-scale EGSB reactor was made of polycarbonate tube with an inner diameter of 32 mm and an effective height of 620 mm, giving a working volume of 0.5 L (Fig. 1). The reactor was equipped with a measurement tape (mm) for sludge bed height monitoring. Reactor temperature was maintained on the recirculation loop by cold plate cooler (TE Technology, Inc.). Four different temperatures (25, 20, 15 and 10 ± 0.1 °C) were tested under invariable influent composition. Temperature change was imposed when effluent composition reached pseudo-steady state.

Synthetic influent was introduced from 2 L influent vessels under nitrogen gas to avoid influent aging. Influent was pumped to reactor bottom at 2 L/d, equivalent to 6 h hydraulic retention time (HRT). Recycling pumping was set to reach 6 m/h vertical velocity necessary to expand the sludge bed. Reactor pH was maintained in the range 8.0–9.0 by a constant supply of potassium phosphate buffer and monitored by electrode (Hanna Instruments) on the recirculation loop (Fig. 1).

2.4. Analytical procedure

Effluent samples were collected daily and analysed immediately. Nitrate (NO_3^-), sulfate (SO_4^{2-}), sulfide (HS^-) and thiosulfate ($S_2O_3^{2-}$) in collected liquid samples (following 0.45 μm filtration) were measured by ion chromatography (Dionex ICS-5000). The concentration of HS^- (as HS^--S) was determined indirectly by potassium permanganate oxidation ($KMnO_4$). Sample separation and elution was performed using an IonPac AS11-HC 2 mm analytical column with potassium hydroxide (KOH) as eluent. Analysis started at 22 mM KOH, gradient started at 6 min, ramped up in 3 min to 45 mM and kept at this concentration for another 4 min. The data acquisition time is 13 min. The injection volume was 10 μl and the flow rate 0.3 ml/min.

2.5. Thiosulfate measurements

Measured effluent concentration of $S_2O_3^{2-}$ and SO_4^{2-} constituted a substantial fraction of the influent sulfur concentration. Applied

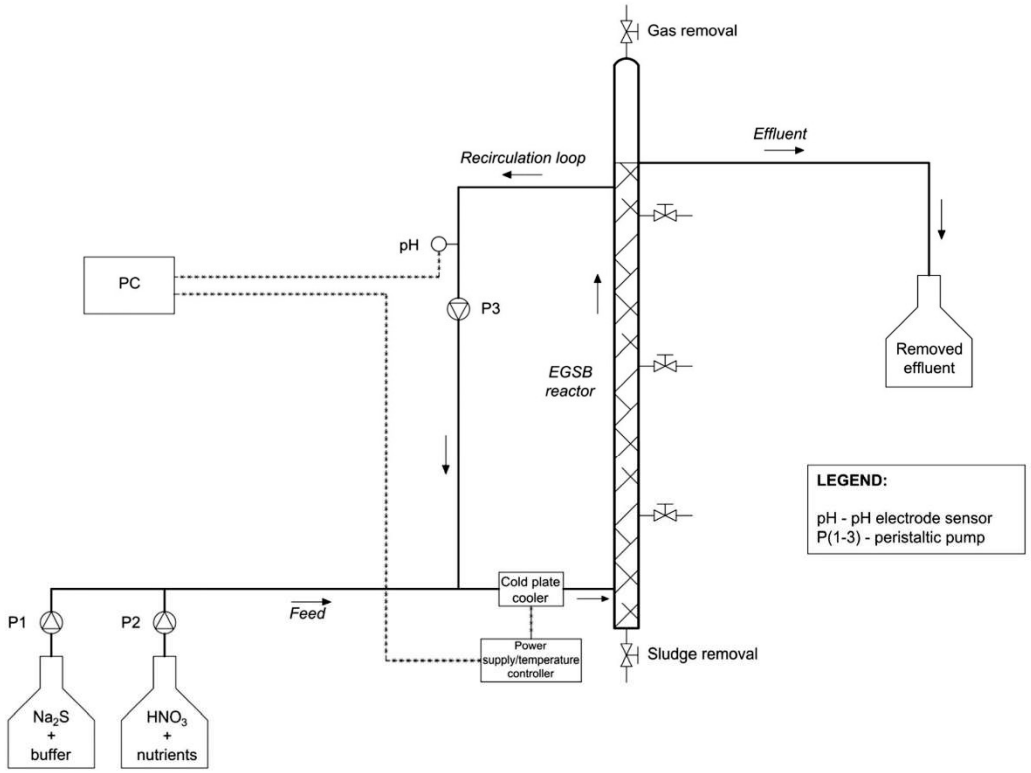

Fig. 1. Experimental setup.

N/S ratio should merely enable S^0 production. $S_2O_3^{2-}$ which is a richer sulfur carrier than SO_4^{2-}, consists of two sulfur atoms with different valence (−II and +VI) and can be disproportionated (Jørgensen, 1990). The $S_2O_3^{2-}$ disproportionation does not require the change in oxidation level of sulfur and leads to HS^- and SO_4^{2-} production as in the Eq. (3).

$$S_2O_3^{2-} + H_2O \rightarrow HS^- + SO_4^{2-} + H^+ \quad (3)$$

Microbial oxidation of HS^- to $S_2O_3^{2-}$ has been reported by several authors, which is often associated with low concentrations and transient formation mediated by abiotic factors and/or phototrophic conditions (Holkenbrink et al., 2011; Steudel et al., 1990). The theoretical catabolic reaction of HS^- oxidation to $S_2O_3^{2-}$ in NO_3 presence shows that the N/S ratio is equal to 0.8 in Eq. (4).

$$HS^- + 0.8NO_3^- + 0.8H^+ \rightarrow 0.5S_2O_3^{2-} + 0.4N_2 + 0.9H_2O$$
$$\Delta G_r^{0\prime} = -393.14\ \text{kJ/reaction} \quad (4)$$

In this study the limited availability of NO_3^- (N/S = 0.35) should not favor the HS^- oxidation to $S_2O_3^{2-}$ to occur. The complete uptake of electron acceptor for $S_2O_3^{2-}$ production would oxidize 1.35 mM HS^-/L (43.3% of influent HS^--S) that is equal to 0.675 mM $S_2O_3^{2-}$/L. Measurements suggest the presence of $S_2O_3^{2-}$ caused by applied analytical method (Sposob et al., 2016). The alkaline eluent used in the analysis cause the oxidation of S^0 present in liquid phase to $S_2O_3^{2-}$ implying that what appears as $S_2O_3^{2-}$ in the analysis is actually S^0. The mass balance of the present study (up to 100% of HS^--S was removed and S^0 and SO_4^{2-} were present as products) supports this understanding and it is therefore assumed, thought-out Results and Discussion, that what appears to be $S_2O_3^{2-}$ is actually S^0.

2.6. Elemental sulfur balance

SOBs have the ability to store S^0 as sulfur globules as their electron reserve (Shively, 1974). The analysis of the amount S^0 attached to the biofilm revealed that similar proportion of S^0 was attached at different sulfur loads (Li et al., 2009). The collected, filtered samples were characterized by turbidity and presence of milky, yellow color. Similar observations are made in several publications (Chen et al., 2008; Doğan et al., 2012; Krishnakumar and Manilal, 1999), suggesting the presence of S^0 in the liquid phase (while measured as $S_2O_3^{2-}$). Thus, two different fractions of S^0 can be distinguished, the first accumulated into the granules (denoted as S^0_{acc}) and a suspended elemental sulfur fraction (S^0_{ss}). The suspended fraction is probably produced on the surface of the granular sludge from which it is detached to become freely disperse in the liquid phase. The S^0_{acc} denotes the S^0 fraction that includes all granular sludge associated sulfur, whether tightly adhered to the surface of the granular sludge, to the internal granular structures, to the internal reactor surface or incorporated within bacteria as sulfur globules as electron reserves. Distinguishing between these two S^0 fractions (S^0_{acc} and S^0_{ss}) is done here based on the elemental sulfur balance as an indirect method for quantification of accumulated elemental

sulfur (S^0_{acc}). Concentration of S^0_{acc} is calculated based on the difference between influent concentration of HS^- and effluent concentrations of HS^-, SO^{2-}_4 and S^0_{ss}, according to Eq. (5). Due to alkaline pH maintained in the EGSB reactor, presence of H_2S in the gas phase is neglected in the balance.

$$S^0_{acc} = HS^-_{inf} - HS^-_{eff} - SO^{2-}_{4eff} - S^0_{ss} \quad (5)$$

3. Results and discussion

3.1. Reactor performance

Reactor performance monitored as pH, NO^-_3 and HS^- removal over 120 days is shown in Figs. 2 and 3. pH did not change significantly with temperature and remained above 8.0, allowing the electron donor to be present in ionized form ranging from average 8.41 at 25 °C to 8.11 at 10 °C (Fig. 2). The highest pH variations were observed at 25 and 20 °C and much less at the lower temperatures, perhaps related to microbial community adaptation, initially from anaerobic digestion to lithoautotrophic conditions and later due to the imposed temperature changes. The imposed temperature changes had not a significant impact on the bioreactor biomass measured as granular bed height level, which during the experimental period remained nearly constant at 1/3 of the reactor height.

Simultaneous removal of NO^-_3 and HS^- at constant sulfur loading rate of 0.4 kg S/m^3 d was achieved at all tested temperatures. NO^-_3 was completely removed and detected in the effluent only in three occasions at the lowest temperature (Fig. 3). The electron donor was also removed up to 100%, but its removal decreased with decreasing temperature (Fig. 3). The average HS^--S removal varied from 98% at 25 °C to 89.2% at 10 °C. The overall reactor effluent concentrations are summarized in Table 1.

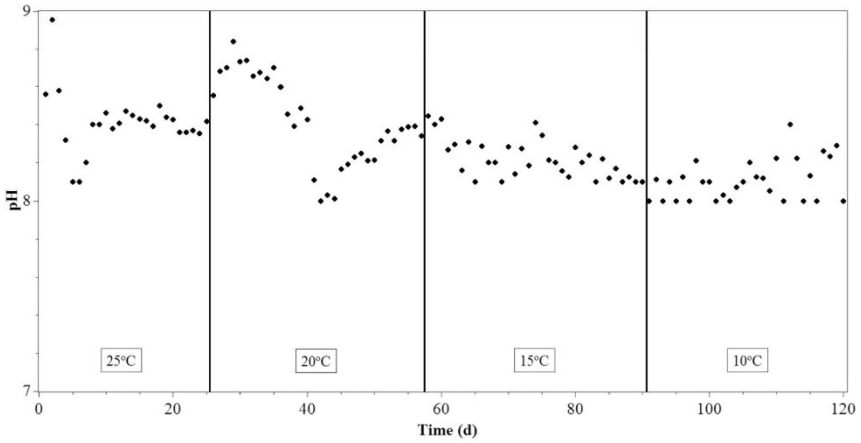

Fig. 2. pH profile with time at 25, 20, 15 and 10 °C.

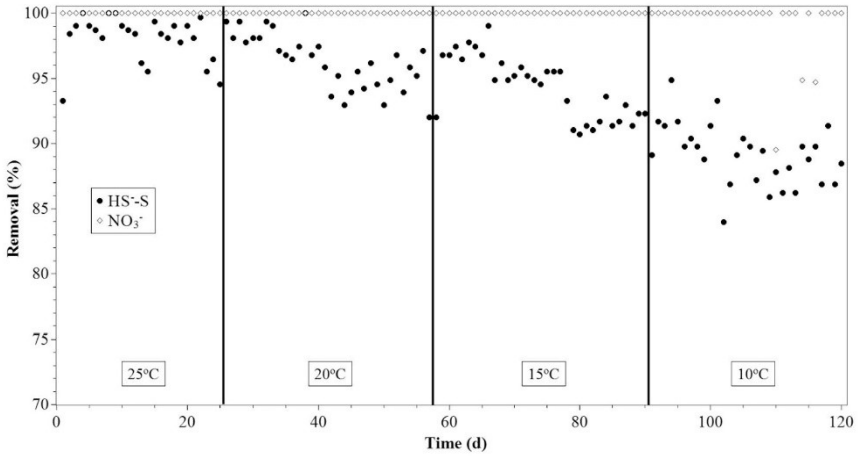

Fig. 3. The substrates (NO^-_3 and HS^--S) removal with time at 25, 20, 15 and 10 °C.

Table 1
Average HS^--S, S^0_{acc}, S^0_{ss}, S^0, SO_4^{2-}, and NO_3^- effluent concentrations at 25, 20, 15 and 10 °C. Percentages in parenthesis indicate fractions of influent sulfur.

Temperature (°C)	HS^--S (mM/L)	S^0_{acc} (mM/L)	S^0_{ss} (mM/L)	$^*S^0$ (mM/L)	SO_4^{2-} (mM/L)	NO_3^- (mM/L)
25	0.06 ± 0.06 (1.9%)	1.41 ± 0.19 (45.2%)	1.2 ± 0.19 (38.5%)	2.61 ± 0.38 (83.7%)	0.45 ± 0.09 (14.4%)	n.d.
20	0.12 ± 0.06 (3.8%)	1.31 ± 0.25 (42.0%)	1.09 ± 0.15 (34.9%)	2.4 ± 0.4 (76.9%)	0.6 ± 0.11 (19.2%)	n.d.
15	0.18 ± 0.07 (5.8%)	0.92 ± 0.15 (29.5%)	1.4 ± 0.07 (44.9%)	2.32 ± 0.22 (74.4%)	0.62 ± 0.08 (19.9%)	n.d.
10	0.34 ± 0.07 (10.9%)	0.57 ± 0.21 (18.3%)	1.52 ± 0.16 (48.7%)	2.09 ± 0.37 (67.0%)	0.69 ± 0.11 (22.1%)	0.07 ± 0.03

n.d. – not detected; $^*S^0 = S^0_{acc} + S^0_{ss}$; ± – standard deviation

HS^- removal efficiencies during biological treatment are often reported between 90 and 100% depending on experimental conditions and reactor design (Syed et al., 2006). Different S^0 yields have been reported as 50, 71, 79 or 88% in Beristain-Cardoso et al. (2008), Huang et al. (2016), Krishnakumar and Manilal (1999) and Li et al., 2009, respectively. S^0 yield obtained at 25 °C (83.7%) is in the upper range of those previously reported (Table 1). S^0 yield dropped with temperature to the lower range reported by others, however, the analytical and quantification procedures differ between reports. The regulation of height/volume of UASB reactor has been reported as a significant factor influencing S^0 production (Huang et al., 2016). The conversion rate has been enhanced from 20–37 to 45–70% in an UASB reactor by *Thiopseudomonas denitrificans* X2 bioaugumentation (Tan et al., 2016). However, the obtained enhancement effect decreased with time.

The percentage shares of sulfur components for all samples (summarized as average values in Table 1) are presented in Fig. 4 to visualize the observed trends and metabolic shift. S^0 was the target product at imposed N/S ratio in the reactor according to Eq. (2). Nonetheless, SO_4^{2-} was always present on the effluent. Studies conducted at conditions focused on S^0 production frequently report accompanying SO_4^{2-} production. This phenomenon have been explained by exposure to atmospheric O_2 as an abiotic factor during sample handling (Cai et al., 2008), where other studies state that SO_4^{2-} production was caused by further oxidation of S^0 accumulated in the reactor (Li et al., 2009). In the presented experiment, the production and share of SO_4^{2-} in sulfur effluent components were increasing with temperature decrease (Fig. 4, Table 1). Simultaneously the oxidation of HS^- to S^0 decreased with temperature. During the experiment, the total 15 °C temperature drop caused an increase of average SO_4^{2-} concentration by 53% (from 0.45 to 0.69 mM/L). The maximum conversion of HS^--S to S^0 reached 90.4% at 25 °C. Average S^0 yield dropped from 83.7% at 25 °C to 67.0% at 10 °C. The fraction of S^0_{ss} was increasing from average 38.5% at 25 °C to 48.7% at 10 °C. This increase in S^0_{ss} fraction may have been caused by the removal of accumulated S^0_{acc}. Alternatively or in addition there may have been an increasing number of microorganisms in suspension at lower temperatures due changes in the granular sludge characteristics causing erosion or detachment of microorganisms (Park et al., 2005; Yang et al., 2016). It was however beyond the scope of this work to investigate such mechanisms. The total 15 °C temperature drop caused a decrease in S^0_{acc} by nearly 2.5 times (Table 1) giving S^0_{acc} at 10 °C equal to 18.3% of influent sulfur.

3.2. Substrates metabolism

An energy analysis based on electron distribution is applied to interpret the observation that imposed temperature changes had not a significant impact on NO_3^- removal while it had strong impact on the relative presence of effluent sulfur components. Since no other electron acceptor was intentionally supplied during the experiment, reduction of NO_3^- had HS^- as a sole electron donor. This indicates that temperature caused a change in the metabolic microbial pathway and their functionality.

The observation that metabolized NO_3^- did not yield only in S^0 suggests the existence of another processes associated with oxidation of reduced sulfur compounds and nitrogen reduction. SOBs can use different ratios of N/S and oxidize reduced sulfur into S^0 and/or SO_4^{2-} (Kleerebezem and Mendez, 2002). Catabolic reactions leading to S^0 or SO_4^{2-} production show that reaction for SO_4^{2-} production is the more exothermic of the two Eqs. (6) and (7). This makes it the most attractive way for chemosynthesis (Muyzer et al., 2013). Production of SO_4^{2-} requires 4 times more NO_3^- than S^0 production. It implies a decrease in standard free Gibbs energy by 3 times and is thereby more exothermic.

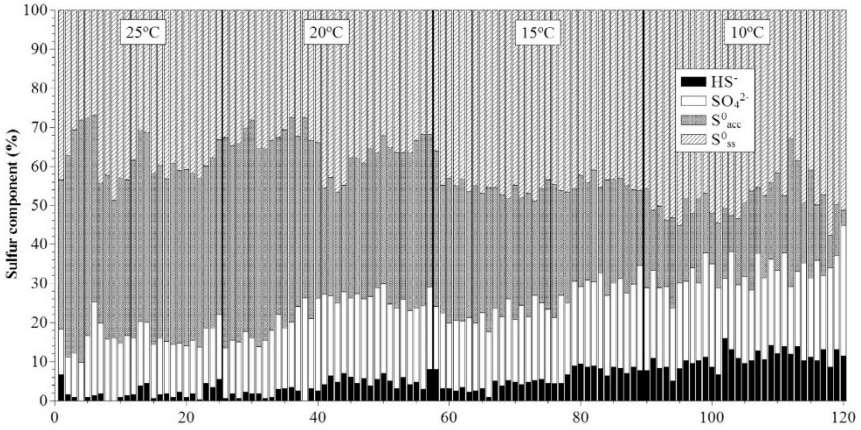

Fig. 4. Percentage share of sulfur components each day for the entire experiment at 25, 20, 15 and 10 °C (based on concentrations expressed as mM S/L).

Table 2
Electron flow as percentages of meq derived from HS^- oxidation, presented as average values for each temperature level tested.

Temperature (°C)	% Metabolized to S^0	% Metabolized to SO_4^{2-}	% Energy output	% Remaining energy as S^0	% as S_{acc}
25	21.3	14.7	36.0	64.0	34.6
20	20.0	19.9	40.0	60.0	32.8
15	19.7	21.1	40.8	59.2	23.5
10	18.8	24.8	43.6	56.4	15.4

$$HS^- + 0.4NO_3^- + 1.4H^+ \rightarrow S^0 + 0.2N_2 + 1.2H_2O$$
$$\Delta G_r^{0'} = -252.13\ \text{kJ/reaction} \quad (6)$$

$$HS^- + 1.6NO_3^- + 0.6H^+ \rightarrow SO_4^{2-} + 0.8N_2 + 0.8H_2O$$
$$\Delta G_r^{0'} = -768.28\ \text{kJ/reaction} \quad (7)$$

By calculating the electron flow as miliequivalents (meq) split between two pathways by temperature it is clear that the overall energy output for maintenance and/or growth did change as cells diminished their energy storing as S^0 and increased SO_4^{2-} production (Table 2). The biomass thereby managed to balance the need for more energy due to decreased temperature by increasing the proportion of HS^- metabolized to SO_4^{2-} from 14.4 to 22.1% (Table 1). This allowed, according to Eqs. (6) and (7), a total metabolic energy production to increase by 7.6%. It can be noted that SO_4^{2-} production did give a 10.1% energy equivalents increase for the HS^- oxidized, where the difference is due to a lower overall HS^- removal efficiency (Figs. 3 and 4). Data presented in Table 2 and Fig. 4 shows that increased presence of HS^- in the effluent follows the increase in SO_4^{2-} share, while the S^0_{acc} decreased from 45.2 (25 °C) to 18.3% at 10 °C.

To evaluate how the energy obtained from NO_3^- reduction has been used, it is assumed that NO_3^- not used for S^0 production was used for SO_4^{2-} production. Due to autotrophic conditions, the amount of NO_3^- used by heterotrophic bacteria using organic matter originating from bacterial lysis was assumed negligible. Calculated uptake of electron donor and acceptor using Eqs. (1) and (2) shows that the probable percentage share of NO_3^- used in the metabolic pathway leading to SO_4^{2-} production increased from 4.4% (25 °C) to 8.9% at 10 °C, suggesting that the SO_4^{2-} production will be even less at temperature >25 °C. The amount of HS^--S oxidized by NO_3^- decreased along with temperature from 88.1 (25 °C) to 75.9% at 10 °C (Table 3). Observed decrease was a result of two factors: incomplete oxidation of HS^- and a second factor related to the observation that 12.2 ± 1.6% of HS^--S was oxidized to SO_4^{2-} using some other unknown electron acceptor(s). Evidently, based on Table 2, there was not enough potential in the supplied NO_3^- to fully account for the observed HS^- oxidation. The flow of unknown electron acceptor(s) could be more complicated than assumed, where it could have an impact on both pathways at unknown ratios. However, the assumption that unknown electron acceptor(s) have only impact on SO_4^{2-} seems to be an appropriate simplification. Here we can only speculate on what other substances than NO_3^- may have served as the electron acceptor, for instance H^+ to give H_2 gas, inorganic carbon to biomass, organic substances or unintended exposure to O_2.

Table 3
The average percentage distribution of electron acceptor in relation to electron donor availability.

Temperature (°C)	% by SO_4^{2-} pathway	% by S^0 pathway	% of HS^--S oxidized by NO_3^-
25	4.4	83.7	88.1
20	6.2	76.9	83.1
15	6.9	74.4	81.3
10	8.9	67	75.9

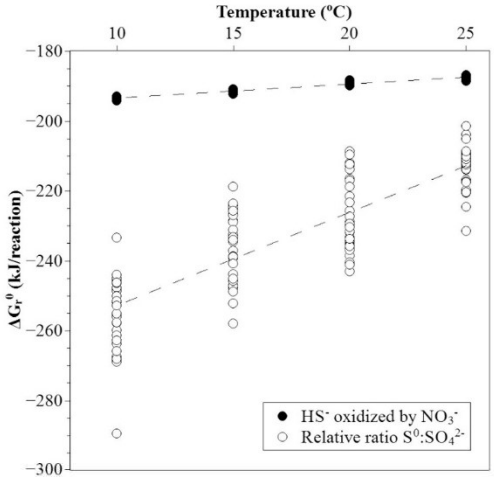

Fig. 5. The comparison of free Gibbs energy between relative S^0:SO_4^{2-} ratio (R^2 = 0.6788) and HS^--S oxidized by NO_3^- (R^2 = 0.9662).

3.3. Free Gibbs energy

The free Gibbs energy is calculated for the four temperatures tested here to evaluate whether changes in free Gibbs energy can explain the observed shift in metabolic pathways. The free Gibbs energy of catabolic reactions used Eqs. (5) and (6) is corrected by H^+, pH and temperature impacts as in Eq. (8) (Rittmann and McCarty, 2001). Calculations include twofold approach where free Gibbs energy was calculated separately for the percentage of HS^- oxidized by NO_3^- and for relative percentage share of two pathways according to Table 3.

$$\Delta G_r^0 = \Delta G_r^{0'} - RTv_{H^+} \ln[10^{-pH}] \quad (8)$$

The free Gibbs energy including the percentage of HS^--S oxidized by NO_3^-, remained relatively stable (Fig. 5): level = −190.4 ± 2.8 kJ/reaction with only 3.4% decrease from 25 to 10 °C. Calculations including the relative share between pathways showed that free Gibbs energy decreased with temperature, making the overall reaction more exothermic with lower temperature (Fig. 5). Free Gibbs ranged from −212.6 (25 °C) to −255.2 at 10 °C (20% decrease).

Obtained values based on relative share between pathways imply increased energy gain for catabolism with the shift towards more SO_4^{2-} production (Table 2), and suggest a linear temperature dependence (Fig. 5). The increased share of HS^- going through the SO_4^{2-} pathway can change the overall biomass yield since, according to Eqs. (1) and (2), the biomass yield is significantly higher when SO_4^{2-} is produced than S^0. The increasing biomass yield from HS^- by increasing the SO_4^{2-} pathway share facilitates to maintain nearly stable free Gibbs energy for catabolism, even at decreasing HS^- removal. It appears that the microbial community tried to compensate for less favorable growth conditions at lower temperatures by a slight shift in metabolic pathways towards a more energy rich pathway. The result of this behavior was almost complete consumption of NO_3^- in connection with

increased SO_4^{2-} production and increased presence of unreacted HS^- with decreasing temperature.

Metabolic pathway shifts can be caused by maintenance energy (m_E) requirements (van Bodegom, 2007). The m_E term is related to some minimal Gibbs energy compensating unavoidable leaks and denaturation processes occurring in organisms, which can be influenced by temperature (Pirt, 1965; Tijhuis et al., 1993).

The observed shift in metabolic pathways may have been caused by microbial competition induced by temperature stress causing changes in the microbial community. An alternative explanation is that the temperature drop induced the metabolic shift in existing organisms. A deeper insight in dynamic changes of microbial community structure caused by temperature stress is necessary to resolve this.

4. Conclusions

Simultaneous NO_3^- and HS^- removal at constant load and N/S ratio was obtained at 25 to 10 °C. HS^--S removal varied from 98% (25 °C) to 89.2% (10 °C) with complete NO_3^- removal. Average S^0 yield ranged from 83.7% at 25 °C to 67% at 10 °C.

Decreased temperature caused significant metabolic changes, which are observed as increased SO_4^{2-} production and decreased elemental sulfur production and accumulation.

The metabolic shift apparently allowed the biomass to obtain more energy per HS^- consumed, hypothesized to be a natural response by the microbiota to compensate temperature-induced changes in catabolic energy requirements.

Acknowledgements

The authors would like to thankYARA AS International and The Research Council of Norway for support of this research.

References

Allen, L.A., 1949. The effect of nitro-compounds and some other substances on production of hydrogen sulphide by sulphate-reducing bacteria in sewage. Proc. Soc. Appl. Bacteriol. 12, 26–38.
Auguet, O., Pijuan, M., Borrego, C.M., Gutierrez, O., 2016. Control of sulfide and methane production in anaerobic sewer systems by means of Downstream Nitrite Dosage. Sci. Total Environ. 550, 1116–1125.
Berg, J.S., Schwedt, A., Kreutzmann, A.-C., Kuypers, M.M.M., Milucka, J., 2014. Polysulfides as intermediates in the oxidation of sulfide to sulfate by Beggiatoa spp. Appl. Environ. Microbiol. 80, 629–636.
Beristain-Cardoso, R., Texier, A.C., Sierra-Alvarez, R., Field, J.A., Razo-Flores, E., Gimez, J., 2008. Simultaneous sulfide and acetate oxidation under denitrifying conditions using an inverse fluidized bed reactor. J. Chem. Technol. Biotechnol. 83, 1197–1203.
Cai, J., Zheng, P., Mahmood, Q., 2008. Effect of sulfide to nitrate ratios on the simultaneous anaerobic sulfide and nitrate removal. Bioresour. Technol. 99, 5520–5527.
Chen, C., Ren, N., Wang, A., Yu, Z., Lee, D.J., 2008. Simultaneous biological removal of sulfur, nitrogen and carbon using EGSB reactor. Appl. Microbiol. Biotechnol. 78, 1057–1063.
Di Capua, F., Milone, I., Lakaniemi, A.-M., Lens, P.N.L., Esposito, G., 2017. High-rate autotrophic denitrification in a fluidized-bed reactor at psychrophilic temperatures. Chem. Eng. J. 313, 591–598.
Doğan, E.C., Türker, M., Dağaçsan, L., Arslan, A., 2012. Simultaneous sulfide and nitrite removal from industrial wastewaters under denitrifying conditions. Biotechnol. Bioprocess Eng. 17, 661–668.
Fajardo, C., Mora, M., Fernández, I., Mosquera-Corral, A., Campos, J.L., Méndez, R., 2014. Cross effect of temperature, pH and free ammonia on autotrophic denitrification process with sulphide as electron donor. Chemosphere 97, 10–15.
Guo, Q., Hu, H.Y., Shi, Z.J., Yang, C.C., Li, P., Huang, M., Ni, W.M., Shi, M.L., Jin, R.C., 2016. Towards simultaneously removing nitrogen and sulfur by a novel process: ana4mmox and autotrophic desulfurization-denitrification (AADD). Chem. Eng. J. 297, 207–216.
Holkenbrink, C., Barbas, S.O., Mellerup, A., Otaki, H., Frigaard, N.-U., 2011. Sulfur globule oxidation in green sulfur bacteria is dependent on the dissimilatory sulfite reductase system. Microbiology 157, 1229–1239.
Huang, C., Li, Z., Chen, F., Liu, Q., Zhao, Y., Gao, L., Chen, C., Zhou, J., Wang, A., 2016. Efficient regulation of elemental sulfur recovery through optimizing working height of upflow anaerobic sludge blanket reactor during denitrifying sulfide removal process. Bioresour. Technol. 200, 1019–1023.
Janssen, A.J.H., Ruitenberg, R., Buisman, C.J.N., 2001. Industrial applications of new sulphur biotechnology. Water Sci. Technol. 44, 85–90.
Jørgensen, B.B., 1990. A thiosulfate shunt in the sulfur cycle of marine sediments. Science 249, 152–154.
Kleerebezem, R., Mendez, R., 2002. Autotrophic denitrification for combined hydrogen sulfide removal from biogas and post-denitrification. Water Sci. Technol. 45, 349–356.
Krishnakumar, B., Manilal, V.B., 1999. Bacterial oxidation of sulphide under denitrifying conditions. Biotechnol. Lett. 21, 437–440.
Li, W., Zhao, Q., Liu, H., 2009. Sulfide removal by simultaneous autotrophic and heterotrophic desulfurization-denitrification process. J. Hazard. Mater. 162, 848–853.
Mahmood, Q., Zheng, P., Cai, J., Wu, D., Hu, B., Li, J., 2007. Anoxic sulfide biooxidation using nitrite as electron acceptor. J. Hazard. Mater. 147, 249–256.
Montalvo, S., Huiliñir, C., Gálvez, D., Roca, N., Guerrero, L., 2016. Autotrophic denitrification with sulfide as electron donor: effect of zeolite, organic matter and temperature in batch and continuous UASB reactors. Int. Biodeterior. Biodegrad. 108, 158–165.
Muyzer, G., Kuenen, J.G., Robertson, L.A., 2013. Colorless sulfur bacteria. In: Rosenberg, E., DeLong, E.F., Lory, S., Stackebrandt, E., Thompson, F. (Eds.), The Prokaryotes: Prokaryotic Physiology and Biochemistry. Springer Berlin Heidelberg, Berlin, Heidelberg, pp. 555–588.
Park, K.Y., Kim, D.Y., Chung, T.H., 2005. Granulation in an upflow anaerobic sequencing batch reactor treating disintegrated waste activated sludge. Water Sci. Technol. 52, 105–111.
Pikaar, I., Rozendal, R.A., Yuan, Z., Keller, J., Rabaey, K., 2011. Electrochemical sulfide removal from synthetic and real domestic wastewater at high current densities. Water Res. 45, 2281–2289.
Pirt, S.J., 1965. The maintenance energy of bacteria in growing cultures. Proc. R. Soc. London. Ser. B. Biol. Sci. 163, 224–231.
Reyes-Avila, J., Razo-Flores, E., Gomez, J., 2004. Simultaneous biological removal of nitrogen, carbon and sulfur by denitrification. Water Res. 38, 3313–3321.
Rittmann, B.E., McCarty, P.L., 2001. Environmental biotechnology: principles and applications. In: McGraw-Hill Series in Water Resources and Environmental Engineering. McGraw-Hill.
Sahinkaya, E., Dursun, N., 2012. Sulfur-oxidizing autotrophic and mixotrophic denitrification processes for drinking water treatment: elimination of excess sulfate production and alkalinity requirement. Chemosphere 89, 144–149.
Shively, J.M., 1974. Inclusion bodies of prokaryotes. Annu. Rev. Microbiol. 28, 167–188.
Sposob, M., Dinamarca, C., Bakke, R., 2016. Short-term temperature impact on simultaneous biological nitrogen-sulphur treatment in EGSB reactor. Water Sci. Technol. 74, 1610–1618.
Steudel, R., Holdt, G., Visscher, P.T., van Gemerden, H., 1990. Search for polythionates in cultures of Chromatium vinosum after sulfide incubation. Arch. Microbiol. 153, 432–437.
Syed, M., Soreanu, G., Falletta, P., Béland, M., 2006. Removal of hydrogen sulfide from gas streams using biological processes – a review. Can. Biosyst. Eng. 48, 1–14.
Tan, W., Huang, C., Chen, C., Liang, B., Wang, A., 2016. Bioaugmentation of activated sludge with elemental sulfur producing strain Thiopseudomonas denitrificans X2 against nitrate shock load. Bioresour. Technol. 220, 647–650.
Tijhuis, L., van Loosdrecht, M.C.M., Heijnen, J.J., 1993. A thermodynamically based correlation for maintenance Gibbs energy requirements in aerobic and anaerobic chemotrophic growth. Biotechnol. Bioeng. 42, 509–519.
van Bodegom, P., 2007. Microbial maintenance: a critical review on its quantification. Microb. Ecol. 53, 513–523.
Wang, X., Zhang, Y., Zhou, J., Zhang, T., Chen, M., 2015. Regeneration of elemental sulfur in a simultaneous sulfide and nitrate removal reactor under different dissolved oxygen conditions. Bioresour. Technol. 182, 75–81.
Wolin, E.A., Wolin, M.J., Wolfe, R.S., 1963. Formation of methane by bacterial extracts. J. Biol. Chem. 238, 2882–2886.
Xu, Y., Chen, N., Feng, C., Hao, C., Peng, T., 2016. Sulfur-based autotrophic denitrification with eggshell for nitrate-contaminated synthetic groundwater treatment. Environ. Technol. 37, 3094–3103.
Yang, W., Lu, H., Khanal, S.K., Zhao, Q., Meng, L., Chen, G.H., 2016. Granulation of sulfur-oxidizing bacteria for autotrophic denitrification. Water Res. 104, 507–519.

Article III

Temperature-induced changes in microbial community under autotrophic denitrification with sulfide

Michal Sposob, Agnieszka Cydzik-Kwiatkowska, Rune Bakke, & Carlos Dinamarca

Published in *Process Biochemistry*, 69, 161-168, 2018.

Process Biochemistry 69 (2018) 161–168

Contents lists available at ScienceDirect

Process Biochemistry

journal homepage: www.elsevier.com/locate/procbio

Temperature-induced changes in a microbial community under autotrophic denitrification with sulfide

Michal Sposob[a,*], Agnieszka Cydzik-Kwiatkowska[b], Rune Bakke[a], Carlos Dinamarca[a]

[a] University College of Southeast Norway, Kjølnes Ring 56, 3918 Porsgrunn, Norway
[b] University of Warmia and Mazury in Olsztyn, Department of Environmental Biotechnology, Sloneczna Str. 45G, 10-709 Olsztyn, Poland

ARTICLE INFO

Keywords:
Autotrophic denitrification
Elemental sulfur recovery
Microbial community change
Sulfide removal
Temperature change

ABSTRACT

This study investigated temperature-induced changes in a microbial community performing autotrophic denitrification with HS^- for S^0 recovery. The study was performed over 120 days in an expanded granular sludge bed (EGSB) reactor at invariable feeding conditions (0.4 kg S/m^3 d loading rate and 0.35 N/S molar ratio). NO_3^- and HS^- were simultaneously removed at 25–10 °C range. Average HS^--S removal was 98 and 89% at 25 and 10 °C, respectively. While NO_3^- was completely removed in studied temperature range. High-throughput sequencing indicated that the transition from methanogenic conditions (inoculum sludge) to the imposed experimental conditions led to development of a Proteobacteria dominated phylum. *β*-Proteobacteria (mainly *Thauera* sp. and *Alicycliphilus* sp.) predominated at 25 °C (64%), when the S^0 accumulation was the highest (45%). Decreasing temperature to 10 °C, reduced both the abundance of *β*-Proteobacteria (2.3 times to 28%) and the accumulation of S^0 (2.5 times to 18%). At 10 °C, chemolithoautotrophic sulfide-oxidizing bacteria belonging to *Sulfurimonas* sp. and *Thiobacillus* sp. were present in the biomass (over 34% of all sequences) while S^0_{ss} and SO_4^{2-} production increased slightly. These results indicate that temperature-induced changes in the microbial community influenced reactor performance and effluent characteristics, especially S^0 accumulation.

1. Introduction

Hydrogen sulfide (H_2S) is a corrosive, harmful and odorous compound found in diverse wastewaters [1–3]. It can be removed by both biological and/or physicochemical methods. Biological treatment methods have many advantages over physicochemical methods, which are costly and can lead to the production of large sludge amounts; thus, require downstream treatment units.

Nitrate (NO_3^-) presence in water causes eutrophication [4] and can have the adverse impact on human health [5]. It is therefore widely regulated by law and has to be reduced to nitrogen gas (N_2) in industrial and municipal wastewater treatment plants. NO_3^- and HS^- can be biologically removed by sulfide-oxidizing bacteria (SOB), where H_2S (or its ionic forms HS^-/S^{2-}) serves as an electron donor for autotrophic denitrification.

The degree of HS^- oxidation in simultaneous removal of NO_3^- and HS^- depends on their molar ratio [6,7] and S^0 and/or SO_4^{2-} production can therefore be controlled by changing the ratio between electron donor and acceptor (Eqs. (1) and (2)).

$$HS^- + 0.4NO_3^- + 1.4H^+ \rightarrow S^0 + 0.2N_2 + 1.2H_2O \quad \Delta G_r^{0'} = -252\ \text{kJ/mol} \quad (1)$$

$$HS^- + 1.6NO_3^- + 0.6H^+ \rightarrow SO_4^{2-} + 0.8N_2 + 0.8H_2O \quad \Delta G_r^{0'} = -768\ \text{kJ/mol} \quad (2)$$

Based on catabolic reactions the oxidation to S^0 is possible at low N/S ratio (0.40, Eq. (1)). At a high N/S ratio (1.60, Eq. (2)), the electron donor is oxidized to SO_4^{2-}. However, the complete description of the studied process should include the biomass production by microbial growth (anabolism). Reactions including biomass based on the energy dissipation method were proposed by Kleerebezem and Mendez [8], where oxidation to S^0 is reflected at N/S = 0.35, whereas oxidation to SO_4^{2-} at N/S = 1.30.

Oxidation to S^0 seems to be a more sustainable pathway for HS^- treatment, since the secondary pollution from SO_4^{2-} production can be avoided. In heterotrophic conditions SO_4^{2-} can be reduced to HS^- by sulfate reducing bacteria (SRB) as shown in Eq. (3) [9].

$$SO_4^{2-} + \text{organic matter} \rightarrow HS^- + H_2O + HCO_3^- \quad (3)$$

The produced S^0 is stored in bacterial inclusion bodies by SOB [10]. Thus, S^0 is accumulated in granular sludge that can be removed from reactor, facilitating sulfur (S) recovery. This kind of resource recovery can be beneficial, and the excess S^0-containing sludge might be used as

* Corresponding author.
E-mail address: michal.sposob@usn.no (M. Sposob).

https://doi.org/10.1016/j.procbio.2018.03.006
Received 13 December 2017; Received in revised form 12 February 2018; Accepted 11 March 2018
Available online 15 March 2018

a soil fertilizer or fungicide [11]. Unlike 'inorganic' S^0, biologically produced S^0 is characterized by hydrophilicity [12].

Studies focused on process optimization for S^0 recovery have been performed [3,13–15]. It has been observed that a transition from low to high N/S ratios can lead to the release of previously accumulated S^0 [6]. Moreover, temperature has an impact on the changes in distribution of sulfur components in the effluent, pointing to metabolic shift to maintain the energy supply at lower temperatures [14].

The impact of operational parameters on microbial structure of biomass and distribution of sulfur compounds during S^0 recovery in autotrophic denitrification reactors is hardly understood. Thus, the aim of the present study is to investigate how the microbial community structure changes in response to temperature change from the mesophilic to the psychrophilic range in autotrophic denitrification EGSB reactor with HS^- as an electron donor.

2. Materials and methods

2.1. Inoculum

The inoculum (total solid content 59.9 g/L with 86% organic fraction) was taken from an up-flow anaerobic sludge blanket (UASB) methane-generating reactor treating wastewater at a paper mill in Halden, Norway. Half of the effective volume of the EGSB reactor was inoculated with this granular sludge. After inoculation, the reactor was fed NO_3^- and HS^- continuously for one month to enrich the sludge before the experimental trail. Feeding conditions and working parameters at enrichment period were as for the first period of experimental trial.

2.2. Synthetic wastewater

The synthetic feed contained $Na_2S{\cdot}9H_2O$ (3.12 mM S/L) with $NaHCO_3$ as the carbon source and phosphate ($H_2PO_4^-/HPO_4^{2-}$) was used as pH buffer to avoid gaseous H_2S by maintaining pH > 8.0. Nitric acid (HNO_3) at the equivalent concentration to N/S = 0.35 molar ratio was used as the electron acceptor source. Additionally, feed contained the stock solutions of minerals and vitamins [14]. Electron donor ($Na_2S{\cdot}9H_2O$) and acceptor (HNO_3) were fed from separate bottles to avoid contamination and possible study-related microbial growth in feed bottles (Fig. 1).

2.3. Experimental setup

The laboratory-scale EGSB reactor was made of polycarbonate with an inner diameter of 32 mm and an effective height of 620 mm, giving a 0.5 L working volume (Fig. 1). The EGSB reactor was operated continuously at 25–10 ± 0.1 °C temperature range in 4 steps under invariable feeding properties (Table 1). Temperature was controlled on the recirculation loop by a cold plate cooler (TE Technology, Inc.).

Feed was introduced from 2 L influent vessels under nitrogen gas to avoid influent aging. Vertical velocity was set to 6 m/h by adjusting the recirculation flow (P3). Reactor pH was maintained above 8.0 by a constant supply of potassium phosphate buffer and was monitored by electrode (Hanna Instruments) placed on the recirculation loop (Fig. 1). Hydraulic retention time was 6 h.

2.4. Analytical procedure and data evaluation

Effluent samples collected daily were analysed immediately. Nitrate (NO_3^-), nitrite (NO_2^-), sulfate (SO_4^{2-}), sulfide (HS^-) and suspended elemental sulfur (S^0_{ss}, measured as thiosulfate $S_2O_3^{2-}$ [14]) in collected liquid samples (following 0.45 µm filtration) were measured by ion chromatography (Dionex ICS-5000). The concentration of HS^- (as HS^--S) was determined indirectly by potassium permanganate oxidation ($KMnO_4$).

At imposed feeding conditions, the accumulation of S^0 was expected. The accumulated fraction of S^0 was denoted as S^0_{acc}, and calculated using sulfur balance equation (Eq. (4)) where the effluent and influent sulfur components are included [16]. Unstable sulfur anion intermediates as $S_4O_6^{2-}$ are assumed present in insignificant quantities for the sulfur balance. H_2S presence in gas phase was neglected in the balance due to pH value (> 8.0) maintained in the reactor.

$$S^0_{acc} = HS^-_{inf} - HS^-_{eff} - SO^{2-}_{4eff} - S^0_{ss} \quad (4)$$

2.5. Molecular methods

Reactor biomass samples were collected at the end of two temperature stages (25 and 10 °C). Additionally, before the experiment start, reactor inoculum sample was collected. Species composition of biomass samples was analyzed. The collected samples were stored at −20 °C. DNA was isolated from the samples using the FastDNA® SPIN Kit for Soil (MP Biomedicals). Purity and concentration of the isolated DNA was measured on a Lite NanoDrop spectrometer (Thermo Scientific). A universal 515F (GTGCCAGCMGCCGCGGTAA) and a 806R (GGACTACHVGGGTWTCTAAT) primer set were used to amplify the archaeal and bacterial 16S rDNA genes [17]. The amplicons were sequenced using the MiSeq Illumina platform in Research and Testing Laboratory (USA). Over 162 thousands of full sequences were obtained.

For chimera detection and removal, UCHIME [18] was used in *de novo* mode with the clustered, denoised data (minimum average quality score of 30 for the base). The reads were condensed into FASTA format and sequences were removed if they had low-quality tags, or were less than half the expected amplicon length or less than 250 bp in length. USEARCH global alignment [19] was used to cluster the sequences into operational taxonomic units (OTUs) with 100% sequence identity. A .NET algorithm utilizing BLASTN+ was used to query the FASTA formatted files with seed sequences for each cluster against a database of NCBI derived sequences. A sequence with an identity score greater than 97% was resolved at the species level; one with a score between 95% and 97%, at the genus level; between 90% and 95%, at the family level; between 85% and 90%, at the order level; 80–85%, at the class level; and 77% to 80%, at the phyla level. Rarefaction analysis was done and showed that the sampling depth was sufficient to accurately characterize the bacterial community.

Alignment of the obtained sequences was performed by Infernal [20]; while clustering by Complete-Linkage Clustering using modules of the RDPipeline (http://rdp.cme.msu.edu/). Sequences were assigned to phylotype clusters at five cutoff levels of 1%, 3%, 5%, 7% and 10% and these data were used for rarefaction analysis with the RDP module. The Shannon-Wiener index of diversity (H') and evenness index (E) were calculated using modules of the RDPipeline [21]. For visualization of the dependence between all present taxa in inoculum and sludge from the EGSB operated at 25 and 10 °C, the Venn diagram was used, generated by Venny software 2.1.0 [22]. The sequences have been deposited in the Sequence Read Archive (SRA) NCBI within BioProject PRJNA398347 as an experiment 'Metagenome of autotrophic denitrification digesters in the presence of HS^-'.

3. Results and discussion

3.1. Substrates removal and products formation

Simultaneous removal of NO_3^- and HS^- was observed at all tested temperatures. Average HS^- removal was 98 and 89% at 25 and 10 °C, respectively. NO_3^- was completely removed during experimental period, with only traces close to the detection limit (below 0.05 mM NO_3^-/L) measured thrice at 10 °C. The NO_2^- presence was not observed in reactor effluent. Reactor pH remained above 8.0 over the experimental period ranging from 8.41 (25 °C) to 8.11 (10 °C).

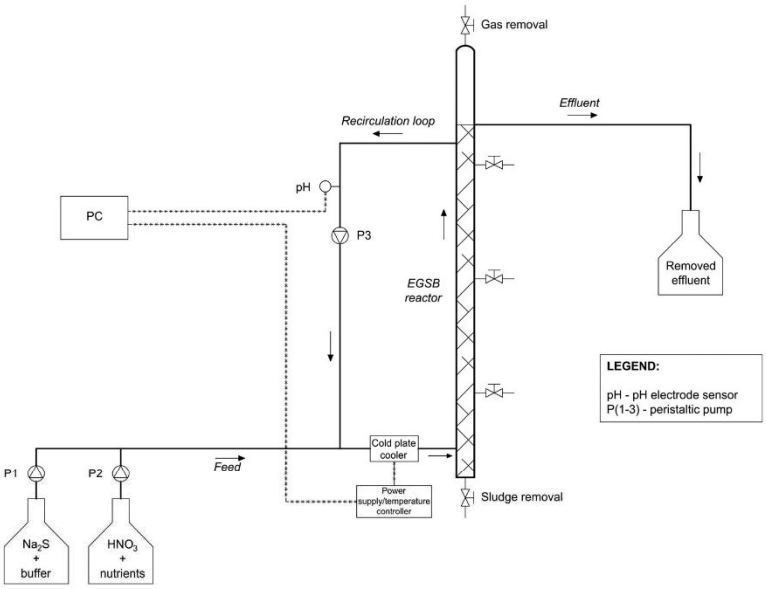

Fig. 1. Experimental setup.

Table 1
Experimental plan.

Temperature (°C)	Time (days)	Influent NO_3^- (mM/L)	Influent HS^- (mM/L)
25	1–25	1.08	3.12
20	26–57		
15	58–90		
10	91–120		

Temperature had a clear impact on HS^- oxidation products distribution (Fig. 2). S^0 yield ($S^0_{acc} + S^0_{ss}$) decreased with temperature from 84 to 67% at 25 and 10 °C, respectively. The S^0_{acc} decreased from 45 to 18%, while S^0_{ss} and SO_4^{2-} production increased. SO_4^{2-} production share increased from 14 to 22%. Simultaneous decrease of HS^- removal and S^0 as product while SO_4^{2-} increase with temperature drop can be related to temperature adaptation mechanism, as oxidation of HS^- to SO_4^{2-} is a more energy-rich pathway than oxidation to S^0. Thus, the observed shift compensates the energy losses on the decreased HS^- removal and S^0 production [14]. Hence, at lower temperatures more NO_3^- per mole of HS^- removed was used. Observed changes are suspected to be related to changes in microbial community with temperature.

3.2. Microbial communities in the inoculum and the EGSB reactor operated at 25 and 10 °C

Illumina high-throughput sequencing shows significant diversity differences between the inoculum, the EGSB reactor sludge at 25 and at 10 °C (Table 2). The overall biomass diversity (H') was highest in the inoculum (7.19), lower at 25 °C (6.60) and lowest at 10 °C (6.19). A similar tendency was observed for species evenness (E) dropping from 0.75 in the inoculum. At 25 °C, the E value was 0.69 and it decreased to 0.64 during EGSB operation at 10 °C. The decrease in both diversity and evenness show that the biomass was inhabited by a lower number of species in autotrophic compared to heterotrophic conditions. Even with lower diversity, the bacterial community is evidently capable of utilizing this inorganic feed at the studied temperature range. The results of the present study show that evaluation of capacity of microbial community to utilize substrates should be mostly focused on species composition and not on the overall diversity and that even community with low diversity can ensure efficient substrates removal.

In all three biomass samples, 231 microbial taxa were identified (Fig. 3). 59.3% of all detected taxa in all studied samples were shared between the communities at 25 and 10 °C. At 25 °C, the microbial community had a low number of individual sequences (only 2.2%); however, the microbial community that developed at 10 °C was unique, and 38 new microbial taxa were identified that were not detected both at 25 °C and in the inoculum (Fig. 3).

Taxa such as *Bacteroides* sp. (Bacteroidetes), *Cytophaga* sp. or Firmicutes, represented mostly by Clostridia class, were numerous in the inoculum and their abundance markedly decreased in the presence of sulfuric compounds in the influent, independent of the temperature (Figs. 4 and 5). The inoculum had the highest share of Archaea (18.6%). Under autotrophic denitrification conditions, the Archaea share diminished to 3.2% and 5.7% at 25 and 10 °C, respectively. Methanogenic Archaea were represented by the Methanobacteria and Methanomicrobia classes. The abundance of *Methanosaeta* sp. belonging to Methanomicrobia was similar at both operational temperatures (1.3–1.4%); however, the abundance of *Methanobacterium* sp. belonging to Methanobacteria increased from 1.7% at 25 °C to 4.2% at 10 °C (Fig. 5).

Bacteria dominated in the EGSB reactor, reaching 96.7 and 94.2% at 25 and 10 °C, respectively. The transition from methanogenic (inoculum origin) to autotrophic denitrification conditions resulted in increased presence of Proteobacteria, which indicates that microorganisms belonging to this phylum are responsible for simultaneous NO_3^- and HS^- removal. Proteobacteria comprised 72.1 and 71.0% of all sequences obtained from the biomass at 25 and 10 °C, respectively, while the share of Proteobacteria in the inoculum was minor (4.8%).

Proteobacteria have been reported to be common in denitrifying bioreactors for simultaneous NO_3^- and HS^- removal [23]. Our study

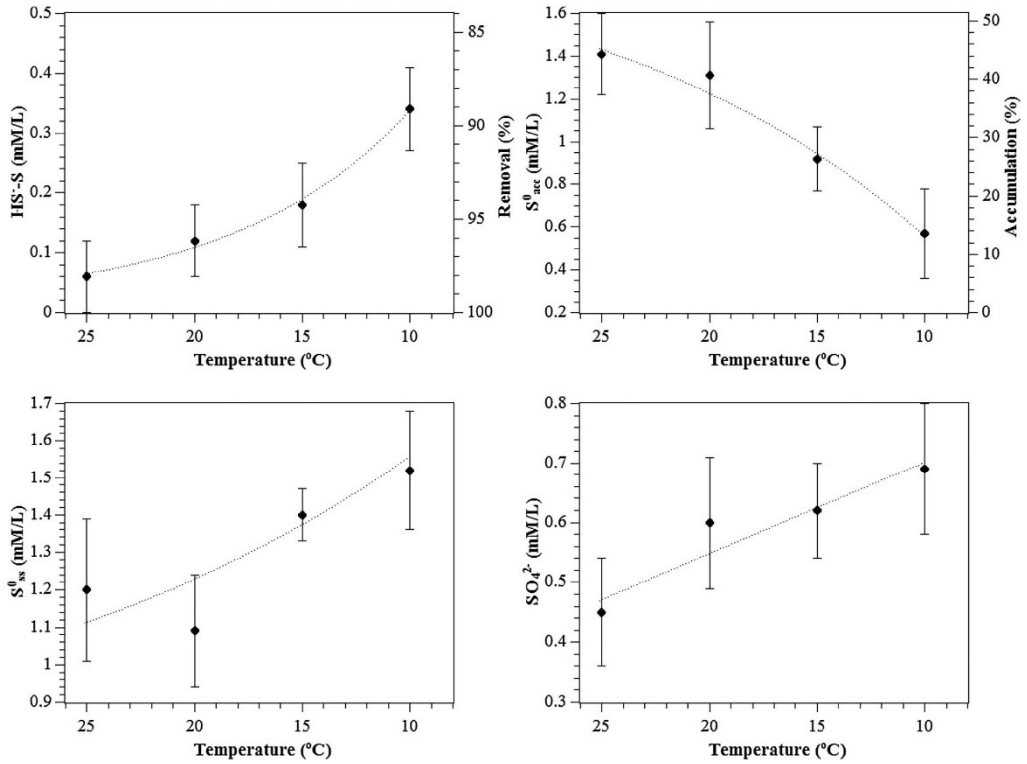

Fig. 2. Average accumulation of S^0_{acc}, removal of HS^--S and concentrations of sulfur components in the effluent from EGSB operated at the temperature range from 25 to 10 °C (error bars show standard deviation).

Table 2
Diversity indexes for inoculum and biomass from EGSB operated at 10 °C and 25 °C.

Sample	No. of OTUs	Shannon-Wiener index of diversity (H')	Evenness index (E)
Inoculum	14,980	7.19	0.75
25 °C	13,656	6.60	0.69
10 °C	15,392	6.19	0.64

point out that the predominant Proteobacteria classes changed depending on the temperature (Fig. 4). At 25 °C, sequences belonging to β-Proteobacteria comprised over 64% of all sequences, while their share decreased below 28% at 10 °C. ε-Proteobacteria, on the other hand, constituted 31.8% at 10 °C (1% at 25 °C), implying a completive advantage of ε-Proteobacteria at low temperature.

Both denitrifiers and SRB coexisted in the EGSB, independent of the operational temperature. Denitrifiers grow faster than SRB and NO_3^- respiration is more energetically favorable than SO_4^{2-} respiration [24]. It is known that some strains of SRB are able to coexist despite selective pressure from NO_3^- [25]. *Desulfomicrobium* was able to remain in the biomass in the nitrate-rich environment and comprised about 1.5% of identified sequences in the biomass when the EGSB was operated at 25 °C in the present study.

Thauera sp. (39.4%) and *Alicycliphilus* sp. (17.6%) representing β-Proteobacteria comprised 57% of all sequences identified in the biomass from the reactor operated at 25 °C (Fig. 5). The genus *Alicycliphilus* includes many nitrate-reducing bacteria that use a broad range of organics for denitrification, however, in this study organic carbon was not

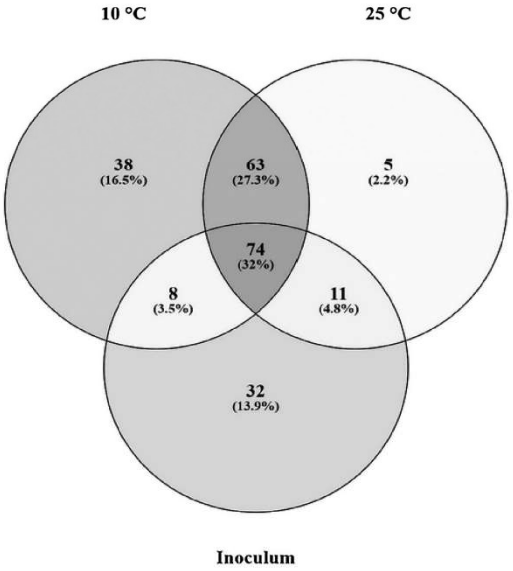

Fig. 3. Venn diagram illustrating the taxa that were shared and unique to the three microbial communities (% value describes the percentage of the total taxa number).

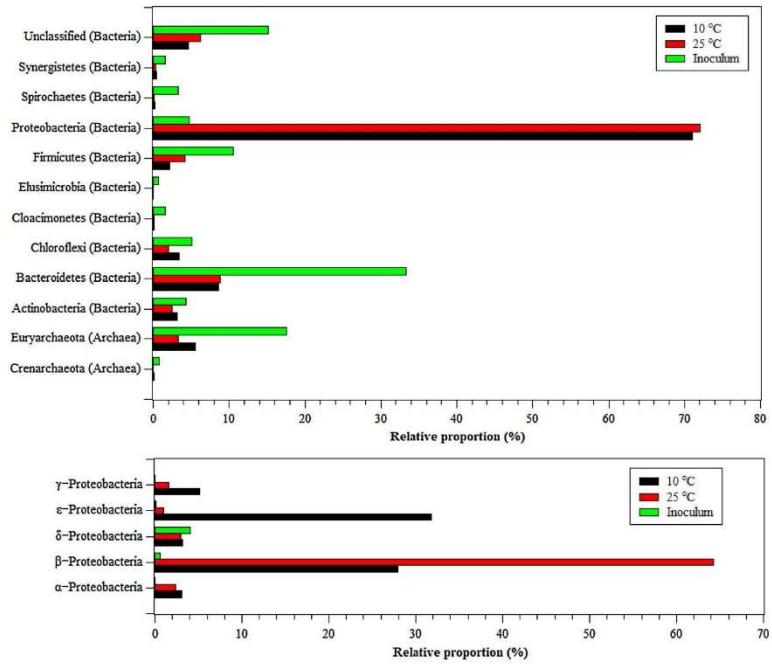

Fig. 4. The relative proportion of 16S rDNA gene sequences at phylum level (upper) and Proteobacteria class level (lower) (> 0.5% threshold).

supplied. Under denitrifying conditions, for example, *Alicycliphilus denitrificans* strain K601 used cyclohexanol, cyclohexanone, monocarboxylic acids (C2–C7), adipate or pimelate as electron donors, and NO_3^-, NO_2^- and O_2 but not SO_4^{2-}, SO_3^{2-} or fumarate as electron acceptors [26]. Bacteria belonging to *Alicycliphilus* sp. are also able to grow anaerobically on acetone or sodium lauryl ether sulfate as sole carbon and energy sources with NO_3^- as an electron acceptor [27,28]. Previous studies have shown that bacteria from genera *Alicycliphilus* are sensitive to the presence of SO_4^{2-} in both bioreactors [29] and microbial electrochemical denitrification systems [30]. Our results show the temperature-sensitivity of members of *Alicycliphilus* sp. and that they prefer higher operational temperatures during autotrophic denitrification in an EGSB.

Thauera spp. are one of the most active denitrifiers in wastewater treatment plants [11] and have been reported to play an important role in removal of quinolones and chemical oxygen demand under denitrifying conditions [31]. *Thauera* spp. were identified as one of the predominant genera during NO_3^- and HS^- removal [32,33] and their presence varied in different parts of the UASB reactor. In the low-level sections of a sludge bed, the number of *Thauera* sp. was highest, and their share in the biomass decreased in the higher parts of the sludge bed [3].

Thauera spp. and *Thiobacillus* spp. convert HS^- to S^0 and NO_3^- to N_2. In the present study, the change in temperature changed the balance between these sulfide-converting genera. The abundance of *Thauera* sp. was nearly 5 times lower at 10 °C (8.2%) than at 25 °C (39.4%), whereas *Thiobacillus* sp. were 3 times more abundant at 10 °C (3.5%) than at 25 °C (0.9%).

Hydrogenophaga sp. was not detected in the inoculum, but its abundance increased to 3.5 − 4.4% in the EGSB reactor in the present

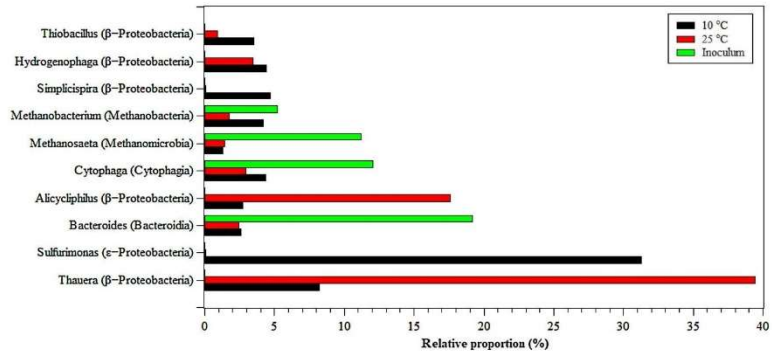

Fig. 5. The relative proportion of the most abundant genera relative proportion of 16S rDNA gene sequences (the list of all detected genera is included in Appendix A).

study. The abundance of hydrogen-oxidizing *Hydrogenophaga* sp. is associated with the amount of hydrogen in the environment. For example, *Hydrogenophaga* sp. predominated in the microbial community of a glass bead biofilm reactor using H_2 as an electron donor to remove NO_3^- at a concentration of 150 mg NO_3/L [34]. In a hydrogenotrophic denitrification reactor supplied with H_2, the relative abundance of *Hydrogenophaga* spp. (30.3–39.3%) was highest with a high and constant hydrogen supply flow rate, whereas *Thauera* spp. (58.5%) and *Methyloversatilis* spp. (26.0%) predominated with a low or intermittent hydrogen supply [35]. However, H_2 was not supplied in the present study, and the production of H_2 was not expected according to the process stoichiometry. The electron balance shows that the supplied NO_3^- was not enough to receive all electrons from HS^- oxidation based on the obtained products [14]. The presence of H_2 consumers observed here, even though no H_2 was supplied, indicates that H_2 production and consumption may have occurred in some not well understood synergistic relationships that can potentially explain the inequality in the electron balance. Potential production of H_2 could be related with fermentation processes where the decaying microorganisms serve as the carbon source.

Previous research has shown that, although *Hydrogenophaga* sp. and *Thauera* sp. are both autotrophic denitrifiers, they differ in tolerance to the presence of organics in wastewater. *Hydrogenophaga* sp. grew well with or without organics while *Thauera* sp. appeared to be the predominant genus (23.6%) in reactors fed inorganic wastewater [36]. The present study indicates that *Hydrogenophaga* sp. tolerated low temperatures in the treatment system better than *Thauera* sp. At the two tested temperatures, the abundance of *Hydrogenophaga* sp. was relatively stable, changing from 3.5 to 4.4%, whereas *Thauera* sp. nearly 5 times more abundant at 25 °C (39.4%) than at 10 °C (8.2%).

Simplicispira sp. occurred (4.7%) only when the EGSB was operated at the lowest temperature in our study. Bacteria from this genus are identified in wastewater treatment systems [37] and some species, e.g. *Simplicispira psychrofila*, possess NO_2^- reductase (NO-forming) activity and are able to denitrify. The denitrifying activity of *Simplicispira* sp. may have supported denitrification at 10 °C when the amount of other denitrifiers in the biomass, such as *Thauera* sp., decreased.

Our results indicate that *Sulfurimonas* spp. predominated (over 31% of all identified sequences) in the biomass only when the EGSB was operated under psychrophilic conditions (Fig. 5). *Sulfurimonas* species are commonly isolated from sulfidic habitats such as hydrothermal deep-sea vents, marine sediments, the ocean's water column, and terrestrial habitats [38]. *Sulfurimonas* spp. have been demonstrated to play an important role in chemoautotrophic processes due to the ability to grow with a variety of electron donors and acceptors [39]. Most *Sulfurimonas* species are capable of growing with hydrogen as electron donor. Some of them such as *S. denitrificans* and *S. hongkongensis* can grow with hydrogen and NO_3^- [39–41], that may explain their high abundance in nitrate-fed EGSB observed here.

3.3. Interrelation between microbial communities and reactor performance

The results presented above show that temperature impacts reactor performance, especially in terms of effluent sulfur products distribution. The considerable decrease in S^0_{acc} (from 45 to 18%) with lower temperatures corresponded to large changes in microbial community composition. To correlate the reactor's product distribution with molecular analysis the two most abundant members of Proteobacteria phylum (β- and ε-Proteobacteria) together with concentrations of four effluent sulfur components (HS^-, S^0_{acc}, S^0_{ss}, and SO_4^{2-}) were interrelated as shown in Fig. 6.

Based on the analysis presented in Fig. 6 the community structure and certain classes correspond best to the obtained effluent characteristic. It is visible in case of β-Proteobacteria represented by a few different species detected in high abundance. The members of β-Proteobacteria such as *Alicycliphilus* sp., *Hydrogenophaga* sp., Burkholderiales, *Simplicispira* sp., *Thauera* sp., and *Thiobacillus* sp. mostly contributed (> 2% of relative abundance) in class structure.

It was also observed that the high abundances of *Thauera* sp. and *Alicycliphilus* sp. (β-Proteobacteria) were related to high level of S^0_{acc} suggesting that β-Proteobacteria were involved in autotrophic denitrification resulting in HS^- oxidation to S^0. The 2.5 times lower S^0_{acc} at 10 °C (compared to 25 °C) was reflected in microbial community changes. At 10 °C under unaltered influent composition, the relative presence of β-Proteobacteria diminished from 64.2% at 25 °C to 27.9% at 10 °C (nearly 2.3 times), thus, to similar degree as S^0_{acc}.

Predominance of *Sulfurimonas* sp. (ε-Proteobacteria) related with increased production of S^0_{ss} and SO_4^{2-} in the effluent when EGSB was operated at 10 °C was observed here. It has been reported that in S^0 production under simultaneous NO_3^- and HS^- removal with oxygen (O_2) addition (microaerophilic conditions) the β- and ε-Proteobacteria presence was minor (< 10%) [42]. While under simultaneous carbon (C), N and S removal, increasing NO_3^- concentration in the influent resulted in increased abundance of ε-Proteobacteria (Arcobacteria and *Sulfurospirillum* sp.) [23]. Increasing concentration of NO_3^- leads to N/S ratio change where at higher ratios oxidation of HS^- to SO_4^{2-} is promoted (Eqs. (1) and (2)). In this study, at 10 °C a change in the microbial community occurred facilitating appropriate conditions for *Sulfurimonas* sp. growth. Based on the interrelation between microbial community and reactor performance the ε-Proteobacteria involvement in S^0_{acc} production is arguable. Development of *Sulfurimonas* sp. could more likely be related to the increased production of S^0_{ss} and SO_4^{2-}. The relation between higher production of these two components and presence of ε-Proteobacteria was reflected in the effluent characteristic. At lower temperature, the amount of NO_3^- used per mole of HS^- oxidized slightly increased leading to lower removal of HS^- due to limited NO_3^- supply.

Psychrophilic conditions (10 °C) were more appropriate for ε-Proteobacteria than for β-Proteobacteria. Lower temperatures favored microorganisms related with complete oxidation of HS^- even if the ratio was kept favorable for S^0 production. The dependence between the structure of microbial community, effluent characteristic and thermodynamic considerations [14] give an interesting information on how the microbial community may compensate energy requirements under different temperature conditions.

The main practical implication of the findings in this study is that efficient autotrophic sulfide removal can be carried out at low temperatures. HS^- can be removed almost as efficient at psychrophilic as at mesophilic temperatures by autotrophic denitrification, even if the microbial communities are different. It appears that more specialized microorganisms (lower diversity) manage to maintain almost complete substrates removal at colder conditions. In psychrophilic conditions, microorganisms accumulate less S^0 than the mesophilic, implying that mesophilic conditions are favorable when sulfur recovery is an aim.

4. Conclusions

The microbial community in an EGSB reactor operated for HS^- removal by autotrophic denitrification changed when temperature was reduced from 25 to 10 °C causing HS^--S removal to drop from 98 to 89% while NO_3^- removal remained complete. Temperature decrease reduced both diversity and evenness of the microbial community. The biomass was predominated by Proteobacteria (5% in the inoculum and over 70% in EGSB) that points to their key involvement in simultaneous NO_3^- and HS^- removal.

The changes in microbial community, triggered by the imposed temperature change, influenced the distribution of sulfur components in the effluent. *Thauera* sp. and *Alicycliphilus* sp. involved in HS^- oxidation to S^0 and its accumulation comprised over 57% of all sequences identified in the EGSB reactor operated at 25 °C. The 2.5 times lower S^0_{acc} at 10 °C (compared to 25 °C) corresponded to decrease in relative presence of both these genera (2.3 times lower) in EGSB operated at

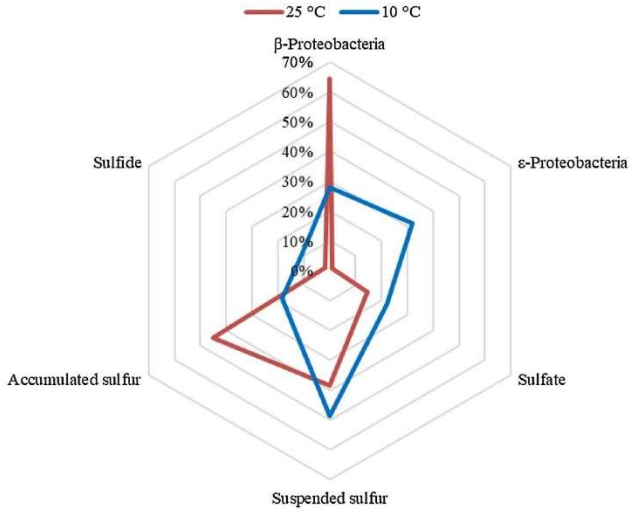

Fig. 6. The interrelation between microbial community and reactor performance at 25 and 10 °C (values on radar plot describe a percentage share in terms of total sulfur effluent for sulfur components and abundance for Proteobacteria).

10 °C.

At 10 °C ε-Proteobacteria (mostly *Sulfurimonas* sp., 31.3%) predominated. Their presence is argued to be related with slightly increased S^0_{ss} and SO_4^{2-} production at the invariable feeding conditions investigated here.

Acknowledgements

The authors would like to thank YARA AS International and The Research Council of Norway for support of this research. We would like to express special thanks to Agnieszka Montusiewicz, PhD (Lublin University of Technology, Poland) for facilitating cooperation between the authors of the manuscript.

Appendix A. Supplementary data

Supplementary data associated with this article can be found, in the online version, at https://doi.org/10.1016/j.procbio.2018.03.006.

References

[1] H. Ma, X. Cheng, G. Li, S. Chen, Z. Quan, S. Zhao, L. Niu, The influence of hydrogen sulfide on corrosion of iron under different conditions, Corros. Sci. 42 (2000) 1669–1683.
[2] F.F. Xia, Y. Su, X.M. Wei, Y.H. He, Z.C. Wu, A. Ghulam, R. He, Diversity and activity of sulphur-oxidizing bacteria and sulphate-reducing bacteria in landfill cover soils, Lett. Appl. Microbiol. 59 (2014) 26–34.
[3] C. Huang, Q. Liu, C. Chen, F. Chen, Y.-K. Zhao, L.-F. Gao, W.-Z. Liu, J.-Z. Zhou, Z.-L. Li, A.-J. Wang, Elemental sulfur recovery and spatial distribution of functional bacteria and expressed genes under different carbon/nitrate/sulfide loadings in up-flow anaerobic sludge blanket reactors, J. Hazard. Mater. 324 (2017) 48–53.
[4] G.F. McIsaac, M.B. David, G.Z. Gertner, D.A. Goolsby, Eutrophication: nitrate flux in the Mississippi river, Nature 414 (2001) 166–167.
[5] L. Knobeloch, B. Salna, A. Hogan, J. Postle, H. Anderson, Blue babies and nitrate-contaminated well water, Environ. Health Perspect. 108 (2000) 675–678.
[6] M. Sposob, R. Bakke, C. Dinamarca, Effects of N/S molar ratio on products formation in psychrophilic autotrophic biological removal of sulfide, Water (Switzerland) 9 (2017).
[7] J. Cai, P. Zheng, Q. Mahmood, Effect of sulfide to nitrate ratios on the simultaneous anaerobic sulfide and nitrate removal, Bioresour. Technol. 99 (2008) 5520–5527.
[8] R. Kleerebezem, R. Mendez, Autotrophic denitrification for combined hydrogen sulfide removal from biogas and post-denitrification, Water Sci. Technol. 45 (2002) 349–356.
[9] G. Tchobanoglous, F.L. Burton, H.D. Stensel, Wastewater Engineering: Treatment and Reuse, fourth edition, (2003).
[10] J.M. Shively, Inclusion bodies of prokaryotes, Annu. Rev. Microbiol. 28 (1974) 167–188.
[11] W. Tan, C. Huang, C. Chen, B. Liang, A. Wang, Bioaugmentation of activated sludge with elemental sulfur producing strain Thiopseudomonas denitrificans X2 against nitrate shock load, Bioresour. Technol. 220 (2016) 647–650.
[12] A.J.H. Janssen, P.N.L. Lens, A.J.M. Stams, C.M. Plugge, D.Y. Sorokin, G. Muyzer, H. Dijkman, E. Van Zessen, P. Luimes, C.J.N. Buisman, Application of bacteria involved in the biological sulfur cycle for paper mill effluent purification, Sci. Total Environ. 407 (2009) 1333–1343.
[13] C. Huang, Z. Li, F. Chen, Q. Liu, Y. Zhao, L. Gao, C. Chen, J. Zhou, A. Wang, Efficient regulation of elemental sulfur recovery through optimizing working height of up-flow anaerobic sludge blanket reactor during denitrifying sulfide removal process, Bioresour. Technol. 200 (2016) 1019–1023.
[14] M. Sposob, R. Bakke, C. Dinamarca, Metabolic divergence in simultaneous biological removal of nitrate and sulfide for elemental sulfur production under temperature stress, Bioresour. Technol. 233 (2017) 209–215.
[15] X. Wang, Y. Zhang, J. Zhou, T. Zhang, M. Chen, Regeneration of elemental sulfur in a simultaneous sulfide and nitrate removal reactor under different dissolved oxygen conditions, Bioresour. Technol. 182 (2015) 75–81.
[16] M. De Graaff, J.B.M. Klok, M.F.M. Bijmans, G. Muyzer, A.J.H. Janssen, Application of a 2-step process for the biological treatment of sulfidic spent caustics, Water Res. 46 (2012) 723–730.
[17] J.G. Caporaso, C.L. Lauber, W.A. Walters, D. Berg-Lyons, C.A. Lozupone, P.J. Turnbaugh, N. Fierer, R. Knight, Global patterns of 16S rRNA diversity at a depth of millions of sequences per sample, Proc. Natl. Acad. Sci. 108 (2011) 4516–4522.
[18] R.C. Edgar, B.J. Haas, J.C. Clemente, C. Quince, R. Knight, UCHIME improves sensitivity and speed of chimera detection, Bioinformatics 27 (2011) 2194–2200.
[19] R.C. Edgar, Search and clustering orders of magnitude faster than BLAST, Bioinformatics 26 (2010) 2460–2461.
[20] E.P. Nawrocki, S.R. Eddy, Infernal 1.1: 100-fold faster RNA homology searches, Bioinformatics 29 (2013) 2933–2935.
[21] T.C.J. Hill, K.A. Walsh, J.A. Harris, B.F. Moffett, Using ecological diversity measures with bacterial communities, FEMS Microbiol. Ecol. 43 (2003) 1–11.
[22] J.C. Oliveros, VENNY. An interactive tool for comparing lists with Venn Diagrams, BioinfoGP of CNB-CSIC, (2007) (http://bioinfogp.cnnb.csic.es/tools/venny/index.ht).
[23] C. Chen, X.-J. Xu, P. Xie, Y. Yuan, X. Zhou, A.-J. Wang, D.-J. Lee, N.-Q. Ren, Pyrosequencing reveals microbial community dynamics in integrated simultaneous desulfurization and denitrification process at different influent nitrate concentrations, Chemosphere 171 (2017) 294–301.
[24] Y. Tang, A. Ontiveros-Valencia, L. Feng, C. Zhou, R. Krajmalnik-Brown, B.E. Rittmann, A biofilm model to understand the onset of sulfate reduction in denitrifying membrane biofilm reactors, Biotechnol. Bioeng. 110 (2013) 763–772.
[25] J. Mohanakrishnan, M.V.W. Kofoed, J. Barr, Z. Yuan, A. Schramm, R.I. Meyer, Dynamic microbial response of sulfidogenic wastewater biofilm to nitrate, Appl. Microbiol. Biotechnol. 91 (2011) 1647–1657.
[26] T. Mechichi, E. Stackebrandt, G. Fuchs, Alicycliphilus denitrificans gen. nov. sp. nov., a cyclohexanol-degrading, nitrate-reducing beta-proteobacterium, Int. J. Syst. Evol. Microbiol. 53 (2003) 147–152.

[27] M.J. Oosterkamp, S. Boeren, S. Atashgahi, C.M. Plugge, P.J. Schaap, A.J.M. Stams, Proteomic analysis of nitrate-dependent acetone degradation by Alicycliphilus denitrificans strain BC, FEMS Microbiol. Lett. 362 (2015).
[28] A.M.S. Paulo, R. Aydin, M.R. Dimitrov, H. Vreeling, A.J. Cavaleiro, P.A. García-Encina, A.J.M. Stams, C.M. Plugge, Sodium lauryl ether sulfate (SLES) degradation by nitrate-reducing bacteria, Appl. Microbiol. Biotechnol. 101 (2017) 5163–5173.
[29] X. Hong, X. Zhang, B. Liu, Y. Mao, Y. Liu, L. Zhao, Structural differentiation of bacterial communities in indole-degrading bioreactors under denitrifying and sulfate-reducing conditions, Res. Microbiol. 161 (2010) 687–693.
[30] V.K. Nguyen, Y. Park, H. Yang, J. Yu, T. Lee, Effect of the cathode potential and sulfate ions on nitrate reduction in a microbial electrochemical denitrification system, J. Ind. Microbiol. Biotechnol. 43 (2016) 783–793.
[31] B. Liu, F. Zhang, X. Feng, Y. Liu, X. Yan, X. Zhang, L. Wang, L. Zhao, Thauera and Azoarcus as functionally important genera in a denitrifying quinoline-removal bioreactor as revealed by microbial community structure comparison, FEMS Microbiol. Ecol. 55 (2006) 274–286.
[32] C. Chen, N. Ren, A. Wang, Z. Yu, D.J. Lee, Microbial community of granules in expanded granular sludge bed reactor for simultaneous biological removal of sulfate, nitrate and lactate, Appl. Microbiol. Biotechnol. 79 (2008) 1071–1077.
[33] C. Wan, B.T. Wong, D.J. Lee, Denitrifying sulfide removal with methanogenic culture, J. Taiwan Inst. Chem. Eng. 43 (2012) 374–385.
[34] D. Park, D.S. Lee, J.Y. Joung, J.M. Park, Comparison of different bioreactor systems for indirect H2S removal using iron-oxidizing bacteria, Process Biochem. 40 (2005) 1461–1467.
[35] R. Eamrat, Y. Tsutsumi, T. Kamei, W. Khanichaidecha, Y. Tanaka, F. Kazama, Optimization of hydrogenotrophic denitrification behavior using continuous and intermittent hydrogen gas supply, J. Water Environ. Technol. 15 (2017) 65–75.
[36] W. Xing, J. Li, P. Li, C. Wang, Y. Cao, D. Li, Y. Yang, J. Zhou, J. Zuo, Effects of residual organics in municipal wastewater on hydrogenotrophic denitrifying microbial communities, J. Environ. Sci. (China) (2017).
[37] S. Lu, S.H. Ryu, B.S. Chung, Y.R. Chung, W. Park, C.O. Jeon, Simplicispira limi sp. nov., isolated from activated sludge, Int. J. Syst. Evol. Microbiol. 57 (2007) 31–34.
[38] M. Labrenz, J. Grote, K. Mammitzsch, H.T.S. Boschker, M. Laue, G. Jost, S. Glaubitz, K. Jurgens, Sulfurimonas gotlandica sp. nov. a chemoautotrophic and psychrotolerant epsilonproteobacterium isolated from a pelagic redoxcline, and an emended description of the genus Sulfurimonas, Int. J. Syst. Evol. Microbiol. 63 (2013) 4141–4148.
[39] Y. Han, M. Perner, The globally widespread genus Sulfurimonas: versatile energy metabolisms and adaptations to redox clines, Front. Microbiol. 6 (2015) 989.
[40] S.M. Sievert, K.M. Scott, M.G. Klotz, P.S.G. Chain, L.J. Hauser, J. Hemp, M. Hügler, M. Land, A. Lapidus, F.W. Larimer, S. Lucas, S.A. Malfatti, F. Meyer, I.T. Paulsen, Q. Ren, J. Simon, K. Bailey, E. Diaz, K.A. Fitzpatrick, B. Glover, N. Gwatney, A. Korajkic, A. Long, J.M. Mobberley, S.N. Pantry, G. Pazder, S. Peterson, J.D. Quintanilla, R. Sprinkle, J. Stephens, P. Thomas, R. Vaughn, M.J. Weber, L.L. Wooten, Genome of the epsilonproteobacterial chemolithoautotroph Sulfurimonas denitrificans, Appl. Environ. Microbiol. 74 (2008) 1145–1156.
[41] L. Cai, M.-F. Shao, T. Zhang, Non-contiguous finished genome sequence and description of Sulfurimonas hongkongensis sp. nov. a strictly anaerobic denitrifying, hydrogen-and sulfur-oxidizing chemolithoautotroph isolated from marine sediment, Stand. Genomic Sci. 9 (2014) 1302–1310.
[42] X.-J. Xu, C. Chen, X. Guan, Y. Yuan, A.-J. Wang, D.-J. Lee, Z.-F. Zhang, J. Zhang, Y.-J. Zhong, N.-Q. Ren, Performance and microbial community analysis of a microaerophilic sulfate and nitrate co-reduction system, Chem. Eng. J. 330 (2017) 63–70.

Article IV

Effects of N/S molar ratio on products formation in psychrophilic autotrophic biological removal of sulfide

Michal Sposob, Rune Bakke, & Carlos Dinamarca

Published in *Water*, 9(7), 476, 2017.

water

MDPI

Article

Effects of N/S Molar Ratio on Product Formation in Psychrophilic Autotrophic Biological Removal of Sulfide

Michal Sposob *, Rune Bakke and Carlos Dinamarca

Department of Process, Energy and Environmental Technology, University College of Southeast Norway, Kjølnes Ring 56, 3918 Porsgrunn, Norway; rune.bakke@usn.no (R.B.); carlos.dinamarca@usn.no (C.D.)
* Correspondence: michal.sposob@usn.no; Tel.: +47-4863-2389

Received: 13 March 2017; Accepted: 27 June 2017; Published: 29 June 2017

Abstract: The excessive H_2S presence in water and wastewater can lead to corrosion, toxicity, and biological processes inhibition—i.e., anaerobic digestion. Production of H_2S can occur in psychrophilic conditions. Biological removal of HS^- by addition of NO_3^- as an electron acceptor under psychrophilic (10 °C) conditions in a continuous flow experiment is evaluated here. Four different N/S molar ratios—0.35, 0.40, 0.60, and 1.30—were tested in an expanded granular sludge bed (EGSB) reactor. Samples were analyzed daily by ion chromatography. Efficient psychrophilic HS^- removal with sulfur products oxidation control by NO_3^- supply is documented. The highest HS^- removal was obtained at N/S = 0.35 and 1.30 (89.1 ± 2.2 and 89.6 ± 2.9%). Removal of HS^- was less at mid-N/S with the lowest value (76.9 ± 2.6%) at N/S = 0.60. NO_3^- removal remained high for all N/S ratios. N/S molar ratio influenced the sulfur products distribution with less S^0 and increase in SO_4^{2-} effluent concentration with increasing N/S ratio. Oxidation of HS^- and accumulated S^0 occurred simultaneously at N/S ratios >0.35. The observations are explained by culture flexibility in utilizing available resources for energy gain.

Keywords: autotrophic denitrification; elemental sulfur recovery; psychrophilic conditions; sulfate production; sulfide removal; N/S ratio impact

1. Introduction

Nitrate (NO_3^-) and sulfide (H_2S) are present in many kinds of wastewater. Their removal is necessary due to their negative environmental and economic impact—i.e., increase of maintenance costs in anaerobic digesters or wastewater treatment plants. Presence of H_2S can lead to corrosion, human toxicity, and biological process inhibition [1]. It has been reported that concentrations of dissolved HS^- in the 100–800 mg/L range can inhibit anaerobic digestion [2]. Additionally, the presence of NO_3^- can inhibit volatile fatty acids (VFAs) production, methanogens, and consequently methane production [3].

Due to the wide diversity of sulfur reducing bacteria (SRB) the production of H_2S can occur also in psychrophilic conditions [4]. The possibility to remove H_2S in psychrophilic conditions by harvesting elemental sulfur (S^0) out of the process line seems to be an interesting opportunity. Many waters and wastewaters are characterized by their low temperatures, especially in cold climates and winter conditions (e.g., Nordic countries). Production of S^0 at low temperatures can become important since heating up to mesophilic conditions can be prohibitively expensive.

NO_3^- and HS^- can be removed simultaneously by sulfide oxidizing bacteria (SOB), where NO_3^- serves as an electron acceptor and HS^- as an electron donor. Simultaneous removal of NO_3^- and HS^- has been studied frequently in auto- and heterotrophic conditions but to our knowledge, nothing was published on continuous flow EGSB at low temperatures and at different N/S ratios. The simultaneous presence of NO_3^- and HS^- in wastewaters is uncommon. Thus, in terms of applicability of the

described process, typically NO_3^- needs to be added to remove HS^- from contaminated water. The usage of NO_3^- as an electron acceptor for HS^- removal can be more cost-effective than O_2, which can also be used in biological HS^- oxidation. NO_3^- has high solubility and can be added at lower costs than O_2 [5].

The simultaneous biological removal of NO_3^- and HS^- can lead to different final products in terms of HS^- oxidation degree depending on relative molar ratio between NO_3^- and HS^- (N/S ratio), while NO_3^- is reduced to nitrogen gas (N_2). Based on theoretical considerations, including both anabolism and catabolism, two different key N/S ratios can be distinguished: 0.35 and 1.30 [6]. At N/S = 0.35 the main final product is S^0 where for 1.30 it is SO_4^{2-}. N/S = 1.30 requires four-times more NO_3^- than at N/S = 0.35 for mainly S^0 production. Mixed products composition occurs at feed ratios between these two values [7]. Previously published batch and continuous flow experiments were focused on appropriate electron donor (reduced sulfur compounds), C/N/S ratios, reactor configurations, and/or pH conditions at mainly mesophilic conditions [8–11]. Psychrophilic conditions are rarely studied [8,12,13], but it has been reported that the removal of NO_3^- decreases at temperature <15 °C [14]. Efficient NO_3^- removal using thiosulfate ($S_2O_3^{2-}$) as an electron donor has, however, been observed at 3 °C [13] and efficient NO_3^- removal at 10 °C with HS^- as an electron donor is reported [15].

The objective of this study is to evaluate effects of different N/S ratios as a strategy to control sulfur product distribution in a continuous flow expanded granular sludge bed (EGSB) reactor at 10 °C.

2. Materials and Methods

2.1. Inoculum and Enrichment

The inoculum was taken from an up-flow anaerobic sludge blanket (UASB) methanogenic reactor treating pulp and paper industry wastewater at Norske Skog Saugbrugs, Halden, Norway. The EGSB reactor was inoculated with 0.25 L of sludge, which had a total solid content of 59.9 g/L with an 86% organic fraction. Imposed lithoautotrophic conditions caused no methane production while sulfur compounds were produced. The data set evaluated here is from an experiment carried out as a continuation study of temperature impact (temperature range 10–25 °C) on sulfur products distribution at constant feed N/S ratio [15].

2.2. Synthetic Wastewater

The EGSB reactor synthetic feed contained $Na_2S{\cdot}9H_2O$ (3.12 mM S/L) with $NaHCO_3$. Potassium phosphate was used as a buffer. Nitrate, which acted as an electron acceptor was supplied at different concentrations 1.08, 1.25, 1.87, and 4.05 mM NO_3^-/L giving N/S ratios 0.35, 0.40, 0.60, and 1.30, respectively (Table 1). Nitrate feed contained also the following stock solutions: (A) NH_4Cl (10 g/L), $MgCl_2{\cdot}6H_2O$ (10 g/L), $CaCl_2{\cdot}2H_2O$ (10 g/L); (B) K_2HPO_4 (300 g/L); (C) $MnSO_4{\cdot}H_2O$ (0.04 g/L), $FeSO_4{\cdot}7H_2O$ (2.7 g/L), $CuSO_4{\cdot}5H_2O$ (0.055 g/L), $NiCl_2{\cdot}6H_2O$ (0.1 g/L), $ZnSO_4{\cdot}7H_2O$ (0.088 g/L), $CoCl_2{\cdot}6H_2O$ (0.05 g/L), H_3BO_3 (0.05 g/L); (D) 10 times concentrated vitamin solution [16]. HNO_3, stock solutions A (10 mL/L), B (2 mL/L), C (2 mL/L), and D (1 mL/L) were dissolved in distilled water. Electron donor ($Na_2S{\cdot}9H_2O$) and acceptor (HNO_3) were fed from separate bottles to prevent contamination and reactions in the feed bottles (Figure 1).

Table 1. Feeding parameters.

Time (Day)	N/S Ratio	NO_3^- (mM/L)	HS^- (mM/L)
1–30	0.35	1.08	3.12
31–44	0.40	1.25	
45–52	0.60	1.87	
53–60	1.30	4.05	

2.3. Experimental Setup

The 0.5 L effective volume laboratory-scale EGSB reactor was made of polycarbonate with an inner diameter of 32 mm and 620 mm effective height (Figure 1), equipped with tape measure for visual sludge bed height monitoring. Reactor temperature was maintained constant at 10 ± 0.1 °C by a cold plate cooler on the recirculation loop (TE Technology, Inc., Traverse City, MI, USA). Four different N/S ratios were tested under invariable temperature and sulfur load imposed according to Table 1.

Synthetic influent was introduced from two 2 L influent vessels under nitrogen gas to avoid influent aging. Influent was pumped into the reactor at 2 L/day, equivalent to 6 h hydraulic retention time. Recycling pump (P3 in Figure 1) was set to maintain 6 m/h reactor up-flow velocity necessary to expand the sludge bed. pH was monitored by electrode (Hanna Instruments) on the recirculation loop.

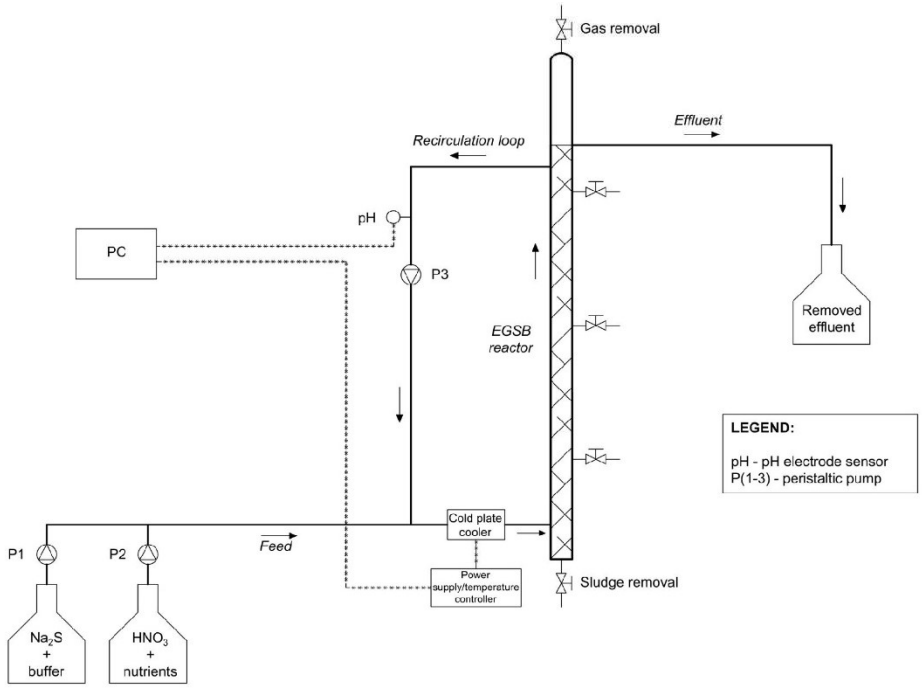

Figure 1. Experimental setup.

2.4. Analytical Procedure

Effluent samples were collected daily and analyzed immediately for nitrate (NO_3^-), nitrite (NO_2^-), sulfate (SO_4^{2-}), sulfide (HS^-), and thiosulfate ($S_2O_3^{2-}$) in collected liquid samples (following 0.45 μm filtration) by ion chromatography (Dionex ICS-5000) using potassium hydroxide (KOH) as the eluent. Sulfide concentration was determined indirectly by potassium permanganate oxidation ($KMnO_4$). Sample separation and elution was performed using an IonPac AS11-HC 2 mm analytical column. Analysis started at 22 mM KOH, gradient started at 6 min, ramped up in 3 min to 45 mM and kept at that concentration for another 4 min. The data acquisition time is 13 min. The injection volume was 10 μL and the flow rate 0.3 mL/min.

2.5. Elemental Sulfur Measurements

Two different fractions of S^0 were distinguished according to Sposob et al. [15]: accumulated into reactor (denoted as S^0_{acc}) and suspended elemental sulfur (S^0_{ss}). Distinguishing between these two S^0

fractions is done based on the elemental sulfur balance as an indirect method for quantification of S^0_{acc}, while S^0_{ss} is equivalent to measured $S_2O_3^{2-}$ [15]. Concentration of S^0_{acc} was calculated based on the difference between influent HS^- concentration and effluent concentrations of HS^-, SO_4^{2-}, and S^0_{ss}, according to Equation (1). H_2S in the headspace was not measured.

$$S^0_{acc} = HS^-_{inf} - HS^-_{eff} - SO_4^{2-}_{eff} - S^0_{ss}, \quad (1)$$

3. Results and Discussion

3.1. Reactor Performance

The electron acceptor was almost completely removed (Figure 2), on average 98.7 ± 2.8% throughout the 60 days experiment, which consisted of four phases with increasing NO_3^- concentration, thereby changing N/S ratio (Table 1). The NO_3^- removal was equal to 96.8 ± 3.9% at the highest N/S ratio and 99.3 ± 2.3% at the lowest ratio. It has been reported that NO_3^- removal can be significantly inhibited at N/S ratios much higher than derived from stoichiometry [17] but this was not the case here. However, the changes in N/S ratio had an impact on HS^- removal with 89.1 ± 2.2 and 89.6 ± 2.9% at N/S ratios of 0.35 and 1.30, respectively, and only 76.9 ± 2.6% at N/S = 0.60 (Figure 2).

Both S^0 forms, accumulated (S^0_{acc}) and suspended (S^0_{ss}), were decreasing with increasing N/S ratios and they were negligible at N/S = 1.30 (Table 2). The negative S^0_{acc} value at N/S = 1.30 implies the oxidation to SO_4^{2-} of the earlier accumulated S^0 in the reactor during lower N/S ratios.

Each increase in NO_3^- resulted in SO_4^{2-} concentration rise, depletion of S^0 fractions and pH drop (Figures 3 and 4). During the last week of the experiment, pH decreased to 7.19 ± 0.31 at N/S = 1.30 due to high SO_4^{2-} production (Figures 3 and 4). At this pH, a larger fraction of HS^- in the unionized form as H_2S could occur compared to the conditions at lower N/S, with higher pH (Figure 4). It is still argued that an insignificant amount of H_2S was stripped off to headspace since: the dissolved H_2S level at pH 7.19 ± 0.31 is calculated to only 0.2 mM/L and H_2S has a high solubility in water (150 mM/L, at 10 °C [18]). Therefore, there is no unaccounted for or missing sulfur in the balance.

Table 2. Process output parameters (concentrations in mM/L).

N/S Ratio	S^0_{acc} [1]	SO_4^{2-}	S^0_{ss}	HS^--S	NO_3^-	pH	Total Sulfur (Effluent) [2]
0.35	0.57 ± 0.21	0.69 ± 0.11	1.52 ± 0.16	0.34 ± 0.07	0.01 ± 0.03	8.11 ± 0.11	2.55 ± 0.21
0.40	0.44 ± 0.32	0.96 ± 0.21	1.24 ± 0.16	0.56 ± 0.15	0.02 ± 0.03	7.92 ± 0.15	2.76 ± 0.36
0.60	0.09 ± 0.20	1.39 ± 0.19	0.91 ± 0.26	0.72 ± 0.08	0.02 ± 0.06	7.65 ± 0.06	3.03 ± 0.2
1.30	−0.69 ± 0.58	3.37 ± 0.83	0.11 ± 0.23	0.32 ± 0.09	0.15 ± 0.16	7.19 ± 0.31	3.81 ± 0.58

Notes: [1] Derived values come from the balance (Equation (1)); [2] Total sulfur (effluent) = SO_4^{2-} + S^0_{ss} + HS^--S.

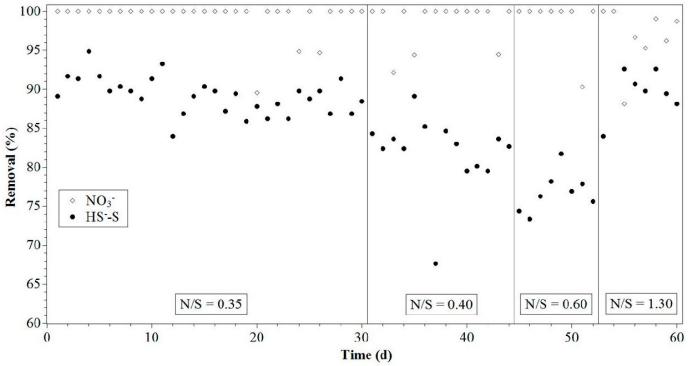

Figure 2. Time series of substrates removal (NO_3^- and HS^-) under different N/S ratios at 10 °C.

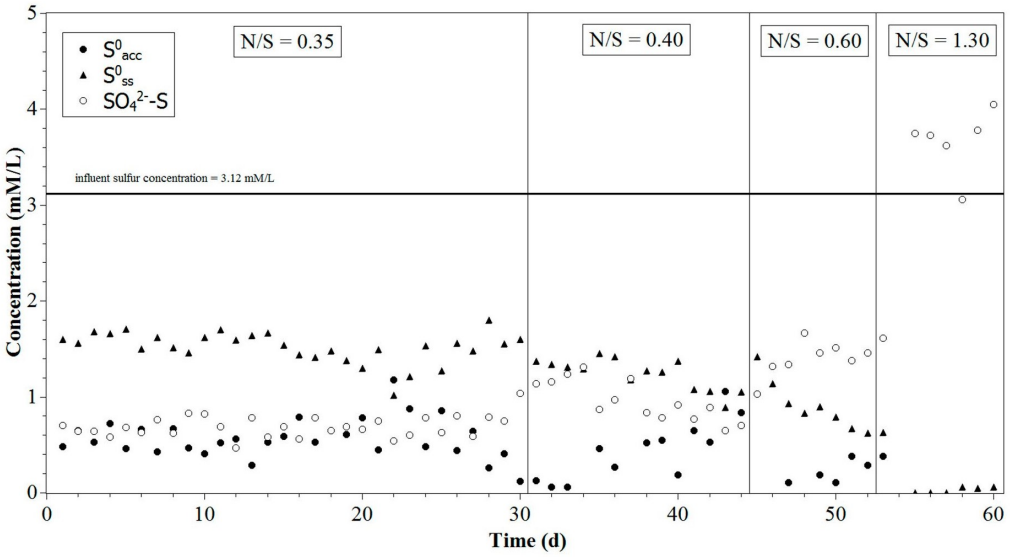

Figure 3. Time series of accumulated (S^0_{acc}) and suspended (S^0_{ss}) elemental sulfur, and sulfate (SO_4^{2-}-S) concentrations under different N/S ratios at 10 °C.

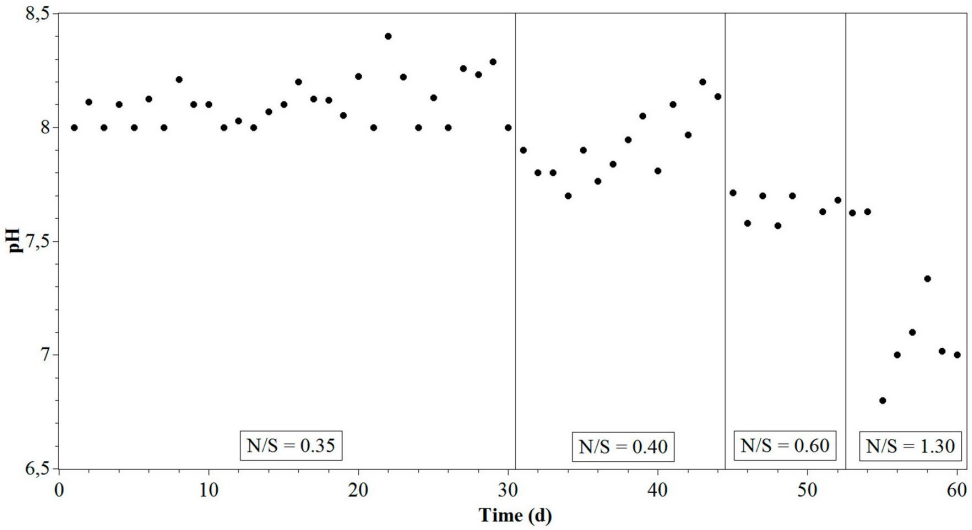

Figure 4. pH vs. time under different N/S ratios at 10 °C.

3.2. Sulfur Components at Different N/S Ratios

The imposed increase in feed NO_3^- concentration had, as expected, an impact on the presence of the four different sulfur components, HS^-, SO_4^{2-} and two fractions of S^0: accumulated (S^0_{acc}) and suspended (S^0_{ss}) (Figure 5).

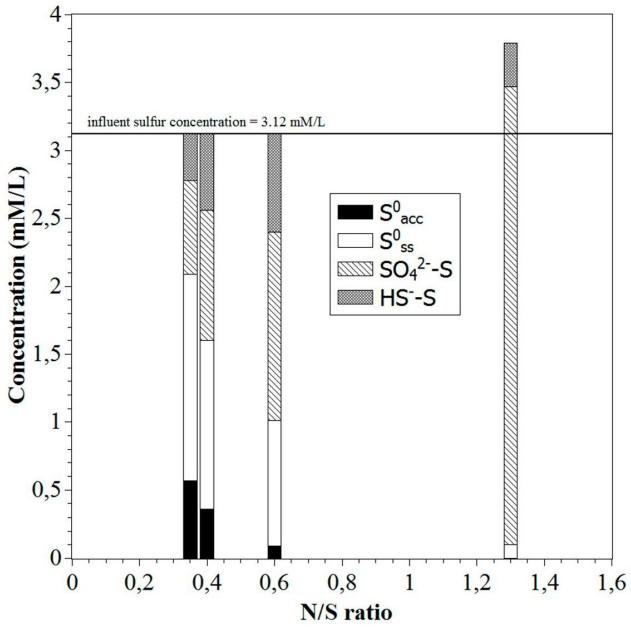

Figure 5. Share of sulfur products under different N/S ratios at 10 °C.

The initially tested N/S ratio revealed that around 11% (0.34 ± 0.07 mM/L) of influent sulfur remained unreacted as HS^-. At this condition, S^0_{ss} was a main fraction of S^0 at a 49% share of influent sulfur while S^0_{acc} constituted 18%, adding up to 67%. A share of 22% of the electron donor was oxidized to SO_4^{2-} at N/S = 0.35. Similar studies performed at mesophilic conditions reveal lower SO_4^{2-} fractions at similar N/S ratio: (1) At 25 °C and N/S = 0.35 the fraction of SO_4^{2-} constituted 14% [15]; (2) At room temperature (22–23 °C) and N/S = 0.32 only 4% of HS^- was converted to SO_4^{2-} [19]. The results confirm previous studies that show temperature impact on HS^- removal and SO_4^{2-} production, where the SO_4^{2-} share increases with decreasing temperature [15].

The slight increase in N/S ratio from 0.35 to 0.40 (equivalent to catabolic reaction in simultaneous NO_3^- and HS^- removal to yield S^0) was imposed to supply sufficient NO_3^- such to obtain the complete removal of HS^-, it however led to less HS^- oxidation. The presence of S^0 fractions also decreased from 67 to 54%, reducing the concentration of S^0_{acc} by 23% and S^0_{ss} by 18% in comparison to the previous (N/S = 0.35) period (Table 2). The electron donor removal decreased, so that 18% of influent sulfur remained unreacted. More of the HS^- oxidized was, however, oxidized to the highest oxidation level (+VI), increasing the SO_4^{2-} share of products from 22 to 31%. This clearly shows that the appropriate N/S ratio for S^0 production is lower than that reflected in the catabolic reaction alone.

S^0_{acc} was almost completely avoided at N/S = 0.60 (3% of influent sulfur, Figure 5). S^0 was still present in the liquid phase (S^0_{ss} = 29% of influent sulfur) but much less than at lower N/S ratios. Concentration of HS^- and SO_4^{2-} at the effluent increased compared to lower N/S ratios. Unreacted HS^-, 23%, 0.72 ± 0.08 mM/L, shows the lowest removal of electron donor during the whole experiment. The increase in SO_4^{2-} was similar as for the transition from 0.35 to 0.40, at N/S = 0.60 had a share of 45%.

Effluent SO_4^{2-} was the main HS^- oxidation product at the highest studied N/S ratio (1.30; NO_3^- = 4.08 mM/L) but its concentration varied more than at lower N/S (3.37 ± 0.83 mM/L). The sum of sulfur components in the effluent was 22% higher than in the influent during this period (Figures 3 and 5), which is explained by the oxidation of previously accumulated sulfur, S^0_{acc}. Similar behavior has been observed during abrupt temperature drops [20]. The slight amount S^0_{ss} (0.11 ± 0.23 mM/L;

4%) observed in this period is assumed to originate from previously accumulated sulfur, S^0_{acc}. Excess effluent compared to influent sulfur must have a temporary nature until the S^0_{acc} in granules is exhausted but the experiment did not last long enough to reach such a steady state.

The observed substrate consumption and products distribution for different ratios between electron acceptor and donor differs from that reported based on catabolic reactions under mesophilic conditions. In comparison, nitrite (NO_2^-) accumulation observed under mesophilic conditions [7] did not occur in the presented work. It has also been reported that SOB like *Thiobacillus denitrificans* oxidizes stored sulfur only when reduced sulfur compounds—i.e., $S_2O_3^{2-}$—have been depleted [21]. However, in this study higher NO_3^- immediately triggered a SO_4^{2-} production increase even when HS^- was not completely oxidized.

It has been reported that changes in N/S ratio under heterotrophic conditions caused changes in products distribution similar to that observed here. Additionally, changes in N/S ratio led to changes in the heterotrophic microbial community structure [22]. There may similarly have been autotrophic community changes in the present study, but this was not investigated. An observed decrease in sludge bed height level by 58% from the lowest to the highest N/S tested here may have been related to microbial community structure changes but the main cause is probably loss of S^0_{acc} from the granules. Oxidation of initially stored S^0_{acc} to recover energy at high N/S ratios, is proposed as the main cause of sludge bed reduction.

3.3. Relation between Experimental and Theoretical Products Distribution

Using N/S ratio as a way to control the fate of HS^- oxidation to either S^0 and/or SO_4^{2-} [9] is further analyzed by comparing theoretical equations [6] and experimental results (Figure 6). Obtained experimental results show the offset from theoretical values with good match only at N/S = 1.30. The observed offset, especially at N/S = 0.35, may be due to a metabolic shift that has been observed in a temperature impact study [15]. It was observed that the production of SO_4^{2-} was increasing at a constant N/S ratio (=0.35) with decreasing temperature, which was hypothesized to be a natural response of microbiota to compensate temperature-induced changes in energy requirements.

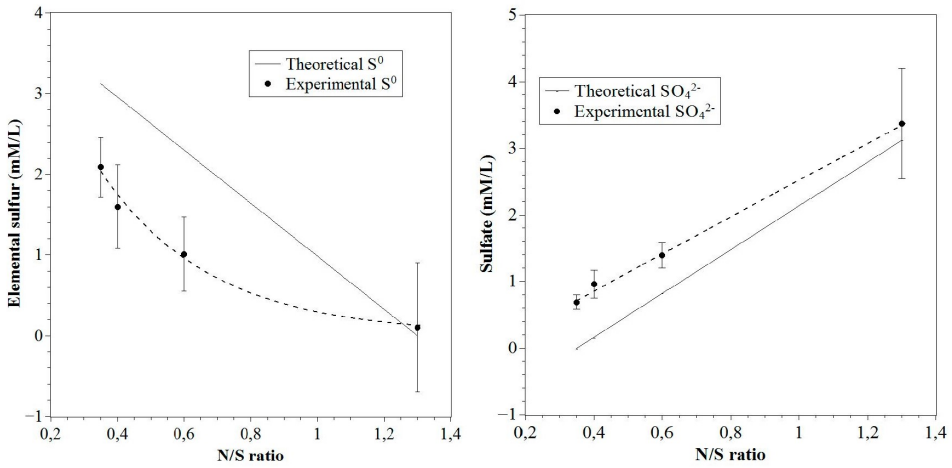

Figure 6. Experimental and theoretical concentration of elemental sulfur (S^0_{acc} + S^0_{ss}) (**left**), and SO_4^{2-} (**right**).

Theoretically, according to the equations given by Kleerebezem and Mendez [6], equal product distribution between S^0 and SO_4^{2-} should be expected at N/S = 0.825 or even at higher ratios, taking into account just the catabolic reactions. Experimentally, however, equal distribution of S^0 and

SO_4^{2-} was reached already at N/S = 0.6. The organisms accumulated some amount of sulfur, S^0_{acc}, as an energy reserve at low N/S ratio. Thus, in addition to temperature effects, the obtained offset at N/S ratios 0.4 and 0.6 may have been influenced by the oxidation of S^0_{acc}. The continuous flow feeding with increasing N/S ratio, facilitated the observation of competition between S^0_{acc} and HS^- as electron donors. This is especially visible at mid-N/S ratios where the S^0_{acc} was evidently, to changing degrees, used as an electron donor together with HS^-, for which removal decreased at the same time. This observation contradicts the previous studies in which it has been reported that the oxidation of accumulated S^0 as an electron reserve can occur only when the reduced sulfur compounds are depleted (HS^- in this case) [21]. The possibility that the organisms can utilize this stored energy by oxidizing S^0_{acc} to SO_4^{2-} also in conditions when surplus HS^- is present implies larger culture flexibility to utilize available resources. The microorganisms may thereby have increased their catabolic energy yield by utilizing differences in free Gibbs energy since the oxidation from S^0 to SO_4^{2-} has a slightly higher ΔG° than from HS^- to SO_4^{2-}, −800.76 and −768.28 kJ/reaction, respectively (Table 3). The exponential-like response for S^0 (Figure 6) may thereby be a result of increased S^0_{acc} oxidation with increased influent NO_3^- concentration. This pathway apparently has an impact and may explain the offset and shape of the exponential-like response of N/S ratio on S^0.

Table 3. Possible reaction of sulfur reduced compounds with nitrate (NO_3^-).

Reaction	ΔG° (1 M of Electron Donor)
$HS^- + 0.4NO_3^- + 1.4H^+ \rightarrow S^0 + 0.2N_2 + 1.2H_2O$	−252.13
$HS^- + 0.8NO_3^- + 0.8H^+ \rightarrow 0.5S_2O_3^{2-} + 0.4N_2 + 0.9H_2O$	−393.14
$HS^- + 1.6NO_3^- + 0.6H^+ \rightarrow SO_4^{2-} + 0.8N_2 + 0.8H_2O$	−768.28
$S^0 + 1.2NO_3^- + 0.4H_2O \rightarrow SO_4^{2-} + 0.6N_2 + 0.8H_2O$	−800.76

The overall percentage distribution of reactants and products (Table 4) shows an imbalance of electrons in the experimental data which implies that some SO_4^{2-} must have been produced through the use of an electron acceptor other than NO_3^-. The percentage of influent sulfur (as HS^-) oxidized by another electron acceptor decreased with increasing N/S ratio from 14 to 8% of influent sulfur. Similar observations have been reported in other studies where the obtained products exceeds what is theoretically expected based on fed electron acceptor [7,15]. Such unintended electron acceptors could be H^+ to give H_2 gas, inorganic carbon to biomass, or exposure to O_2.

Table 4. Comparison of theoretical and experimental percentage share of products and electron acceptors uptake.

N/S Ratio	Theoretical Share (%)		Experimental Share (%)		NO_3^- Uptake Share (%)		SO_4^{2-} Produced by Another Electron Acceptor (mM/L)
	S^0	SO_4^{2-}	S^0	SO_4^{2-}	S^0	SO_4^{2-}	
0.35	100	0	67	22	67	33	0.41 (13%) [1]
0.40	95	5	54	31	46	54	0.44 (14%)
0.60	74	26	32	45	18	82	0.22 (7%)
1.30	0	100	4 [2]	108	1	99	0.26 (8%)

Notes: [1] In parenthesis percentage of influent sulfur concentration; [2] only S^0_{ss} included.

4. Conclusions

The lowest and highest N/S ratios, 0.35 and 1.30, did not differ in HS^- removal, with 89.1 ± 2.2% and 89.6 ± 2.9%, respectively. Less HS^- removal was obtained at intermediate N/S ratios with the lowest, 76.9 ± 2.6%, at N/S = 0.60.

The products from the studied N/S ratios deviated from theoretical predictions, except at N/S = 1.30. Additionally, equal product distribution between S^0 and SO_4^{2-} occurred at a lower N/S ratio than theoretically expected. This implies that the reactions in continuous flow bioreactors are more complicated than accounted for in standard stoichiometric models.

Increasing N/S feed ratio caused an increase in SO_4^{2-} production and depletion of stored S^0. The S^0 accumulated during the low N/S feed ratio was utilized at higher N/S, thus, leading to SO_4^{2-} production to recover stored energy. The oxidation of S^0 occurred even though excess HS^- was available at higher feed N/S ratios (>0.35). These phenomena can explain the lower removal of HS^- at mid-N/S ratios and the highest sulfur concentration obtained in the effluent at N/S = 1.30.

Efficient psychrophilic biological HS^- removal with NO_3^- as an electron acceptor in an EGSB process is documented and elemental sulfur (S^0) harvesting can be obtained through careful NO_3^- supply control.

Acknowledgments: The authors would like to thank YARA AS International and The Research Council of Norway for support of this research.

Author Contributions: Carlos Dinamarca and Michal Sposob conceived and designed the experiment and all authors were involved in analyzing the data; Michal Sposob performed the experiments and analyzed all the samples; Michal Sposob, Rune Bakke and Carlos Dinamarca contributed to writing the paper.

Conflicts of Interest: The authors declare no conflict of interest.

References

1. Pokorna, D.; Zabranska, J. Sulfur-oxidizing bacteria in environmental technology. *Biotechnol. Adv.* **2015**, *33*, 1246–1259. [CrossRef] [PubMed]
2. Chen, Y.; Cheng, J.J.; Creamer, K.S. Inhibition of anaerobic digestion process: A review. *Bioresour. Technol.* **2008**, *99*, 4044–4064. [CrossRef] [PubMed]
3. Zhou, Z.; Yu, Z.; Meng, Q. Effects of nitrate on methane production, fermentation, and microbial populations in in vitro ruminal cultures. *Bioresour. Technol.* **2012**, *103*, 173–179. [CrossRef] [PubMed]
4. Knoblauch, C.; Sahm, K.; Jørgensen, B.B. Psychrophilic sulfate-reducing bacteria isolated from permanently cold Arctic marine sediments: Description of *Desulfofrigus oceanense* gen. nov., sp. nov., *Desulfofrigus fragile* sp. nov., *Desulfofaba gelida* gen. nov., sp. nov., *Desulfotalea psychrophila* gen. nov., sp. nov. and *Desulfotalea arctica* sp. nov. *Int. J. Syst. Evol. Microbiol.* **1999**, *49*, 1631–1643.
5. Auguet, O.; Pijuan, M.; Borrego, C.M.; Gutierrez, O. Control of sulfide and methane production in anaerobic sewer systems by means of Downstream Nitrite Dosage. *Sci. Total Environ.* **2016**, *550*, 1116–1125. [CrossRef] [PubMed]
6. Kleerebezem, R.; Mendez, R. Autotrophic denitrification for combined hydrogen sulfide removal from biogas and post-denitrification. *Water Sci. Technol.* **2002**, *45*, 349–356. [PubMed]
7. Cai, J.; Zheng, P.; Mahmood, Q. Effect of sulfide to nitrate ratios on the simultaneous anaerobic sulfide and nitrate removal. *Bioresour. Technol.* **2008**, *99*, 5520–5527. [CrossRef] [PubMed]
8. Fajardo, C.; Mora, M.; Fernández, I.; Mosquera-Corral, A.; Campos, J.L.; Méndez, R. Cross effect of temperature, pH and free ammonia on autotrophic denitrification process with sulphide as electron donor. *Chemosphere* **2014**, *97*, 10–15. [CrossRef] [PubMed]
9. Beristain-Cardoso, R.; Sierra-Alvarez, R.; Rowlette, P.; Flores, E.R.; Gómez, J.; Field, J.A. Sulfide oxidation under chemolithoautotrophic denitrifying conditions. *Biotechnol. Bioeng.* **2006**, *95*, 1148–1157. [CrossRef] [PubMed]
10. Huang, C.; Li, Z.; Chen, F.; Liu, Q.; Zhao, Y.; Gao, L.; Chen, C.; Zhou, J.; Wang, A. Efficient regulation of elemental sulfur recovery through optimizing working height of upflow anaerobic sludge blanket reactor during denitrifying sulfide removal process. *Bioresour. Technol.* **2016**, *200*, 1019–1023. [CrossRef] [PubMed]
11. Mahmood, Q.; Zheng, P.; Cai, J.; Wu, D.; Hu, B.; Li, J. Anoxic sulfide biooxidation using nitrite as electron acceptor. *J. Hazard. Mater.* **2007**, *147*, 249–256. [CrossRef] [PubMed]
12. Xu, Y.; Chen, N.; Feng, C.; Hao, C.; Peng, T. Sulfur-based autotrophic denitrification with eggshell for nitrate-contaminated synthetic groundwater treatment. *Environ. Technol.* **2016**, *37*, 3094–3103. [CrossRef] [PubMed]
13. Di Capua, F.; Milone, I.; Lakaniemi, A.M.; Lens, P.N.L.; Esposito, G. High-rate autotrophic denitrification in a fluidized-bed reactor at psychrophilic temperatures. *Chem. Eng. J.* **2017**, *313*, 591–598. [CrossRef]
14. Yamamoto-Ikemoto, R.; Komori, T.; Nomuri, M.; Ide, Y.; Matsukami, T. Nitrogen removal from hydroponic culture wastewater by autotrophic denitrification using thiosulfate. *Water Sci. Technol.* **2000**, *42*, 369–376.

15. Sposob, M.; Bakke, R.; Dinamarca, C. Metabolic divergence in simultaneous biological removal of nitrate and sulfide for elemental sulfur production under temperature stress. *Bioresour. Technol.* **2017**, *233*, 209–215. [CrossRef] [PubMed]
16. Wolin, E.A.; Wolin, M.J.; Wolfe, R.S. Formation of methane by bacterial extracts. *J. Biol. Chem.* **1963**, *238*, 2882–2886. [PubMed]
17. Oh, S.E.; Kim, K.S.; Choi, H.C.; Cho, J.; Kim, I.S. Kinetics and physiological characteristics of autotrophic dentrification by denitrifying sulfur bacteria. *Water Sci. Technol.* **2000**, *42*, 59–68.
18. Carroll, J.J.; Mather, A.E. The solubility of hydrogen sulphide in water from 0 to 90 °C and pressures to 1 MPa. *Geochim. Cosmochim. Acta* **1989**, *53*, 1163–1170. [CrossRef]
19. An, S.; Tang, K.; Nemati, M. Simultaneous biodesulphurization and denitrification using an oil reservoir microbial culture: Effects of sulphide loading rate and sulphide to nitrate loading ratio. *Water Res.* **2010**, *44*, 1531–1541. [CrossRef] [PubMed]
20. Sposob, M.; Dinamarca, C.; Bakke, R. Short-term temperature impact on simultaneous biological nitrogen-sulphur treatment in EGSB reactor. *Water Sci. Technol.* **2016**, *74*, 1610–1618. [CrossRef] [PubMed]
21. Schedel, M.; Trüper, H.G. Anaerobic oxidation of thiosulfate and elemental sulfur in Thiobacillus denitrificans. *Arch. Microbiol.* **1980**, *124*, 205–210. [CrossRef]
22. Chen, C.; Xu, X.J.; Xie, P.; Yuan, Y.; Zhou, X.; Wang, A.J.; Lee, D.J.; Ren, N.Q. Pyrosequencing reveals microbial community dynamics in integrated simultaneous desulfurization and denitrification process at different influent nitrate concentrations. *Chemosphere* **2017**, *171*, 294–301. [CrossRef] [PubMed]

Article V

Modeling N/S ratio and temperature effects in simultaneous biological denitrification and sulfide oxidation

Michal Sposob, Rune Bakke, & Carlos Dinamarca

Published in *Proceedings of the 58th Conference on Simulation and Modelling (SIMS 58)*, 138, 41-47, 2017.

Modeling N/S ratio and temperature influences on simultaneous biological denitrification and sulfide oxidation

Michal Sposob[1] Rune Bakke[1] Carlos Dinamarca[1]

[1]Department of Process, Energy and Environmental Technology, University College of Southeast Norway, Norway
michal.sposob@usn.no

Abstract

A model describing the simultaneous removal of NO_3^- and HS^- by microorganisms is presented here. The oxidation of HS^- (electron donor) can be controlled by the appropriate dosage of NO_3^-. The developed model, which includes variable process stoichiometry, attempts to predict the distribution of sulfur oxidation products. Stoichiometric coefficients are based on a 150 days experimental study of temperature (25-10 °C) and N/S ratio (0.35-1.30) effects. The model can be used as a prediction tool for autotrophic denitrification with HS^-. Elemental sulfur production is included in the mathematical model, however, its accumulation and release (as SO_4^{2-}) with increasing feed N/S ratio (e.g. leading to higher effluent than feed total sulfur mass at N/S = 1.30) is not simulated. A conceptual model to account for biological accumulation and release of elemental sulfur is proposed here.

Keywords: autotrophic denitrification, elemental sulfur production, mathematical modeling, sulfate production

1 Introduction

The presence of sulfide (H_2S) in wastewaters is an important issue concerning wastewater networks and treatment plants maintenance due to its corrosive properties (Ma et al., 2000). Low concentrations of H_2S (lower than 10 mg/L) are present in domestic wastewaters (Pikaar et al., 2011). The exposure to H_2S in gaseous form is toxic to human even at low concentrations and can paralyze the olfactory nerves and lead to death (Reiffenstein et al., 1992).

Biological wastewater treatment plants used to remove carbon, nitrogen and phosphorus can be inhibited by extensive presence of H_2S (Chen et al., 2008; Jin et al., 2013; Joye and Hollibaugh, 1995). It has been reported that anaerobic digestion process can be inhibited at concentrations from 50 mg H_2S/L (Chen et al., 2008). H_2S presence can vary due to the high complexity of the sulfur (S) cycle and its partial overlapping with cycles of other elements (i.e. C, Fe, Hg, N and Se). Knowledge of these cycles can be used for biochemical H_2S control and S removal.

Physicochemical H_2S removal is often used for H_2S removal (desulfurization) in industrial scale. The Claus process, where elemental sulfur (S^0) is recovered from H_2S-containing gases under high temperature and oxygen (O_2) supply, is the most common method. Biological treatment, utilizing the unique properties of microorganisms, is gaining attention due to the environmental and economic advantages. Biological H_2S removal from wastewaters utilizes the ionic forms HS^- and/or S^{2-} (depending on pH) as the electron donor, while usually nitrate (NO_3^-), nitrite (NO_2^-) and O_2 are electron acceptor sources. The usage of these electron acceptors is not mutually exclusive, so they can be used together and separately. Addition of more than one electron acceptor can be applied to enhance the H_2S removal (Wang et al., 2015). Due to advantages such as a higher solubility of NO_3^- than O_2, NO_3^- usage is studied here. It is argued that the continuous flow expanded granular sludge bed (EGSB) bioreactor is the most efficient design for biological desulfurization (Cai et al., 2010). Data from a previous EGSB study (Sposob et al., 2017a; 2017b) are used here.

The oxidation of HS^- can be controlled by the ratio between electron acceptor and electron donor to influence the relative amounts of the oxidation products: S^0 and sulfate (SO_4^{2-}). Extensive experimental and theoretical studies on the appropriate conditions for simultaneous N and S removal, i.e. C/N/S ratio, pH, load and temperature, have been conducted (Di Capua et al., 2017; Guo et al., 2016; Huang et al., 2016; Mahmood et al., 2007; Montalvo et al., 2016; Reyes-Avila et al., 2004; Sposob et al., 2017a). Modeling can facilitate further understanding and optimization of simultaneous biological NO_3^- and HS^- removal. So far, a few models based on artificial neural networks (Wang et al., 2009) and kinetic approach (Wang et al., 2010; Xu et al., 2016, 2014) have been developed. The kinetic models are based on batch experiments where only the initial phase of the process is accounted for. Fixed stoichiometry based on assumed chemical reactions or based on calculated and/or experimentally obtained yield values also limits published models, since the ratio between electron acceptor and electron donor can completely alter the output (Cai et al., 2008; Sposob et al., 2017b). The models describing simultaneous removal of NO_3^- and HS^- should take into account the fact that effluents from this kind of treatment can contain several products

especially at low N/S ratios. This is challenging since it has been observed in long-term experiment that SO_4^{2-} and S^0 were produced at the same time at feed N/S ratio that theoretically should lead to S^0 production only (Sposob et al., 2017a; Tan et al., 2016). It has also been observed that temperature has an impact on effluent sulfur components at constant N/S ratio (Sposob et al., 2017a). Thus, the need for the modeling including multicomponent effluent characteristic is required, especially in cases where lower N/S ratios are modeled.

The objective of this study is to develop a model for simultaneous removal of NO_3^- and HS^- at different N/S ratios and temperatures, which can be used to predict the distribution of produced sulfur components.

2 Methods and model development

2.1 Experimental design

The experimental trial was performed in a 0.5 L laboratory-scale EGSB reactor continuously fed by synthetic wastewater over 150 days. The feeding parameters are given in Table 1.

Table 1. Feeding parameters.

Time (d)	*Temperature (°C)*	*N/S ratio*	*NO_3^- (mM/L)*	*HS^- (mM/L)*
1-25	25	0.35	1.08	3.12
26-57	20			
58-90	15			
91-120	10			
121-134		0.40	1.25	
135-142		0.60	1.87	
143-150		1.30	4.05	

Synthetic wastewater was supplied from two feed tanks (separate for electron acceptor and donor) to avoid contamination and possible reactions in feeding tank. In addition to electron acceptor and donor sources, vitamins, buffer, macro- and microelements were supplied as described in Sposob et al. (2017a), where the more detailed description of experiment is given.

2.2 Stoichiometry

The model is developed and evaluated based on the stoichiometry derived by Kleerebezem and Mendez, (2002) and data from continuous flow expanded granular sludge bed (EGSB) experiments (Sposob et al., 2017a; 2017b). The collected data consists information about concentrations of accumulated elemental sulfur (S^0_{acc}), nitrate (NO_3^-), sulfate (SO_4^{2-}), sulfide (HS^-) and suspended elemental sulfur (S^0_{ss}) measured as thiosulfate ($S_2O_3^{2-}$). Accumulated sulfur (S^0_{acc}) was calculated based on the difference between influent HS^- concentration and effluent concentrations of HS^-, SO_4^{2-} and S^0_{ss}, according to Eq. 1 (Sposob et al., 2017a).

$$S^0_{acc} = HS^-_{inf} - HS^-_{eff} - SO_4^{2-}_{eff} - S^0_{ss} \quad (1)$$

The basic chemical reactions (Eqs. 2, 3) and reactions combining both anabolism (biomass production) and catabolism (energy release) (Eqs. 4, 5) according to Kleerebezem and Mendez (2002) serve as the core for the model. However, these equations assume production of only one sulfur component at specific N/S ratio and does not include temperature impact.

$$HS^- + 1.6NO_3^- + 0.6H^+ \rightarrow 0.8N_2 + SO_4^{2-} + 0.8H_2O \quad (2)$$

$$HS^- + 0.4NO_3^- + 1.4H^+ \rightarrow 0.2N_2 + S^0 + 1.2H_2O \quad (3)$$

$$3HS^- + 3.9NO_3^- + 0.2NH_4^+ + HCO_3^- + 1.7H^+ \rightarrow CH_{1.8}O_{0.5}N_{0.2} + 1.95N_2 + 3SO_4^{2-} + 2.3H_2O \quad (4)$$

$$14.5HS^- + 5NO_3^- + 0.2NH_4^+ + HCO_3^- + 20.3H^+ \rightarrow CH_{1.8}O_{0.5}N_{0.2} + 2.5N_2 + 14.5S^0 + 17.4H_2O \quad (5)$$

The new stoichiometry applied here includes simultaneous NO_3^- and HS^- removal and possibility to produce two sulfur components: S^0 (without distinguishing the S^0 fractions) and SO_4^{2-} according to Eq. 6.

$$aNO_3^- + bHS^- \text{-} S \rightarrow cS^0 + dSO_4^{2-} + eN_2 \quad (6)$$

Where c and d depend on feed molar ratio between a and b (N/S ratio) and temperature (T) (Eqs. 7, 8).

$$c = f(\text{N/S; T}) \quad (7)$$

$$d = f(\text{N/S; T}) \quad (8)$$

2.3 Kinetics

Process kinetics is modeled based on the Monod equation for reaction rates and assuming one general microbial community of sulfide oxidizing bacteria (SOB). The growth of microorganisms is thus described using the Bailey's equation that includes both required substrates (Eq. 9). The biomass concentration is assumed constant in the simulations due to the conditions with high biomass content in the EGSB reactor and low biomass yield of autotrophic denitrification bacteria (Tchobanoglous et al., 2003), implying that reactor biomass changes are insignificant during the experiments used in this study. The growth parameters maximum growth rate (μ_{max}) and half-saturation constants (K_{HS^-}, K_{NO3^-}) applied are given in Table 2.

$$\mu = \mu_{max} \cdot X_{SOB} \left(\frac{S_{HS^-}}{K_{HS^-} + S_{HS^-}}\right)\left(\frac{S_{NO_3^-}}{K_{NO_3^-} + S_{NO_3^-}}\right) \quad (9)$$

Table 2. Growth parameters.

Parameter	*Value*	*Source*
μ_{max}	4.25 d^{-1}	(Wang et al., 2010)
$K_{NO_3^-}$	7.84 mM NO_3^-/L	(Xu et al., 2016)
K_{HS^-}	1.8 mM S^{2-}/L	

The mathematical model is implemented in the AQUASIM simulation software (Eawag, Switzerland). The established model is calibrated and used to simulate removal of NO_3^- and HS^-. Simulation results are

compared with the obtained experimental data published in Sposob et al. (2017a, 2017b).

2.4 Temperature

Temperature has an impact on bacterial kinetic coefficients like μ_{max} and K_S leading to changes in the treatment efficiency. During the experimental trial the electron donor (HS^--S) removal changed from 98 (25 °C) to 89 % at 10 °C. Temperature also influenced the effluent composition of sulfur components in the experiment modeled here (Figure 1). Electron acceptor (NO_3^-) removal was not significantly influenced by temperature as it was completely removed (effluent NO_3^- was detected only three times during 120 days temperature-trial).

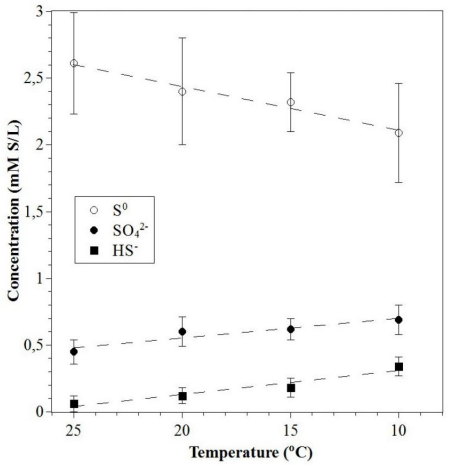

Figure 1. Average concentration of sulfur components at 25-10 °C and N/S = 0.35 (Sposob et al., 2017a).

With decreasing temperature and invariable feeding pattern, the share of S^0 decreased while SO_4^{2-} together with HS^- increased. Performed free Gibbs energy calculations ($\Delta G^{0'}$) revealed that the reaction energy at the different temperatures remained nearly constant due to this shift in products formation from S^0 to SO_4^{2-} (Sposob et al., 2017a). The reaction energy maintained at invariable feeding conditions is dependent on the relationships given in Eqs. 10 and 11. The culture evidently preferred to use more NO_3^- per mole of HS^- at lower temperatures. Whether this is due to a shift in microbial community or a metabolic shift within cells is currently under investigation. Until such information is available an empirical temperature effect is implemented in the model by temperature dependent stoichiometric coefficients (Table 3) based on the experimental results given in Figure 1.

$$Reaction\ energy = oxidation\ to\ S^0 + oxidation\ to\ SO_4^{2-} \quad (10)$$

$$Reaction\ energy \approx constant \quad (11)$$

Table 3. Temperature coefficient for stoichiometric parameters calculated based on the experimental trial.

Temperature	T_{sulfur}	$T_{sulfate}$
25	0.84	0.14
20	0.77	0.19
15	0.74	0.2
10	0.67	0.22

2.5 N/S ratio

Changes in N/S ratio have been reported as a way to control the level of HS^- oxidation (Cai et al., 2008). However, the results at different ratios at 10 °C show a significant offset from the theoretical values (Figure 2). The highest offset was obtained for S^0. Experimental results equaled the theoretical values only at N/S = 1.30. A more detailed description of N/S ratio impact at psychrophilic conditions (10 °C) is given in Sposob et al. (2017b). Modeling effects of N/S ratios in Eq. 7 and 8 based on these observations is implemented through correction coefficients given in Table 4.

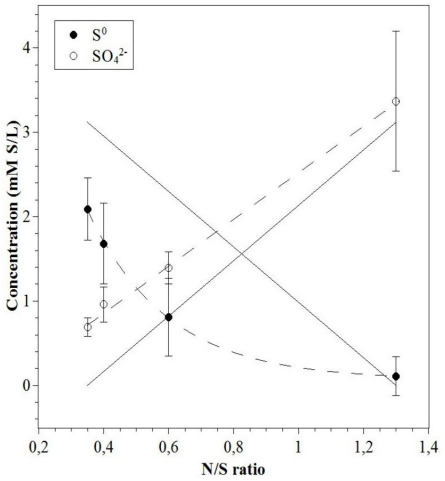

Figure 2. Average concentration of sulfur components at different N/S ratios at 10 °C. Whole lines are theoretical values based on Eqs. 4, 5 while dotted line connects the given experimental values.

Table 4. N/S ratio coefficient for stoichiometric parameters calculated based on the experimental trial.

N/S ratio	N/S_{sulfur}	$N/S_{sulfate}$
0.35	1	1
0.40	0.81	1.41
0.60	0.48	2.05
1.30	0.06	4.36

DOI: 10.3384/ecp1713841

3 Results and Discussion

Simulations, with the calculated coefficients (Table 3) of products distribution (S^0 and SO_4^{2-}) with different temperatures and constant feed N/S = 0.35 behaves similar to the experimental results (Figure 3). The implemented model with the temperature coefficients (Table 3) simulates the pseudo-steady state relative amounts of effluent S^0 and SO_4^{2-}. This may seem obvious since the coefficients are calculated based on average values for each temperature case of the same data set. The model, however, also simulates the transitions in relative amounts of products occurring following each 5 °C temperature drop (the initial part of each of the three last panels in Figure 3) quite accurately. The model significantly improved predictions at N/S = 0.35 compared to the equations (Eqs. 3, 5) that predict S^0 production only and no temperature effect.

Increasing the model complexity, including diversification of microbes and/or the implementation of energy terms, can further improve the model for better prediction of HS^- removal and products distribution for a wider range of conditions. However, further experimental investigations are required to implement such.

Experimental data and predictions based on Kleerebezem and Mendez (2002) equations (Eqs. 4, 5) are compared in Figure 2 regarding N/S ratio effects on products distribution. The observed offset between experimental and theoretical values could be partly due to the oxidation of earlier accumulated S^0 (reaction 3 in the schematic presentation of the studied process in Figure 4), but this is not explicitly included in the mathematical model. The reaction energy from HS^- oxidation is increasing with increased amount of NO_3^- supplied. Probably both of these energy related phenomena influence the products distribution but insufficient results are yet available to distinguish these. Thus, further model refinement to include both hypothesized energy reactions separately is not attempted and the cumulative effect observed experimentally are covered by the coefficients given in Tables 3 and 4 and simulated (Figure 5).

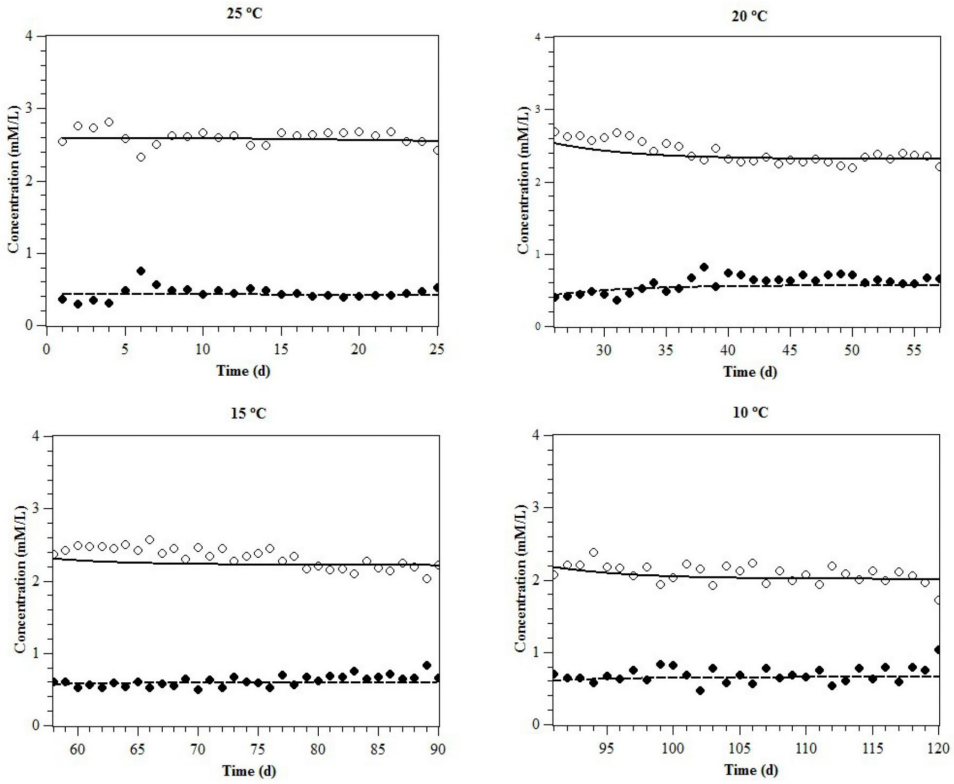

Figure 3. Model simulation results in comparison to experimental results at different temperatures. Solid and dash line represent simulated results for S^0 and SO_4^{2-}, respectively. Scatter points represent experimental results for S^0 (○) and SO_4^{2-} (●).

DOI: 10.3384/ecp1713841

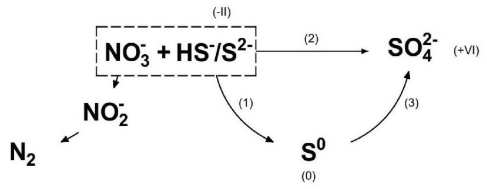

Figure 4. The scheme of autotrophic denitrification with HS^- as electron donor.

The simulations with the applied coefficients related to N/S ratio (Table 4) significantly improved predictions compared to those in Figure 2, except for N/S = 1.30, where simple stoichiometric calculations matched the experimental values best. The poor simulation of experimental results at N/S = 1.30 is assumed to be due to the fact that reaction 3 in Figure 4 is not explicitly accounted for in the model and that this reaction is especially important at this stage. This is due to the experimental scenario which at the beginning was focused on S^0 production leading to its accumulation, as energy storage for the microorganisms. This S^0 energy reserve in the reactor was oxidized to SO_4^{2-} and is especially visible at N/S = 1.30. This implies that a more refined future model of simultaneous biological removal of HS^- and NO_3^- needs to consider the effect of S^0 accumulation and its possible oxidation (Figure 4) as occurred here under N/S ratio effects trial.

The energy related aspects discussed here are not included in the previously published models since these are based mainly on batch experiments and high N/S ratio situations. The observed phenomena probably occur only in cases when the N/S ratio is in or close to the range investigated here and are most observable when increasing from low (S^0 production related) to high N/S ratios (SO_4^{2-} production related). It can therefore be useful to develop the model further to better account for accumulation and consumption of S^0. Some relevant information is available, such as: kinetics for S^0 leaching and usage as electron donor is available (Franzmann et al., 2005; Gourdon and Funtowicz, 1998; Koenig and Liu, 2001). Models including similar accumulation phenomena related to energy storage are developed, i.e. ASM2d where the accumulation and

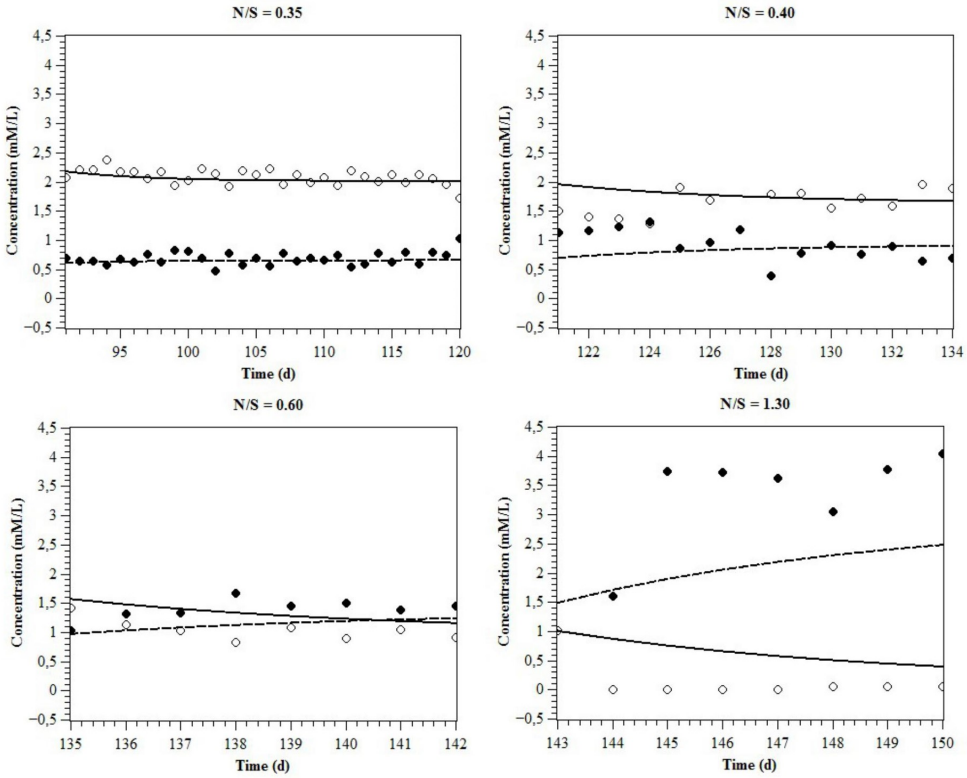

Figure 5. Model simulation results in comparison to experimental results at different N/S ratios at 10 °C. Solid and dash line represent simulated results for S^0 and SO_4^{2-} respectively. Scatter points represent experimental results for S^0 (○) and SO_4^{2-} (●).

consumption of polyhydroxybutyrate (PHB) and polyphosphate (PP) are taken into account (Henze et al., 1999). However, the factors triggering the oxidation of accumulated S^0 are not clear. It has been reported that the oxidation can only occur when the source of reduced sulfur compounds is depleted (Schedel and Trüper, 1980), but oxidation of accumulated S^0 can obviously occur (e.g. Figure 2) and be influenced by both temperature and N/S ratio changes when HS^- (sulfur reduced compound) is available (Sposob et al., 2017b, 2016). The observation that S^0 leaching increases with temperature (Franzmann et al., 2005) should also be accounted for in the further model development.

4 Conclusions

The presented model can serve as a prediction tool for autotrophic denitrification with HS^- as supplied electron donor, to account for effects of temperature and feed N/S ratio.

The model was able to simulate sulfur compound products distribution at different temperatures, more accurately at low than higher N/S ratios (N/S range 0.35 to 1.30).

The phenomena of S^0 production included in the mathematical model does not take into account its accumulation and release (as SO_4^{2-}). Thus, adequate prediction of products distribution caused by N/S ratio step increases (leading to higher concentration of sulfur components in the effluent than fed into the reactor) was not obtained. Therefore, a conceptual model is proposed to account for biological accumulation and release of S^0. Further investigations on N/S ratio effects on S^0 accumulation and release can yield a more refined model of simultaneous biological removal of HS^- and NO_3^-.

Acknowledgements

The authors would like to thank YARA AS International and The Research Council of Norway for support of this research.

References

Cai, J., Zheng, P., and Mahmood, Q. Effect of sulfide to nitrate ratios on the simultaneous anaerobic sulfide and nitrate removal. *Bioresource Technology*, 99(13):5520–5527, 2008.

Cai, J., Zheng, P., and Mahmood, Q. Influence of transient pH and substrate shocks on simultaneous anaerobic sulfide and nitrate removal. *Journal of Hazardous Materials*, 174(1–3):162–166, 2010.

Chen, Y., Cheng, J. J., and Creamer, K. S. Inhibition of anaerobic digestion process: A review. *Bioresource Technology*, 99(10):4044–4064, 2008.

Di Capua, F., Milone, I., Lakaniemi, A. M., Lens, P. N. L., and Esposito, G. High-rate autotrophic denitrification in a fluidized-bed reactor at psychrophilic temperatures. *Chemical Engineering Journal*, 313:591–598, 2017.

Franzmann, P. D., Haddad, C. M., Hawkes, R. B., Robertson, W. J., and Plumb, J. J. Effects of temperature on the rates of iron and sulfur oxidation by selected bioleaching Bacteria and Archaea: Application of the Ratkowsky equation. In *Minerals Engineering* 18:1304–1314, 2005.

Gourdon, R., and Funtowicz, N. (1998). Kinetic model of elemental sulfur oxidation by Thiobacillus thiooxidans in batch slurry reactors: Effects of surface characteristics and suspended solid concentration. *Bioprocess Engineering*, 18(4):241–249, 1998.

Guo, Q., Hu, H. Y., Shi, Z. J., Yang, C. C., Li, P., Huang, M., Ni, W. M., Shi, M. N., and Jin, R. C. Towards simultaneously removing nitrogen and sulfur by a novel process: Anammox and autotrophic desulfurization-denitrification (AADD). *Chemical Engineering Journal*, 297, 207–216, 2016.

Henze, M., Gujer, W., Mino, T., Matsuo, T., Wentzel, M. C., Marais, G. V. R., and Van Loosdrecht, M. C. M. (1999). Activated Sludge Model No.2d, ASM2d. *Water Science and Technology* 39:165–182, 1999.

Huang, C., Li, Z., Chen, F., Liu, Q., Zhao, Y., Gao, L., Chen, C., Zhou, J., and Wang, A. Efficient regulation of elemental sulfur recovery through optimizing working height of upflow anaerobic sludge blanket reactor during denitrifying sulfide removal process. *Bioresource Technology*, 200:1019–1023, 2016.

Jin, R. C., Yang, G. F., Zhang, Q. Q., Ma, C., Yu, J. J., and Xing, B. S. The effect of sulfide inhibition on the ANAMMOX process. *Water Research*, 47(3):1459–1469, 2013.

Joye, S. B., and Hollibaugh, J. T. Influence of sulfide inhibition of nitrification on nitrogen regeneration in sediments. *Science*, 270(5236):623–625, 1995.

Kleerebezem, R., and Mendez, R. Autotrophic denitrification for combined hydrogen sulfide removal from biogas and post-denitrification. *Water Science and Technology*, 45(10):349–356, 2002.

Koenig, A., and Liu, L. H. Kinetic model of autotrophic denitrification in sulphur packed-bed reactors. *Water Research*, 35(8):1969–1978, 2001.

Ma, H., Cheng, X., Li, G., Chen, S., Quan, Z., Zhao, S., and Niu, L. The influence of hydrogen sulfide on corrosion of iron under different conditions. *Corrosion Science*, 42(10):1669–1683, 2000.

Mahmood, Q., Zheng, P., Cai, J., Wu, D., Hu, B., and

Li, J. Anoxic sulfide biooxidation using nitrite as electron acceptor. *Journal of Hazardous Materials*, 147(1–2):249–256, 2007.

Montalvo, S., Huiliñir, C., Gálvez, D., Roca, N., and Guerrero, L. Autotrophic denitrification with sulfide as electron donor: Effect of zeolite, organic matter and temperature in batch and continuous UASB reactors. *International Biodeterioration and Biodegradation*, 108:158–165, 2016.

Pikaar, I., Rozendal, R. A., Yuan, Z., Keller, J., and Rabaey, K. (2011). Electrochemical sulfide removal from synthetic and real domestic wastewater at high current densities. *Water Research*, 45(6):2281–2289, 2011.

Reiffenstein, R. J., Hulbert, W. C., and Roth, S. H. Toxicology of hydrogen sulfide. *Annual Review of Pharmacology and Toxicology*, 32(1):109–134, 1992.

Reyes-Avila, J., Razo-Flores, E., and Gomez, J. Simultaneous biological removal of nitrogen, carbon and sulfur by denitrification. *Water Research*, 38(14–15):3313–3321, 2004.

Schedel, M., and Trüper, H. G. Anaerobic oxidation of thiosulfate and elemental sulfur in Thiobacillus denitrificans. *Archives of Microbiology*, 124(2–3):205–210, 1980.

Sposob, M., Bakke, R., and Dinamarca, C. Effects of N/S molar ratio on products formation in psychrophilic autotrophic biological removal of sulfide. *Water*, 9(7):476, 2017a.

Sposob, M., Bakke, R., and Dinamarca, C. Metabolic divergence in simultaneous biological removal of nitrate and sulfide for elemental sulfur production under temperature stress. *Bioresource Technology*, 233:209–215, 2017b.

Sposob, M., Dinamarca, C., and Bakke, R. Short-term temperature impact on simultaneous biological nitrogen-sulphur treatment in EGSB reactor. *Water Science and Technology*, 74(7):1610–1618, 2016.

Tan, W., Huang, C., Chen, C., Liang, B., and Wang, A. Bioaugmentation of activated sludge with elemental sulfur producing strain Thiopseudomonas denitrificans X2 against nitrate shock load. *Bioresource Technology*, 220:647–650, 2016.

Tchobanoglous, G., Burton, F. L., and Stensel, H. D. (2003). *Wastewater Engineering: Treatment and Reuse (Fourth Edition). Wastewater Engineering, Treatment, Disposal and Reuse,* 2003.

Wang, A., Liu, C., Han, H., Ren, N., and Lee, D. J. Modeling denitrifying sulfide removal process using artificial neural networks. *Journal of Hazardous Materials*, 168(2–3):1274–1279, 2009.

Wang, A., Liu, C., Ren, N., Han, H., and Lee, D. Simultaneous removal of sulfide, nitrate and acetate: Kinetic modeling. *Journal of Hazardous Materials*, 178(1–3):35–41, 2010.

Wang, X., Zhang, Y., Zhou, J., Zhang, T., and Chen, M. Regeneration of elemental sulfur in a simultaneous sulfide and nitrate removal reactor under different dissolved oxygen conditions. *Bioresource Technology*, 182:75–81, 2015.

Xu, G., Yin, F., Chen, S., Xu, Y., and Yu, H. Q. Mathematical modeling of autotrophic denitrification (AD) process with sulphide as electron donor. *Water Research*, 91:225–234, 2016.

Xu, X., Chen, C., Wang, A., Guo, W., Zhou, X., Lee, D. J., Ren, N., and Chang, J. S. Simultaneous removal of sulfide, nitrate and acetate under denitrifying sulfide removal condition: Modeling and experimental validation. *Journal of Hazardous Materials*, 264:16–24, 2014.

Doctoral dissertation no. 11
2018

—

Biological hydrogen sulfide removal with nitrate

Dissertation for the degree of Ph.D

—

Michal Sposob

—

ISBN: 978-82-7206-485-2 (print)
ISBN: 978-82-7206-486-9 (online)

usn.no